Exploiting zebrafish model by transgenic technology for the study of gastrointestinal diseases

In Hye Jung

The Graduate school

Yonsei University

Graduate Program for Nanomedical Science

Exploiting zebrafish model by transgenic technology for the study of gastrointestinal diseases

A Dissertation

Submitted to the Graduate School of Yonsei University

in partial fulfillment of the

requirements for the degree of

Doctor of Philosophy

In Hye Jung

July 2014

This certifies that the dissertation Of In Hye Jung is approved.

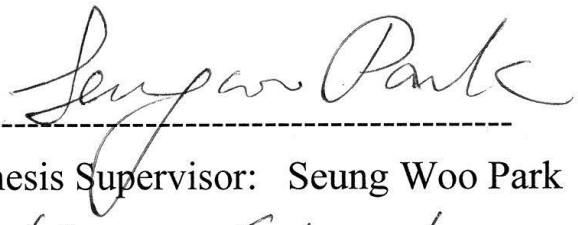

Thesis Supervisor: Seung Woo Park

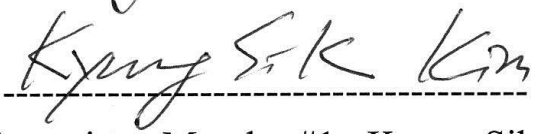

Thesis Committee Member#1: Kyung Sik Kim

Thesis Committee Member#2: Jae Young Cho

Thesis Committee Member#3: Dug Young Kim

Thesis Committee Member#4: Kang Taek Lee

The Graduate School
Yonsei University
July 2014

Acknowledgements

아직도 science가 무엇인지 잘 모르는 저로서 벌써 이렇게 학위 논문을 쓰고 있다니 놀랍기만 합니다. 잠시 지난날들을 돌이켜 보면 무엇보다 먼저 부족한 저를 잘 이끌어 주신 지도 교수님이신 박승우 교수님께 진심으로 감사와 고마움을 전하고 싶습니다. 세브란스 소화기내과 의사겸 교수님이시라 진료도 보시고 학생지도도 하시느라 늘 바쁘시지만 어느 자연대 교수님보다 더 열정적으로 항상 연구실에서 실험하시는 모습을 보여주시고 사수로서 실험 방향이나 문제점들을 해결하시는 모습을 보며 정말 많은 것을 배웠습니다.

어릴 때부터 생선비린내도 싫어하던 제가 제브라피쉬라는 실험동물 모델인 물고기로 365일을 거의 같이 지내면서 열정과 애정으로 저의 30대를 동고동락 한 것 같습니다. 매일 아기 키우는 것과 같은 물고기들을 잘 관리 사육하고 연구하여 이렇게 좋은 성과를 얻고 학위를 마칠 수 있도록 지도하여 주심을 진심으로 감사드립니다. 또한, 항상 어려울 때 옆에서 묵묵히 도와준 저의 또 다른 스승인 남편한테 고마움과 미안함을 함께 전합니다.

처음 협소한 시스템과 장소인 의과 대학 신관 3층 공용 랩 실험실에서 생활하다가 작년에 신관 5층 전용 제브라피쉬룸과 연구실이 생겨 이사가면서 너무나 좋아했던 기억들이 어제 일처럼 스쳐 지나갑니다.

연구하는데 많은 도움과 정신적 지주인 소화기 내과 정다운 박사, 신장내과 순하, 보영, 혜영, 지선이, 혼자인 저에게 선후배 같아서 학위 과정 동안

즐거웠고, 방학중 한국에 들어 올때마다 우리 실험실이라며 실험실을 지켜주는 미국 의대생 현규, 띠동갑 예비 소화기내과 의사샘 가람이, 눈빛만 봐도 다 아는 병리학교실 도희, 다혜, 유경이한테 고마운 마음을 전하고 싶습니다. 주말마다 물고기 관리해주는 나의 든든한 조력자 민희한테도 고마움을 전하고 싶습니다.

사랑하는 나의 아빠, 엄마, 시부모님, 윤혜 언니, 재철이, 재엽이, 형부, 조카 세나, 세원이 다시 한번 사랑한다고 말을 전하고 싶습니다. 그리고 기쁠 때나 어려울 때나 함께 있어준 가족 친지들에게도 고마운 마음을 전합니다.

마지막으로 바쁘신 와중에 시간을 내어 심사에 와 주신 김경석 교수님, 조재용 교수님, 김덕영 교수님, 이강택 교수님께도 감사의 인사를 드립니다.

2014년 6월
정 인혜올림

Table of contents

Pancreas-specific expression using Ptf1a regulatory element

Chapter 1.Aberrant pancreatic expression of hedgehog ligands in transgenic zebrafish induces progressive fibrosis by recruiting and activating myofibroblasts through paracrine signaling

Liver-specific expression using LFABP regulatory element

Chapter 2.Interleukin-6 mediated chronic inflammation induces hepatocellular carcinoma in transgenic zebrafish

Intestinal-specific expression

Chapter 3.Platform for intestine-specific expression of transgenes

List of figures

Chapter 1

Chapter2

Chapter 3

List of table

Chapter 1

Chapter 2

Chapter 3

Abbreviations

AFP	Alpha-fetoprotein
Akt1	Abelson non-receptor tyrosine kinase
Apaf	Apoptotic protease activating factor 1
Appa	Appa amyloid beta (A4) precursor protein a
ASMA	Alpha smooth muscle Actin
BAC	Bacterial artificial chromosome
Bax	BCL2-associated X protein
Bcl2	B-cell lymphoma 2
BrdU	5-bromo-2'-deoxyuridine
CCND1	Cyclin D1
CDKI	Cyclin dependent kinase inhibitor
Cis	Cis citrate synthase
CPA	Carboxypeptidase A
DAPI	4’,6-Diamidino-2-phenyindole
DCLK1a	Doublecortin-like kinase 1a ,
Mcl1a	Myeloid cell leukemia sequence 1a
DMSO	Dimethyl sulfoxide
DTT	1,4-dithiothreitol
EDTA	Ethylenediaminetetraacetic acid
Eif1a	Eukaryotic initiation factor

EGTA	Ethylene glycol tetraacetic acid
Erk1	Extracellular signal-regulated kinase 1
FITC	Fluorescein isothiocyanate
Foxa3	Forkhead box A3
GAPDH	Glyceraldehyde 3-phosphate dehydrogenase
GATA6	GATA-binding factor 6
Gli1	GLI family zinc finger 1
GFP	Green fluorescent protein
GFAP	Glial fibrillary acidic protein
Her4	Hairy-related 4
HEPES	4-(2-hydroxyethyl)-1-piperazineethanesulfonic acid
HIF1α	Hypoxia inducible factor 1α
HPI-4	Hh Primary Inhibitor-4
hpf	Hours post fertilization
Ihha	Indian Hedgehog
IFABP	Intestinal fatty acid binding protein-
IL	Interleukin
IFNγ1	Interferon gamma 1
NOS2	Nitric oxide synthase 2
JAK	Janus Kinase
MAPK1	Mitogen-activated protein kinase 1
MBP	Maltose binding protein
Mcl1A	Myeloid cell leukemia sequence 1a

Mdm2	Mouse double minute 2 homolog
MMP	Matrix metalloprotease
MTD	Maximal tolerable dose
MT1-MMP	Membrane type 1 metalloprotease
Myca	Myelocytomatosis oncogene a
Olig2	Oligodendrocyte transcription factor
Rac1	Ras-related C3 botulinum toxin substrate 1
RFP	Red fluorescent protein
PBS	Phosphate-buffered saline
PCNA	Proliferating cell nuclear antigen
PDGFA	Platelet-derived growth factor subunit A
PI3K	Phosphatidylinositol 3-kinase
Pim1	Proviral integration site 1
Ptc1	Patched1
Pft1a	Pancreas transcription factor 1 subunit alpha
PFA	Paraformaldehyde
PMSF	Phenylmethylsulfonyl fluoride
PHH3	Phosphohistone H3
p-mTOR	Phospho- mammalian target of rapamycin
p-RS6K	Phospho- ribosomal protein S6 kinase
p-4EBP1	Phosphorylated 4E-binding protein 1
SDS-PAGE	Sodium dodecyl sulfate polyacrylamide gel electrophoresis
S100	S100 calcium binding protein B

Shha	Sonic Hedgehog
Smo	Smoothened
SOCS3	Sppressor of cytokine signaling 3
STAT	Signal transducer and activator of transcription
TIMP2	Tissue inhibitor of metalloproteinase 2
TGF- β	Transforming growth factor beta
UAS	Upstream activating sequence
UBB	Ubiquitin B
Xiap	X-linked inhibitor of apoptosis protein

Pancreas - specific expression using

Ptf1a regulatory element

Chapter 1

Aberrant pancreatic expression of hedgehog ligands in transgenic zebrafish induces progressive fibrosis by recruiting and activating myofibroblasts through paracrine signaling

1. Abstract

Hedgehog (Hh) signaling is frequently up-regulated in fibrogenic pancreatic diseases including chronic pancreatitis and pancreatic cancer. Although recent series suggest exclusive paracrine activation of stromal cells by Hh ligands from epithelial components, debates still exist on how Hh signaling works in pathologic conditions. To explore how Hh signaling affects the pancreas, transgenic phenotypes of zebrafish over-expressing either Indian Hh or Sonic Hh were investigated. This investigation was done along with green fluorescence protein (GFP) to enable real-time observation, or GFP alone as control, at the ptf1a domain. Transgenic embryos and zebrafish were serially observed for transgenic phenotypes, and investigated using quantitative reverse transcription-polymerase chain reaction (qRT-PCR), in situ hybridization, and immunohistochemistry.

The results showed that over-expression of Ihh or Shh reveals virtually identical

phenotypes. Hh induced morphologic changes in the developing pancreas without derangement in acinar differentiation. The transgenic zebrafish showed progressive pancreatic fibrosis intermingled with proliferating ductular structures, which is accompanied by the destruction of the acinar structures. Both myofibroblasts and ductular were activated and proliferated by paracrine Hh signaling, showing restricted expression of Hh downstream components including Patched1 (Ptc1), Smoothened (Smo), and Gli1/2 in those Hh-responsive cells. Hh ligands also induced matrix metalloproteinases (MMPs), especially MMP9 in all Hh-responsive cells, and transform growth factor-ß1 (TGFß1) only in ductular cells. Aberrant Hh over-expression, however, did not cause pancreatic tumors. On treatment with inhibitors, the embryonic phenotypes were found to be reversed by either cyclopamine or Hedgehog Primary Inhibitor-4 (HPI-4). Pancreatic fibrosis was only prevented by HPI-4.

This study provides strong evidence of Hh signaling which induces pancreatic fibrosis through paracrine activation of Hh-responsive cells *in vivo*. Induction of MMPs and TGFß1 by Hh signaling expands on the current understanding of how Hh signaling affects fibrosis and tumorigenesis. These experiments showed that the transgenic models can be a valuable platform in exploring the mechanism of fibrogenic pancreatic diseases which are induced by Hh signaling activation.

Key words: Matrix metalloproteinase, transforming growth factor-ß, Hedgehog inhibitor, paracrine action

2. Introduction

Hh ligands are secreted glycoproteins and they initiate hedgehog signaling upon binding to Patched (Ptc) receptors. The signaling is transmitted through Smoothened (Smo)'s activation, resulting in the Gli-mediated transcriptional up-regulation of Hh target genes. This signaling plays a critical role in both physiologic and pathologic conditions by participating in cell differentiation and tissue patterning during early embryonic development and in tissue homeostasis as well as tumorigenesis in adult organs [1, 2]. The Desert Hedgehog (Dhh) is known to be largely restricted by gonads during embryonic development [3, 4]. On the other hand, the Indian Hedgehog (Ihh) and Sonic Hedgehog (Shh) are expressed in various organs, including the endoderm and the gastrointestinal tract; thereby showing an overlapped expression, suggesting that they are functionally redundant [5,6].

The pancreas is one of the organs where Hh signaling is strictly controlled. Although inactivation of Hh signaling is a crucial event for proper pancreatic development and differentiation, this signaling is frequently reactivated in fibrogenic pancreatic diseases. For instance, chronic pancreatitis and pancreatic ductal adenocarcinoma, with several components of Hh pathway are frequently and often markedly up-regulated in early stages of those conditions [7-9].Thus, these are representative of pancreatic diseases accompanying prominent desmoplastic reaction, in which active Hh signaling is somehow involved in fibrogenesis. An *in vitro* study revealed enhanced migration of pancreatic stellate cells by exogenous Ihh[10].

Moreover, the impact of Hh signaling on fibrosis does not seem to be confined to the pancreas. It also exerts an effect on fibrosis of the lungs, bile duct, and liver. This suggests that a similar paradigm works in various organs [11-13].

It has been well-documented that Hh signaling relies on paracrine action for proper patterning of the gastrointestinal tract during murine development [14]. Though evidence from recent observation has suggested a paracrine mechanism for Hh signaling in both physiologic and pathologic conditions [15], an autocrine mechanism cannot be completely excluded in certain types of malignancy [16, 17]. These findings reflect the possible existence of cell-type or organ-dependency, necessitating further clarification of Hh signaling. This raises a question regarding pathologic consequences of aberrantly expressed Hh ligands in the exocrine pancreas.

Since the early 1980s, the zebrafish has been widely used for the study of genetics and developmental biology, and is often exploited as a disease model [18]. Conservation of the genetic program strengthens the power of using the zebrafish model in simulating human diseases. Frequently, the orthologs of the human gene are duplicated in zebrafish. The orthologs of Ihh and Shh are also duplicated in zebrafish, suggesting the existence of redundancy within subtypes. Recent advances in technology have facilitated the establishment of transgenic zebrafish with greater efficiency and convenience. The implication of Hh signaling and pancreatic fibrosis has been firmly documented as a result of *in vitro* studies [10], specimens of diseased pancreas [19], and xenograft model of pancreatic cancer [20]. Nonetheless the direct effect of an aberrant Hh expression on the pancreas has not clearly established. In an

earlier study [21], the authors demonstrated that precancerous lesions developed in the pancreas of Pdx1-Shh transgenic mice. However, they did not mention any findings which are relevant to pancreatic fibrosis. Therefore, the present study was designed to investigate the effects of Hh ligands in the exocrine pancreas of transgenic zebrafish in which Ihha or Shha is over-expressed in the ptf1a domain. The results show *in vivo* evidence that Hh ligands cause pancreatic fibrosis by paracrine activation of myofibroblasts, as well as ductular cells.

3. Materials and Methods

1. Ethics Statement

It was not necessary to obtain approval by the Laboratory Animal Committee at Yonsei University College of Medicine. The current committee does not request approval when non-mammalian models are used for experiments. This study, however, was strictly carried out to minimize suffering. All live images of embryos were taken under anesthesia using E3 media with 0.3mg/mL tricaine. All adult zebrafish to be processed for experiments were euthanized by immersion in an ice-water bath.

2. Transgenesis

Transgenic constructs were generated by modifying JD21-UAS: GFP-Kras, a kind gift from Steven D. Leach, which allows Tol2- to mediate transgenesis and is designed to co-express the transgene along with green fluorescence protein (GFP) which

enabled real-time observation (Fig. 2A).The cDNA for zebrafish Ihha (GenBank accession No. BC133983.1) was purchased from Openbiosystem Co., and zebrafish Shha (GenBank accession No. BC162395) was cloned using cDNA generated from three day-old wild-type embryos (AB line, ZIRC ZL1).While using polymerase with the proofreading function (Invitrogen), the GFP sequence including a polyA site was PCR amplified from pEGFP1 vector (Clontech) using F-GFP-Nco1/R-GFPpA-Xho1 primers. It was then digested and inserted into Nco1/Xho1 sites of JD21-UAS:GFP-Kras to generate JD21-UAS:GFPpA-Kras. Ihha and Shha were amplified with PCR usingF-Ihha-Mlu1/R-Ihha-Cla1 and F-Shha-Mlu1/R-Shha-Cla1 primers, respectively, then inserted into Mlu1/Cla1 sites of JD21-UAS: GFP-Kras, separately to generate JD21-UAS:Ihha and JD21-UAS:Shha. Each UAS: Ihha and UAS: Shha sequence was PCR amplified using F-UAS-Xho1/R-Ihha-Cla1 and F-UAS-Xho1/R-Shha-Cla1, respectively. It was then inserted into Xho1/Cla1 sites of JD21-UAS-GFPpAKras, separately, to generate the final transgene constructs JD21-UAS: GFP-UAS: Ihha and JD21-UAS:GFP-UAS:Shha.Schematic illustration for the generation of transgene construction is shown in Figure 1. The control construct was generated by digesting JD21-UAS-GFPpA-Kras with Xhol1/Cla1, blunting, and then self-ligation. . JD21-Ins-DsRed was generated for targeted expression of biomarker in pancreatic beta cells. Upstream a 1kb sequence of the preproinsulin gene was PCR amplified from genomic DNA using F-Ins1kb-Apa1/R-Ins1kb-Nco1 primers and inserted into Apa1/Nco1 sites of JD21-UAS-GFPpA.Then, DsRed was PCR amplified from pDsRed-monomer-N1 (PT3795-5, Invitrogen Co.) using F-DsR-Nco1/R-DsR-Cla1 and inserted into

Nco1/Cla1 site of JD21-Ins-GFPpA. All constructs were sequenced and verified using appropriate primers. Primers used for transgene constructs are listed in Table 1.

Each injection mixture was made by reconstituting Tol2-transposase mRNA (20 ng/ul) and a transgene construct (20 ng/ul) in Danieu's buffer mixed with 0.03% phenol red. Single-cell stage Tg(Ptf1a:Gal4) embryos were transferred to a molded agarose dish and 4pL of injection mixture was introduced by yolk injection using a MMPI-2 micro injector. Approximately 50% of injected embryos survived. On day two, embryos showing GFP at the Ptf1a domain were selected using a fluorescence microscope, raised until adulthood, and out-crossed to generate F1 transgenic zebrafish. The utilization of Tol2-mediated transgenesis greatly enhanced the transgenic efficiency that 25-50% of F0 zebrafish from each construct gave rise to F1 offspring expressing transgenes. In each clutch of F1 embryos, approximately 10% showed transgene expression. Among the F1 progenies, embryos showing faithful expression were selected and raised to produce F2 progenies. All transgenes were transmitted into normal Mendelian ratios. Transgenic zebrafish were raised in a standardized aquaria system (Genomic-Design, Daejeon, Korea) according to standard protocols. Embryos to be processed for whole mount examination of GFP expression or ISH analyses were placed in 0.003% phenylthiourea at 24 hours post-fertilization (hpf) to inhibit pigmentation.

3. Histology and Immunohistochemistry (IHC)

Histologic evaluation was performed in a subset of F2 transgenic zebrafish at

1,3,6,9, and 12-month(s). Hematoxylin and eosin (H&E) staining and IHC were performed according to the standard protocols. Primary antibodies used for immunohistochemistry were rabbit anti-α-smooth muscle actin (α-SMA) (Abcam ab15734, 1:500), rabbit anti-Smoothened (Smo) (Abcam ab72130, 1:200), rabbit anti-Gli1 (Upstate AB3444, 1:500), rabbit anti-Gli2 (Abcam ab26056, 1:300), mouse anti-Transforming growth factor ß1 (TGFß1) (R&D MAB1835, 1:500), rabbit anti-matrix metalloproteinase 9 (MMP9) (Abcam ab38898, 1:500), mouse anti-cytokeratin (CK) AE1/AE3 (Abcam ab961, 1:500), mouse anti-proliferating cell nuclear antigen (PCNA) (Abcam ab29, 1:1000), and rabbit anti-phosphohistone H3 (pHH3) (Cell Signaling 9701, 1:200). Horse radish peroxidase (HRP)-conjugated secondary antibodies were utilized and colored using DAB solution. Slides were counterstained with hematoxylin, dehydrated, and mounted with Histomount (Zymed Co.).

4. Western blotting

A western blot hybridization was performed as previously described [22], using the exocrine pancreas dissected under a fluorescence microscope from 4 month-old zebrafish. The zebrafish pancreas does not form a single solid organ, but exists as thread-like structures being dispersed between visceral organs and embedded in fatty tissues. For each group, samples were collected from 20 to 30zebrafish and processed for protein extraction. Proteins were resolved by 10% SDSP-gels, blotted onto a nitrocellulose membrane, stained for 5 minutes with Ponceau S, blocked for 1 h in 5% milk in PBST, incubated over night at 4℃ with a primary antibody in blocking buffer,

washed 4 times with PBST, and incubated for 1h with horseradish peroxidase-conjugated secondary antibody. Labeled proteins were detected by ECL reagents and Hyperfilm ECL (Amersham Biosciences).

5. In situ hybridization (ISH)

ISH was performed either using 4% paraformaldehyde-fixed whole embryos or on 4-um sections of 4% paraformaldehyde-fixed, paraffin-embedded tissues as described previously [23]. To generate riboprobes, the corresponding coding sequences were PCR amplified from cDNA, TA cloned into pCRII vector (Invitrogen, CA, USA), and sequence-verified. Then, digoxigenin-labelled riboprobes were generated with the IVT kit (Roche Applied Science, Germany) using SP6 or T7 RNA polymerase depending on the orientation of the inserts. Primers used for TA cloning are listed inTable 3. Hybridized embryos or sections were bound with alkaline phosphatase-conjugated anti-Dig antibody, and colored using NBT/BCIP solution. Sections were counterstained with neutral red and mounted with Histomount.

6. Whole mount immonofluorescence

Whole mount immunofluorescence was ISH was performed using 4% paraformaldehyde-fixed whole embryos essentially as described previously [23].Embryos were incubated overnight in10% goat serum with rabbit anti-CPA (Rockland, 100-4152), washed 3 times with PBST, and then incubated overnight in 10% goat serum with Cy3-conjugated anti-rabbit antibody (Jackson Labs). To identify individual acinar cells, photographs were obtained by using a Zeiss 700 confocal

microscope with a 10X eye lens and a 20X objective lens.

7. Imaging

Photographs were obtained using an Olympus BX51 for slide sections and an Olympus MVX10 for whole mount embryos. If not indicated, all section images were taken with a 10X eye lens and a 40X objective lens. If needed, zoom functions were used to obtain further magnified images.

8. Semi-quantitative and quantitative reverse transcription-PCR (RT-PCR)

RT-PCR was performed using the exocrine pancreas dissected under a fluorescence microscope from three-month old zebrafish. For each group, samples were collected from five to six zebrafish and processed for RNA extraction. Real-time, quantitative RT-PCR was performed as previously described [18], using 7300 Real Time PCR System (Applied Biosystems, Foster city, CA) with the QuantiTectTMSYBRGreen PCR Kit (Qiagen, Valencia, CA). Samples were in triplicate, and all experiments were repeated three time using separately prepared samples. Statistical analysis was performed using SPSS 11 software. Statistical significance for quantitative RT-PCR was analyzed by the Mann-Whitney U test. Primer sequences are shown in Table 2.

9. Treatment with Hedgehog inhibitors

To antagonize Hh signaling, either cyclopamine (Sigma-Aldrich Co., C4116) or Hh Primary Inhibitor-4 (HPI-4) (Sigma-Aldrich Co., H4541) was used [32]. For short-term phenotypic reversal, Tg(Ptf1a-Gal4/UAS:GFP-UAS:Ihha) embryos were treated in a

petri dish from 32 hpf when Ptf1a expression first appeared in the primordial exocrine pancreas for five days with the maximal tolerable doses (MTDs) that would not impair embryonic development. MTDs were measured by treating embryos with a serial escalation of doses from 100 nM, which were 1uM for HPI-4 and 15uM for cyclopamine. Next, 12 day-old Tg(Ptf1a-Gal4/UAS:GFP-UAS:Ihha) larvae were treated in a 1L-breeding cage with Hh inhibitors for an extended period of up to six weeks. The MTDs (lethal in less than 25%) were measured again revealing 5uM for HPI-4 and 500 nM for cyclopamine. Cage water was daily refreshed and inhibitors were newly added. At week six, juvenile zebrafish were processed for histologic evaluation.

4. Results

1. Targeted expression of transgenes and short-term phenotypes

In order to express transgenes from a zebrafish pancreas, Tg (Ptf1a:Gal4) zebrafish [24] had previously been established by bacterial artificial chromosome (BAC) and allowed binary expression by Gal4-UAS system. Transgene constructs were generated to co-express either Ihha or Shha along with green fluorescence protein (GFP) which enabled real-time observation (Fig. 2A). From each construct, 7 independent transgenic lines were successfully established: Tg(Ptf1a-Gal4/UAS:GFP-UAS:Ihha), Tg(Ptf1a-Gal4/UAS:GFP-UAS:Shha), and Tg(Ptf1a-Gal4/UAS:GFP). The transgene expression levels estimated by GFP, however, varied among the F1 progenies depending on their

parental zebrafish. All independent lines were separately maintained.

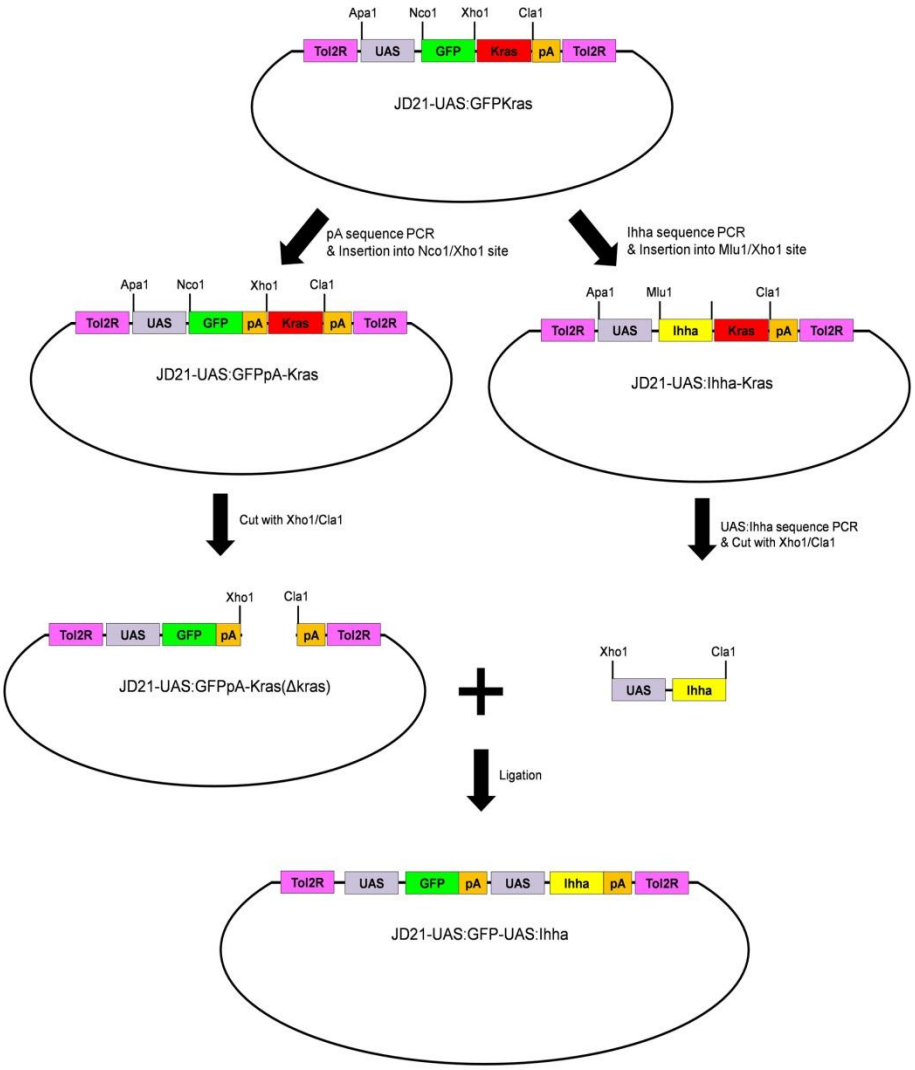

Figure 1. Schematic illustration for the generation of transgene constructs.

Table 1 . Primers used for the generation of transgene constructs.

Primers	Sequence
F-GFP-Nco1	5'-ATACCATGGTGAGCAAGGGCGAGGAG-3'
R-GFP-Xho1	5'-ATACTCGAGATACATTGATGAGTTTGGAC-3'
F-Ihha-Mlu1	5'-ATAACGCGTGCCACCATGCGTCTCCCCGTGGTGTT-3'
R-Ihha-Cla1	5'-ACTAATCGATTCATCTATCATTGTCCATCA-3'
F-Shha-Mlu1	5'-ATAACGCGTGCCACCATGCGGCTTTTGACGAGAGT-3'
R-Shha-Cla1	5'-ACTAATCGATTCAGCTTGAGTTTACTGACA-3'
F-Ins1kb-Apa1	5'-ACTAGGGCCCATTTAACTTCAGCCCACAGTCT-3'
R-Ins1kb-Nco1	5'-CACACTGCCATGGTCACACT-3'
F-DsR-Nco1	5'-ATACCATGGATGGACAACACCGAGGACGTC-3'
R-DsR-Cla1	5'-ACTAATCGATCTACTGGGAGCCGGAGTGGCGGG-3'
F-UAS-Xho1	5'-ATACTCGAGCTCTGCTAACCATGTTCATG-3'
F-UAS-Seq	5'-TCAGCCTCACTTTGAGCTCC-3'

F-UAS-Seq was used for sequence verification of constructs. Underlined GCCACC sequence was inserted to satisfy Kozak sequence for proper transcription. Underlines, restriction enzyme sequences.

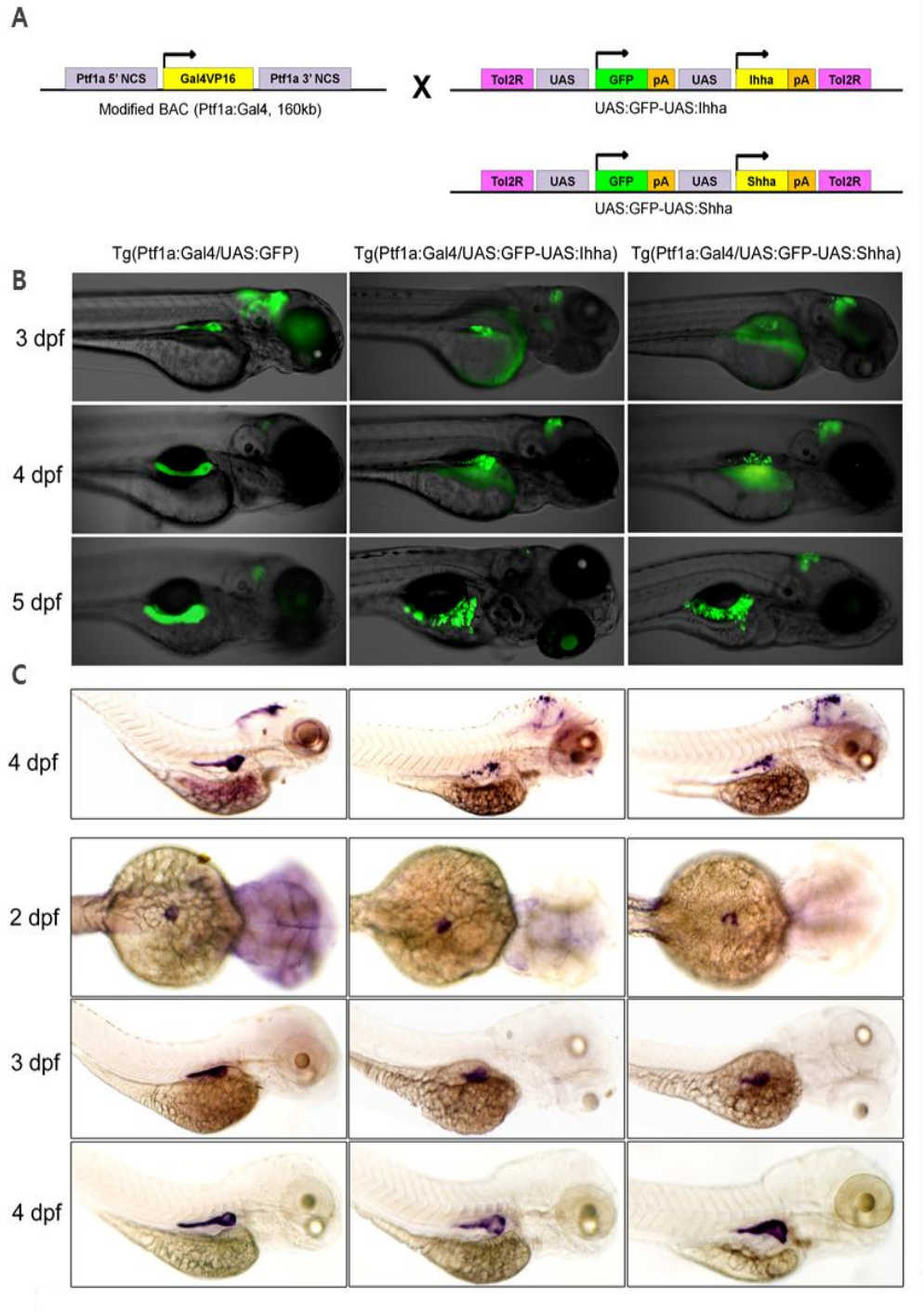
A
Ptf1a 5' NCS
Gal4VP16
Ptf1a 3' NCS
Modified BAC (Ptf1a:Gal4, 160kb)
X
Tol2R
UAS
GFP
pA
UAS
Ihha
pA
Tol2R
UAS:GFP-UAS:Ihha
Tol2R
UAS
GFP
pA
UAS
Shha
pA
Tol2R
UAS:GFP-UAS:Shha
Tg(Ptf1a:Gal4/UAS:GFP)
Tg(Ptf1a:Gal4/UAS:GFP-UAS:Ihha)
Tg(Ptf1a:Gal4/UAS:GFP-UAS:Shha)
B
3 dpf
4 dpf
5 dpf
C
4 dpf
2 dpf
3 dpf
4 dpf

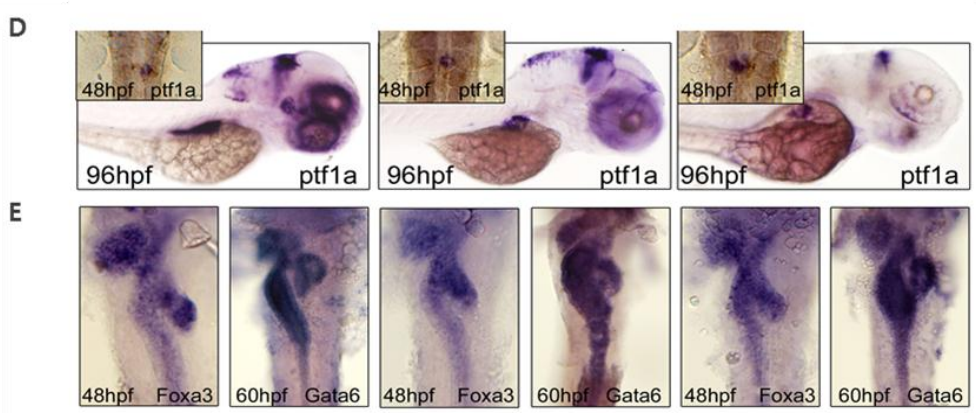

Figure 2. Short-term phenotypes. (**A**) Transgenesis strategy. (**B, C**) Inverted fluorescence and transgene ISH images show mosaic pattern of transgene expression in Hh ligand-expressing embryos. (**D**) Whole mount ISH for ptf1a at 48 and 96hpf. Inlet figures are dorsal views with anterior to the top. A, anterior. Hh over-expression did not impair migration of ptf1a-expressing exocrine progenitor cells, showing ptf1a positive exocrine cells surrounding principal islet at 48 hpf. (**E**) Whole mount ISH for Foxa3 and Gata6, endodermal markers during development. Dorsal views with anterior to the top. The FoxA3 and Gata6 are properly expressed in the liver, intestine, and exocrine pancreas, and the endodermal morphologies are not affected by Hh over-expression. L, Liver; I, Intestine; P, Exocrine pancreas.

When transgene expression was evaluated by GFP expression or by ISH, it was found to be spatiotemporally restricted to the Ptf1a domain (Fig. 2B, C). In control embryos, GFP was expressed throughout the whole exocrine pancreas. In Hh ligand-expressing embryos, patterns of transgene expression were not homogeneous throughout the whole exocrine pancreas, but rather, were mosaic for GFP and Hh ligands expression somewhat due to an unknown cause. Acinar cells surrounding the principal islet tended to show more robust expression of the transgenes. In developing zebrafish, the ptf1a-positive cells first appear at the left side of the endoderm, migrate across the midline, and eventually encircle the principal islet at 48 hpf. The migration of the exocrine progenitor cells was not affected by Hh expression, showing the doughnut-shaped ptf1-expressing exocrine pancreas at 48 hpf (Fig. 2D, 3A). Next, in order to visualize the developing endoderm, ISH was performed for endodermal markers, FoxA3 and Gata6 at 48 and 60 hpf, respectively [25, 26].These transcriptional factors were properly induced in the liver, intestine, and exocrine pancreas. Also, endodermal morphologies were not deranged by Hh over-expression (Fig. 2E).

The endocrine or exocrine differentiation was not compromised by Hh over-expression (Fig. 3). To visualize the endocrine pancreas, each line was crossed with Ins-DsRed transgenic zebrafish. The emergence of RFP-positive endocrince cells was not different from that of control (Fig. 3A). The anterior endocrine cells appear as a small dot like structure at the rostral side of the principal islet and are visible in approximately 50% of the control embryos, which was also not affected by Hh over-expression (Fig 3A). The exocrine differentiation was evaluated by trypsin, elastase,

and carboxypeptidase A (CPA) expression. The appearance of trypsin expression at 48 hpf did not temporally differ from that of the control embryos. The expression of other exocrine markers, such as elastase and CPA were also properly induced (Fig. 3B, C). Aberrant Hh expression, however, caused morphologic changes of exocrine pancreas when estimated by GFP expression or by ISH. The exocrine pancreas in Hh-expressing embryos showed a short, slender, and tortuous posteriorly-growing pancreas with a relatively prominent head compared to that of the control, which was evident at 4 and 5 dpf and exaggerated at 12 dpf (Fig. 3B, C). Confocal imaging of CPA immunofluorescence staining revealed proper exocrine differentiation of individual acinar cells regardless of transgene expression, suggesting that the exocrine differentiation program was not affected by Hh over-expression.

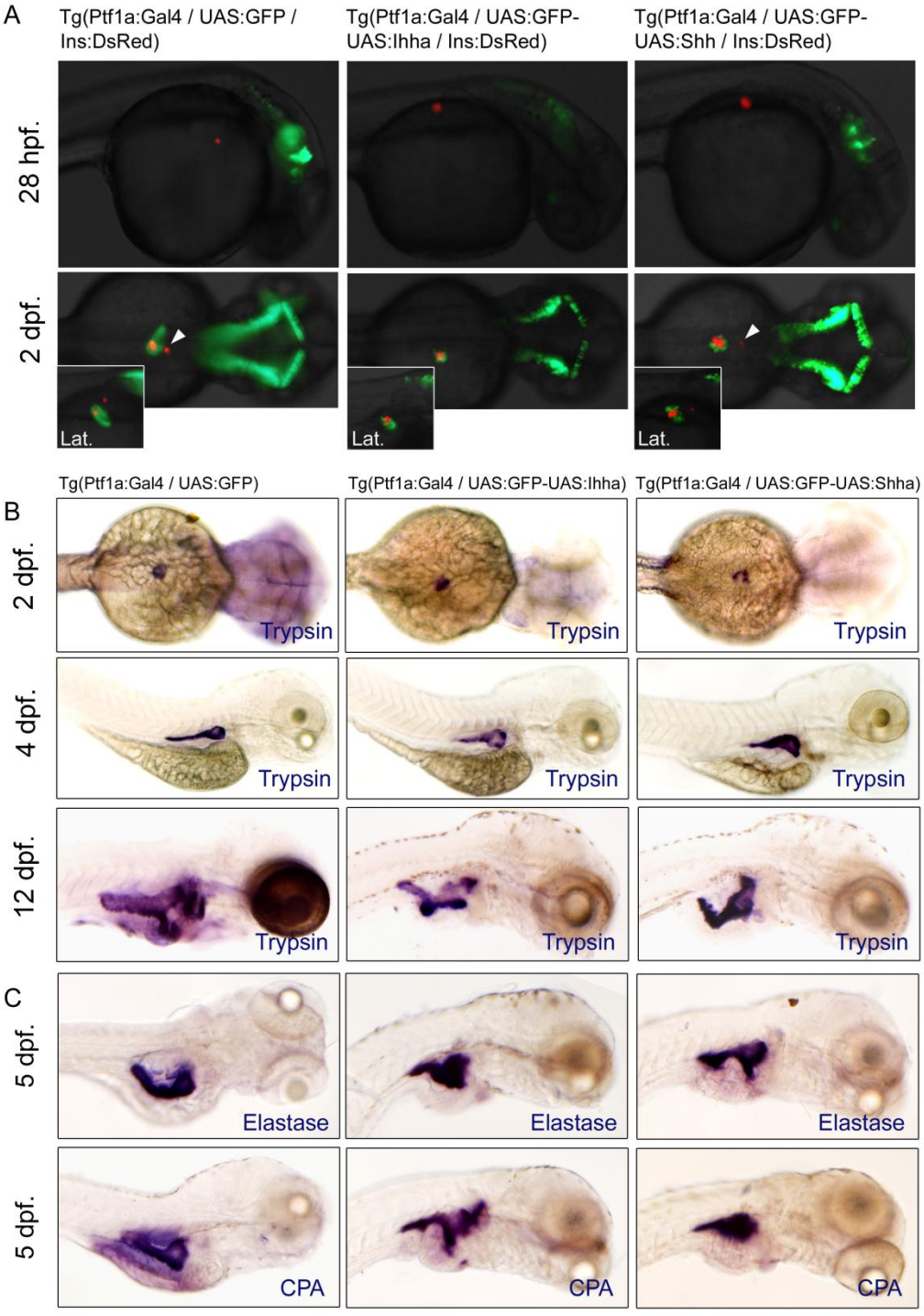
A
Tg(Ptf1a:Gal4 / UAS:GFP / Ins:DsRed)
Tg(Ptf1a:Gal4 / UAS:GFP-UAS:Ihha / Ins:DsRed)
Tg(Ptf1a:Gal4 / UAS:GFP-UAS:Shh / Ins:DsRed)
28 hpf.
2 dpf.
Lat.
Lat.
Lat.
B
Tg(Ptf1a:Gal4 / UAS:GFP)
Tg(Ptf1a:Gal4 / UAS:GFP-UAS:Ihha)
Tg(Ptf1a:Gal4 / UAS:GFP-UAS:Shha)
2 dpf.
4 dpf.
12 dpf.
Trypsin
C
5 dpf.
Elastase
5 dpf.
CPA

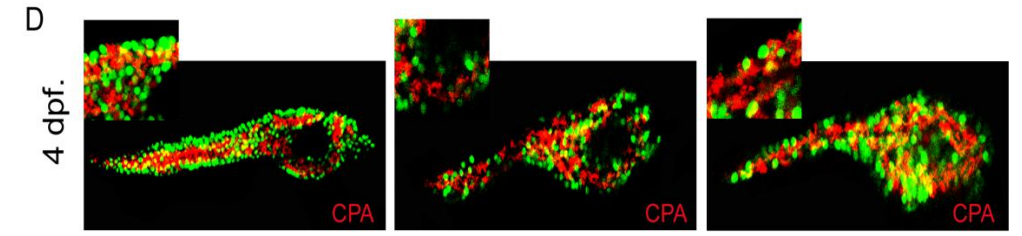

Figure 3. Unaffected endocrine and exocrine differentiation by Hh over-expression. (A) Fluorescence images showing the endocrine (RFP) and exocrine pancreas (GFP). When each transgenic fish is crossed with Ins-DsRed zebrafish, the development of insulin-expressing endocrine pancreas is not impaired by Hh over-expression. A smaller dot-like insulin-positive structure (white arrowheads) which corresponds to the anterior endocrine cells is observed in approximately half of the control and Hh-expressing embryos. (B, C) Whole mount ISH for trypsin, elastase, and carboxypeptidase A (CPA) at different time points. Over-expression of Hh ligands does not compromise the exocrine differentiation of the zebrafish pancreas, as evidenced by the proper and timely expression of trypsin. Expression of the other exocrine markers is also unaffected by Hh over-expression. Hh over-expression, however, induces subtle morphologic changes of the exocrine pancreas, showing a short, slender, and tortuous posterior pancreas compared to those of controls, which is evident by ISH for exocrine markers at 4 and 5 dpf and exaggerated at 12 dpf. (D) Confocal images of immunofluorescence staining for CPA. Regardless of transgene (GFP) expression, most acinar cells express CPA, suggesting unaffected exocrine differentiation by Hh over-expression. Lat., lateral.

2. Aberrant Hedgehog ligands cause pancreatic fibrosis

All Hh-expressing zebrafish from independent lines revealed a varying degree of pancreatic fibrosis and the desmoplasia was accumulated as the zebrafish aged (Fig.4). Among the 3 groups of independent lines from each construct, single representative line per group which revealed consistent and robust expression of transgenes was selected. Both Ihh and Shh induced pancreatic fibrosis undistinguishable by histology alone. It is notable that Shh induced phenotypically more severe pancreatic fibrosis than Ihh at the given time points. The pancreatic fibrosis was progressive and manifested at as early as the age of one month (Fig.4A). Fibrotic bands segregated and compartmentalized the exocrine glands, which resulted in the marked destruction of acinar structures at three months (Fig.4B). Though typical lesions with fibrosis did not involve infiltration of inflammatory cells, transgenic zebrafish occasionally revealed inflammatory lesions similar to acute pancreatitis in humans, demonstrating infiltration of inflammatory cells, fluid collection, and necrosis (Fig.4C,D). These findings, however, were unusual and appeared in less than 10% of the Hh-expressing zebrafish pancreas; therefore, it appeared to be caused by ductal obstruction resulting from fibrosis.

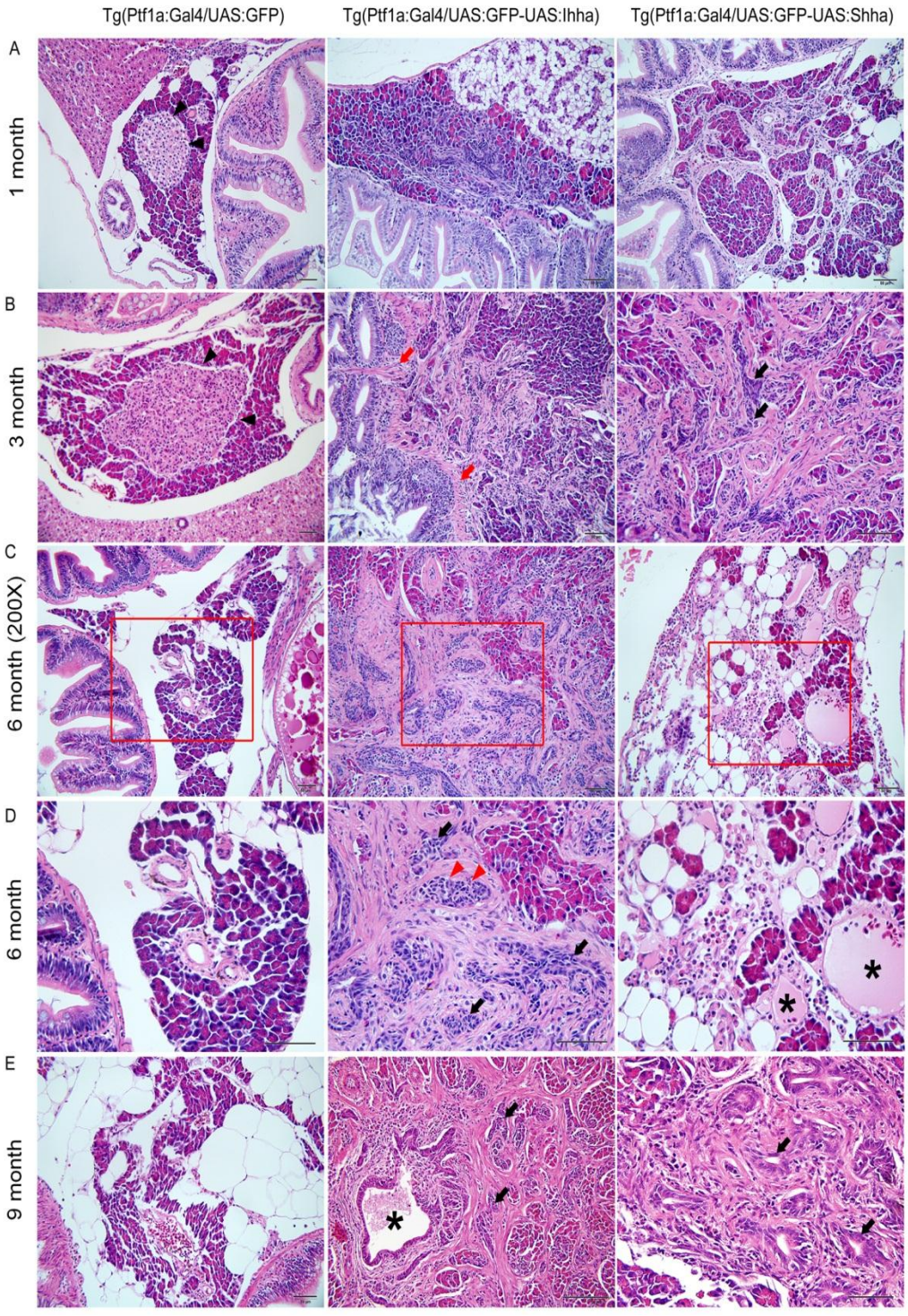
Tg(Ptf1a:Gal4/UAS:GFP)
Tg(Ptf1a:Gal4/UAS:GFP-UAS:Ihha)
Tg(Ptf1a:Gal4/UAS:GFP-UAS:Shha)
A
1 month
B
3 month
C
6 month (200X)
D
6 month
E
9 month

Figure 4. Histopathologic findings showing progressive pancreatic fibrosis. (A) Progressive pancreatic fibrosis starts at as early as 1-month old in Hh-expressing transgenic zebrafish. In non-fibrotic area, Individual morphology of the pancreatic acini and acinar cells is not unusual. (B) A principal islet is seen in control, which is well-circumscribed by acinar cells (black arrowheads). In Hh-secreting lines, accumulation of fibrosis results in the destruction of the morphologic architecture, which is prominent even at 3 months. Fibrotic bands are contiguous from the bowel wall forming adhesion between the bowel and the pancreas (red arrows), suggesting recruitment of myofibroblasts from the muscle layer of the bowel. Along with fibrosis, an increasing number of ductular structure appears within fibrotic area at 3 months of age (black arrows). (C, D) The pancreas at 6-months old. (D) An enlarged view of the red box in (C). Contrary to the islet of control in B, some islets of the Hh-expressing pancreas are completely encircled by fibrosis (red arrowheads), which is typical finding in chronic pancreatitis of human. The number of ductular structure further increased (black arrows). Occasionally, acute pancreatitis-like changes are noted, showing the infiltration of inflammatory cells and cystic space filled with mucinous material (asterisks). (E) The exocrine pancreas of 9 month-old zebrafish shows more accumulation of fibrosis and ductular structures (black arrows). At center image, a large pancreatic duct (asterisk) is seen, being surrounded by fibrosis and ductular structures. If not specified, microscopic images are 400X.Bars, 50 μm.

The fibrotic changes were typically observed in the pancreas between the liver and gut, where the exocrine pancreas surrounded the principal islet. Interestingly, this corresponded to the area where the transgene expression was most robust. A prominent fibrotic area revealed a discernable whitish plaque in the entire dissected viscera and corresponded with the spot showing strong GFP expression (Fig. 5A). On ISH for Hh molecules which are co-expressed with GFP, transgene expression was strictly restricted to pancreatic acinar cells (Fig.5B) which express a transcription factor Ptf1a over a lifetime. In the non-fibrotic area, however, the acinar and cellular morphology were well-preserved, suggesting acinar destruction was secondary to the accumulation of fibrotic change.

Proliferating myofibroblasts were invariably positive for α-SMA (Fig. 5D). The majority of the activated myofibroblasts seemed to come from the gut wall as the fibrotic strands were outstretching from the gut wall, forming an adhesion between the bowel and pancreas (Fig.4B). α-SMA's reactivity was also noted in the muscle layer of the gut and pancreatic duct in control. Fibrotic bands found to be positive for α-SMA stain, also formed a contiguous strand from the gut wall (Fig.5D), suggesting recruitment and activation of myofibroblasts from the muscle layers of the gut. Myofibroblasts in the pancreatic ductal wall were also activated and proliferated as the muscle layers thickened and expressed α-SMA (Fig.5D). Occasionally, α-SMA-reactive cells were observed within the control pancreas, suggesting the presence of putative pancreatic stellate cells in the zebrafish pancreas (Fig.5D). The source of proliferating myofibroblasts along with the preferential change in fibrosis around the

principal islet suggested that Ihha or Shha recruited and activated any myofibroblasts in the vicinity of the pancreas where secreted Hh ligands could reach and mediate any effect.

Interestingly, proliferation of ductular structures was also noted at the age of three months, showing dense fibrotic bands intermingled with ductules (Fig.4B). Along with the progression of fibrosis, the ductular structures had also accumulated within the fibrotic area. To see whether these ductular structures were formed by proliferation or by mere entrapment of existing ductules, IHC for PCNA and pHH3 was performed. The majority of ductular cells were strong-reactive to PCNA and many of them also expressed pHH3 (Fig.5E, F), suggesting that the ductular structures were formed by enhanced proliferation.

The Hh signaling has been considered as a mediator of gastrointestinal tumorigenesis for many years, and Pdx1-Shh mice have shown metaplastic change and PanIn-like lesions [21]. However, the abnormal over-expression of Hh molecules did not cause pancreatic tumors in this study. . Those Hh-expressing transgenic zebrafish were further investigated for more than a year without finding any evidence of tumor foci or precancerous lesions.

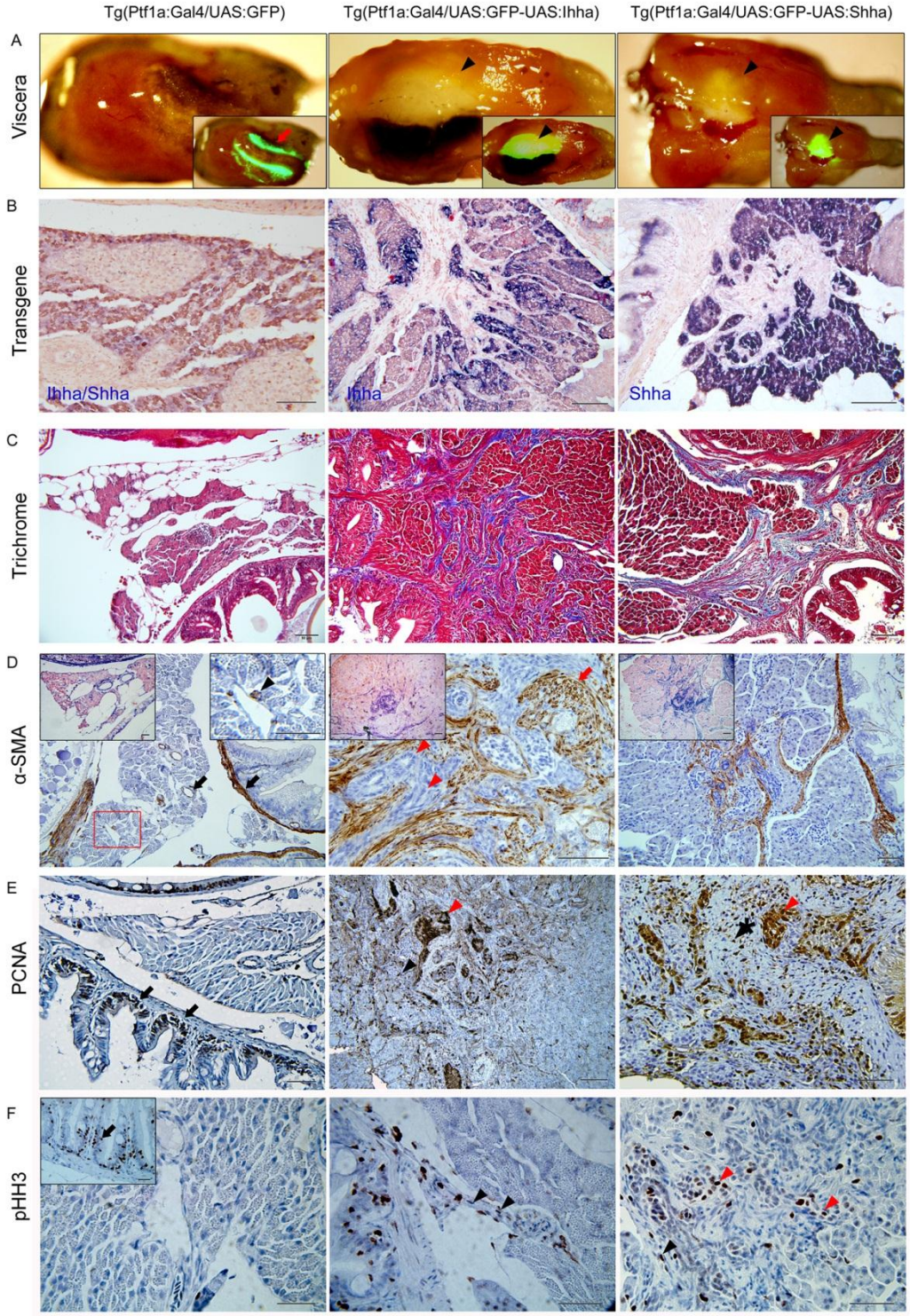
Tg(Ptf1a:Gal4/UAS:GFP)
Tg(Ptf1a:Gal4/UAS:GFP-UAS:Ihha)
Tg(Ptf1a:Gal4/UAS:GFP-UAS:Shha)
A
Viscera
B
Transgene
Ihha/Shha
Ihha
Shha
C
Trichrome
D
α-SMA
E
PCNA
F
pHH3

Figure 5. Hh-induced pancreatic fibrosis and proliferation of myofibroblasts. (A) Dissected whole viscera from 4 month-old zebrafish showing transgene (GFP) expression. Ventral views. Left, anterior. The pancreas of control appears as a thread-like structure between the bowel and visceral organs (arrow). In Hh ligand-expressing pancreas, prominent fibrosis around the principal islets forms whitish plaque-like lesions showing robust GFP expression (arrowheads). Inlets are merged in bright and fluorescence images. (B) ISH for transgene expression. The control pancreas reveals negligible expression of either Ihha or Shha. In the Hh-expressing pancreas, transgene expression is strictly restricted to acinar cells with nil expression at myofibroblasts or ductular cells. (C) Trichrome stains showing fibrotic bands. (D) IHC for α-SMA. Muscle layers of the bowel and large pancreatic ductal wall are reactive to α-SMA in control (black arrows). Infreqeuently, α-SMA-positive cells are noted (black arrowhead) in the parenchyme of control pancreas suggesting presence of stellate cells. Infilitrating myofibroblasts are invariably reactive to α-SMA while proliferating ductular cell are not (red arrowheads). Note the thickened and α-SMA-reactive intrapancreatic duct wall (red arrow). Left inlets (200X) are ISH images. Right inlet is an enlarged view of the box. (E, F) IHC for PCNA and pHH3. Within the fibrotic area, both ductular cells (red arrowheads) and myofibroblasts (black arrowheads) are frequently reactive to both PCNA and pHH3, suggesting enhanced proliferation. Intestinal crypt cells are also frequently reactive to both PCNA and pHH3 (black arrows) and used as internal control. If not specified, microscopic images are 400X. Bars, 50 μm.

3. Differential genes involved in Hedgehog signaling and fibrosis

In order to identify differentially expressed genes, GFP-expressing pancreases were dissected under a fluorescence microscope and pancreas samples were extracted from 4-5 of each transgenic zebrafish, which were processed for RT-PCR. Among the Hh components, real-time RT-PCR revealed up-regulation in most of the downstream components including Ptc1, Smo, Gli1, and Gli2a as well as transgenes compared to the control, which suggested the presence of cells with active Hh signaling (Fig. 6A,B). The signaling pathways relevant to fibrosis comprise a long list of genes and gene families. An exemplary list of genes that might have been modulated by aberrant expression of Hh ligands was seleted. Among the tested genes, RT-PCR revealed marked up-regulation of TGFß1aand MMP9, and mild to modest up-regulation of others, including membrane type 1 matrix metalloproteinase b (MT1MMPb), MMP2, interleukin1b (IL1b), TGFß2, and platelet derived growth factor Aa (PDGFAa) (Fig. 6A,B). A western blot hybridization was carried out using pooled samples from 4 month-old zebrafish with antibodies reactive to zebrafish antigen, which also recapitulated RT-PCR findings (Fig. 6C).

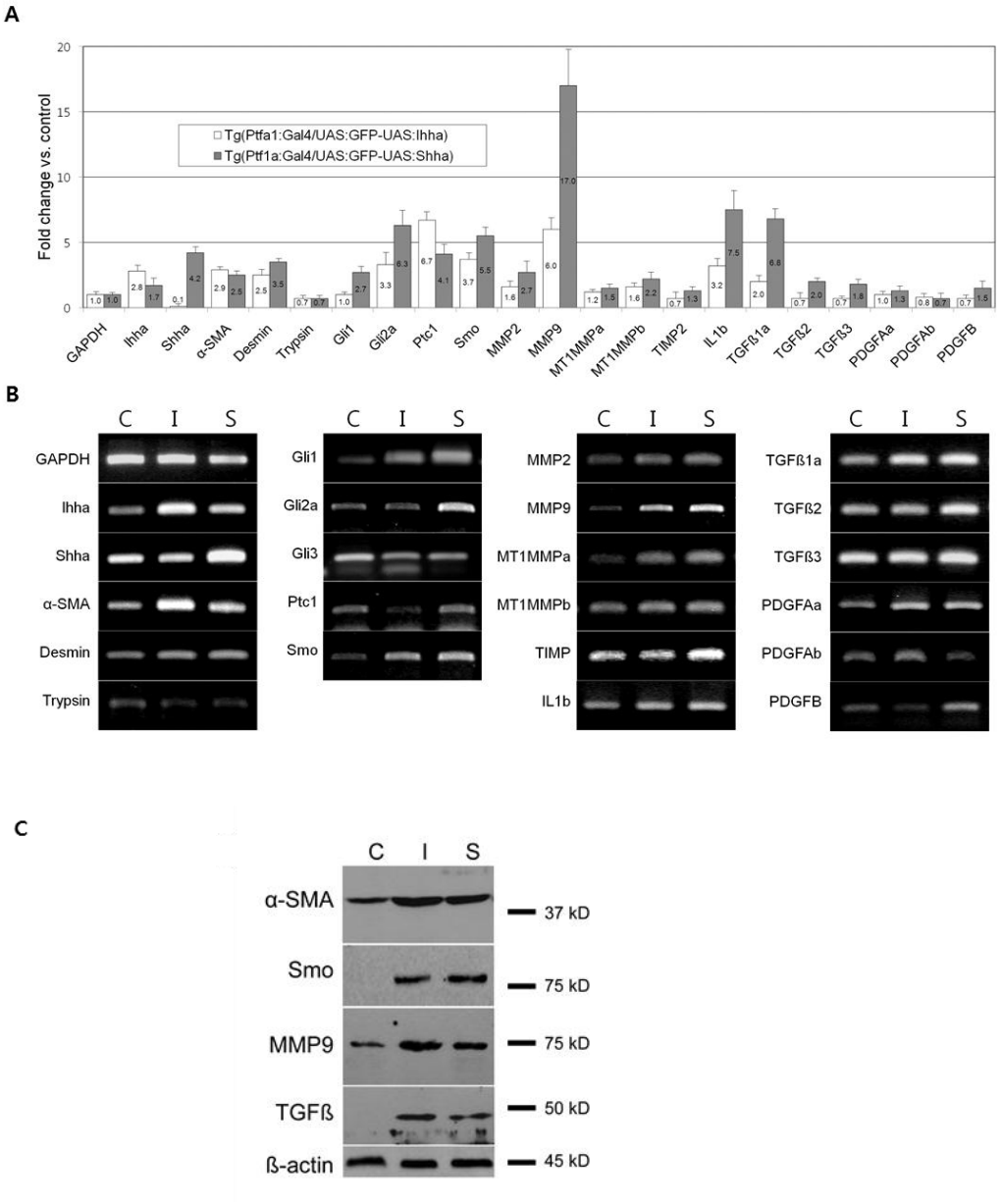

Figure 6. RT-PCR and Western blot. Pancreas from 3-4 month-old zebrafish was dissected under a fluorescence microscope. C, Tg(Ptf1a-Gal4/UAS:GFP); I, Tg(Ptf1a-Gal4/UAS:GFP-UAS:Ihha); S, Tg(Ptf1a-Gal4/UAS:GFP-UAS:Ihha). (A) Real-time RT-PCR showing differential expression of the components of the Hh pathway and fibrosis by Hh over-expression. Note the prominent up-regulation of MMP9 and

TGFß1a. (B) Electrophoretic images of RT-PCR products recapitulate real-time PCR data. (C) A western blot hybridization using available antibodies which are reactive to zebrafish antigens also recapitulates RT-PCR findings. α-SMA, 42 kD; Smo, 85 kD; MMP9, 75 kD; TGFß, 45 kD; ß-actin, 45 kD. * P<0.05 versus control.

Table 2. Primers used for RT-PCR.

Genes	Sense (5'-3')	Antisense (5'-3')	Product length (bp)
GAPDH	AAAGTCACCGCCATCAACGAC	CCTTAACCTCACCCTTGTACTT	173
Ihha	ATGCGTCTCCCCGTGGTGTT	TGGCTCCCAGTGTCTTCTCG	175
Shha	GCTTTTGACGAGAGTGCTGCT	TAAGGTCTTCTCCGCGACAT	163
α-SMA	GTGTGACGACGAAGAAAGCA	TTCTGCCCCATTCCTACCAT	153
Desmin	ACGAAATATTCAGCCTCCGC	GAGCTCTTGGTCACCTCGTA	152
Trypsin	GAAGGCTTTCATTCTTCTGGCTCTTT	GGTTGCTGATCAGAGAGCCA	171
Gli1	ATGCCAGTGGATATGCAGCC	GGCCATGGAGGGATTATACA	183
Gli2a	ATGGAGACCACAAGTCCCAC	CTTCCTTCATGATGCCGCAT	179

Ptc1	ATGGCCTCGGATCCCAGAGA	CCCACAGCTTTCCCCTTAGA	167
Smo	CAAGCGCCCCTGCTCCATTGTT	TGCGTGTACGGCAAAGGCGA	186
MMP2	GTTGAAGGACACGCTGAAGAAA	GGGTGTGCCCTAAGATTCTG	191
MMP9	ATGAGACTTGGAGTCCTGGC	TTAGCATTGGAGATGACCGC	209
MT1MMPa	ATGTTACCGAAACTGCAGACG	GATTTAGGAGAGCGAATCGC	173
MT1MMPb	ATGATCTGGAGCGGGTTTAC	CAGGCCGTAGAATCTCTGCA	201
TIMP2	TGAAGAGCGTCAGGAGCTGTA	GCTTGATCGGGTTCCCATAA	197
IL1b	CATGCGGGCAATATGAAGTC	CATTTTGTGCTGCGAAGTCC	170
TGFß1a	GTTGGTTTGCTTGGTGCTGA	ATCTTCTGTCCGTCGTCGTC	186
TGFß2	TGAACTTGTACGTCTTGAGCC	GATCTCAGGAGGACTGCTCA	167
TGFß3	AAAGGACTGCTGTTTGTTCTG	ATCCCTGGTGCTGTTGTAGA	216
PDGFAa	CGCTGATCCACTTTCTCGTC	CGTCCTCCAGCACTTCATTC	171

PDGFAb	ATGAGAACCTTATTCTGCTGC	ATGGTGCTTCTGCTTGACCT	207
PDGFB	GGACCCTCTTCCTCCATCTCT	GGCTTCTGGGAAGACGTTTG	164

4. Paracrine activation of responsive cells by Hedgehog ligands

Histologic expression of the Hh signaling components was assessed by either IHC or ISH, depending on the availability of an antibody that was cross-reactive to zebrafish antigen. Though Ptc1 theoretically counteracts the activation of Smo, the Hh ligand needs Ptc1 receptor to bind and initiate Hh signaling [27]. Ptc1 expression was restricted to proliferating myofibroblasts and ductular cells (Fig. 7A). The expression of Smo assessed by IHC was virtually identical to the Ptc1 expression (Fig. 7B). In control zebrafish, muscle layers of the bowel and pancreatic ducts also expressed both Ptc1 and Smo (Fig.7A, B), suggesting paracrine activation of these Ptc1/Smo-positive cells by secreted Hh molecules. Similarly to α-SMA, Smo-reactive cells were occasionally noted within the control pancreas (Fig.7B), which seemed to be the counterparts of pancreatic stellate cells. To further verify Hh signaling activation in responsive cells, the expression of Gli genes, the final mediator of Hh signaling by ISH, was evaluated. The expression of both Gli1 and Gli2a was again strictly restricted to myofibroblasts and ductular cells (Fig. 7C, D). Even though, there exists a non-canonical pathway leading to the Gli1 expression [28], the Gli2 expression represents actual activation of the canonical Hh pathway [29, 30]. None of the acinar cells were reactive to Gli1 or Gli2a. The expression of Hh components in both myofibroblasts and ductular cells suggest that these two cellular compartments are responsive to Hh ligands secreted from acinar cells, activated, and proliferated to form dense fibrotic area intermingled with ductular structures.

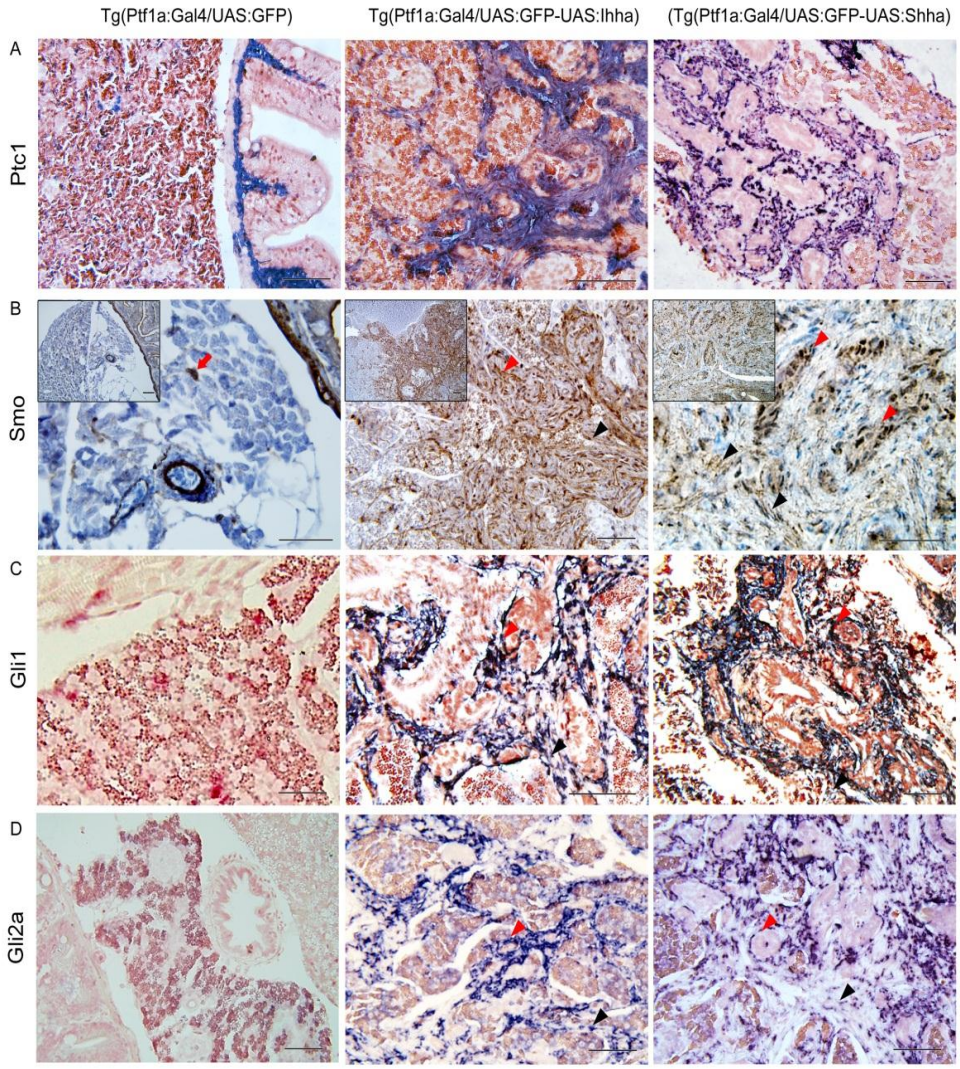

Figure 7. Expression of the downstream components of Hh signaling at 6 month-old zebrafish pancreas. (A) ISH for Ptc1. In control Ptc1 is expressed in the muscle layer of bowel and pancreatic duct. In the Hh-expressing pancreas, both proliferating myofibroblasts and ductular cells express Ptc1. (B) IHC for Smo reveals strong expression in a wide area of fibrosis. Both myofibroblasts and ductular cells are reactive to Smo. Likely to α-SMA immunostaining, Smo-reactive cells (red arrow) are

occasionally noted in the parenchyma of the control pancreas. Inlets are 200X images. (C, D) ISH for Gli1 and Gli2a. Whereas, the control pancreas reveals a negligible degree of Gli1 and Gli2a expression, activated myofibroblasts and ductular cells express Gli1 and Gli2a. (B-D)Black arrowheads, myofibroblasts; Red arrowheads, ductular cells. If not specified, microscopic images are 400X. Bars, 50 μm.

5. Hedgehog ligands induce MMPs and TGFß1 in Hedgehog-responsive cells

MMPs function in the regulation of the extracellular matrix (ECM) organization by degrading ECM gives way to cellular migration. Thus, induction of MMPs is necessary for the progression of fibrosis. RT-PCR showed that induction of MMP9 was the most striking among the MMP genes evaluated in this study. While MMP2 was modest, MT1MMPs were mildly elevated. An immunostaining analysis revealed that both Hh-responsive myofibroblasts and ductular cells strongly expressed MMP9 with nil expression in acinar cells, which suggests that activated Hh signaling was responsible for induction of MMP9 (Fig. 8A).

TGFß family members also play important roles in fibrosis as well as tumorigenesis. Crosstalk between Hh and TGFß signaling has been found, and both genes are often co-expressed in epithelial compartments [13, 31]. Contrary to the MMP9, TGFß1 expression was strictly restricted only to proliferating ductular cells which were also reactive to the pan-cytokeratin antibody (Fig. 8B). This finding gives an important clue as to how active Hh signaling is involved in pancreatic tumorigenesis. Although, TGFß1 induction might have contributed to the aggravation of desmoplasia, it was not primarily responsible for fibrosis because ductular proliferation was not prominent until three months, when pancreatic fibrosis was already found. Unlike MMP9 and TGFß1, the expression of PDGFAa and IL1b was restricted to myofibroblasts (Fig.8C, D).

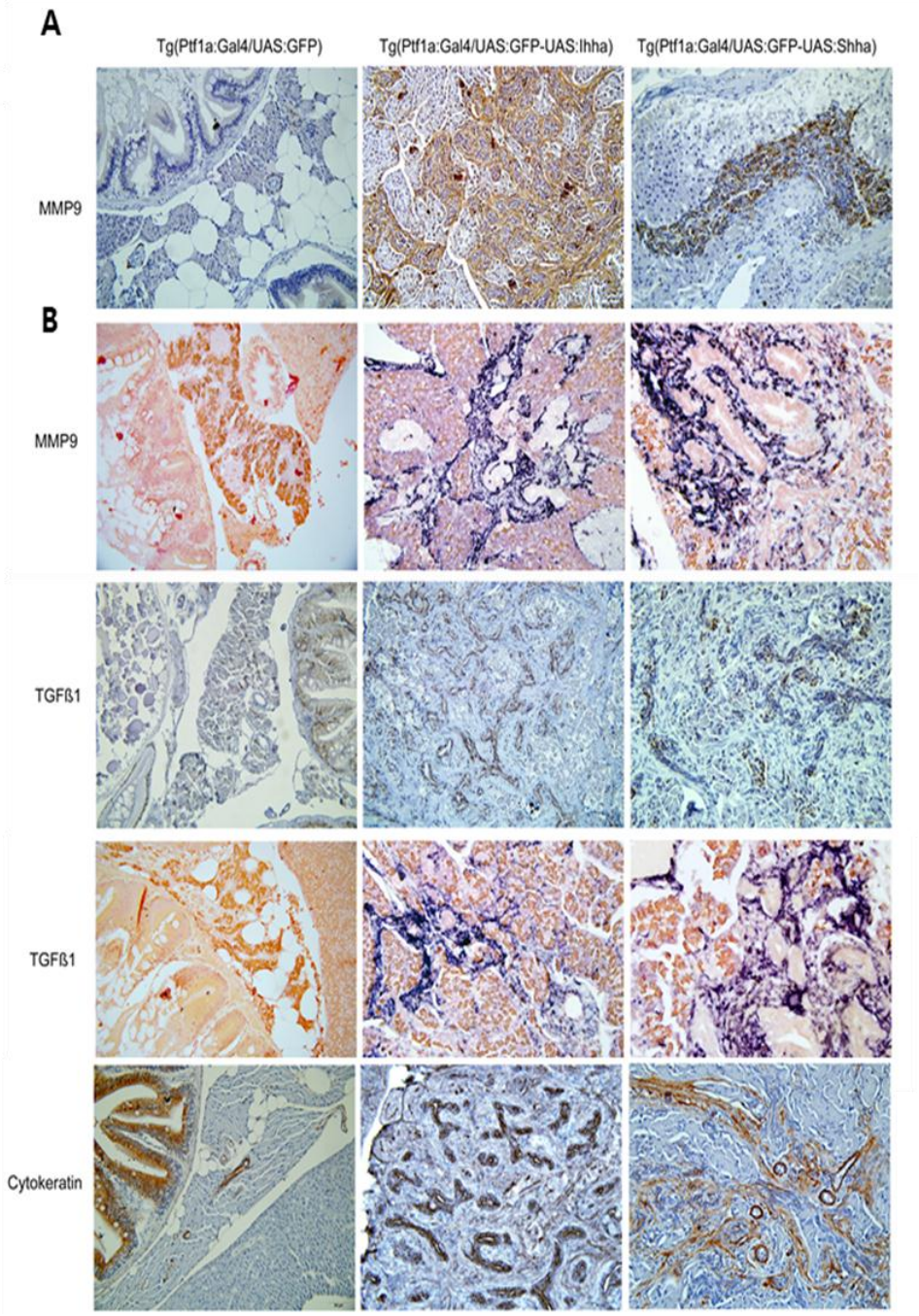
A
Tg(Ptf1a:Gal4/UAS:GFP)
Tg(Ptf1a:Gal4/UAS:GFP-UAS:Ihha)
Tg(Ptf1a:Gal4/UAS:GFP-UAS:Shha)
MMP9
B
MMP9
TGFß1
TGFß1
Cytokeratin

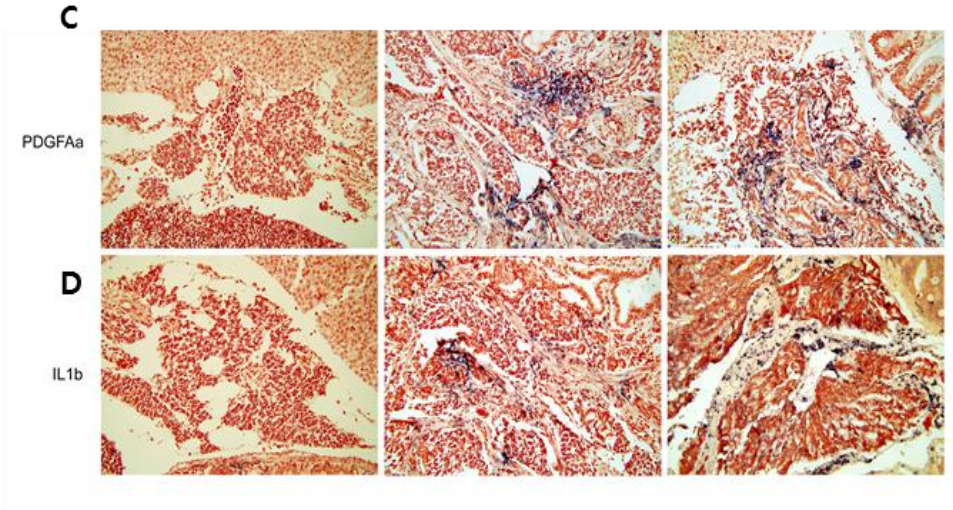

Figure 8. Expression of genes involved in fibrosis at 6 months. (A) IHC and ISH (inlets) showing MMP9 expression in proliferating myofibroblasts and ductular cells. (B) IHC for TGFß1. Contrary to MMP9, TGFß1 is expressed only in proliferating ductular cells which are also positive for cytokeratin. (C, D) ISH for PDGFAa and IL1b. Transcripts of both genes are detected in a small subset of proliferating myofibroblasts and ductular cells. (A-C, red arrowheads, ductular cells). Microscopic images are 400X. Bars, 50 μm.

Table 3. Primers used for TA cloning to generate riboprobes

Genes	Sense (5'-3')	Antisense (5'-3')	Product length (bp)
Trypsin	ATGAAGGCTTTCATTCTTCTG	TCATGGTGTTTCTGATCCAG	730
Elastase	ATGTTCGCCCTCATCCTAGC	TTAGTTGTTCATCATGACCT	813
CPA5a	ATGAAGAGGCTGCTGGTGCT	TTAATAAGGGTTATTCTTGG	1260
Ptf1a	ATGGACACTGTGTTGGATCC	TTAGGAAATGAAATTAAAGGG	798
GATA6	ATGTATCAGACCCTGGCCA	CCCACCAGTGTTGAAGAGT	1007
FoxA3	ATGTTGAGCTCCGTGAAGAT	CGACTTGAGGTCCATCTTCT	1176
Ihha	ATGCGTCTCCCCGTGGTGTT	TCATCTATCATTGTCCATCA	1242
Shha	ATGCGGCTTTTGACGAGAGT	TCAGCTTGAGTTTACTGACA	1257
αSMA	GTGTGACGACGAAGAAAGCA	CTTCATCATACTCCTGCT	1099
Gli1	AGTTCGTTTGCCACTGGAAG	ACGTTGCTCAAGCTGTTAAA	1492

Gli2a	GTTTCCCGAGTCCCAGACTG	CCAACTCCAGCAGAAGTACC	1447
Ptc1	TGAAGCCTGAAACTAAGACTGT	TCAGGAGAAGGACTTTGCAA	1363
MMP9	CTGCTCCATTGTTGGAAGCT	TTCTTTCCCACTCAGCTTGA	1367
IL1b	CATGCGGGCAATATGAAGTC	CTAGATGCGCACTTTATCCT	818
PDGFAa	CGCTGATCCACTTTCTCGTC	TCACCTTATATCTGCTGTGT	578

6. Phenotypic Reversal by Hedgehog Inhibitors

The zebrafish model has been spotlighted for its feasibility in *in vivo* screening of candidate drugs due to a lower cost and a higher efficiency than with mouse models. To investigate the feasibility of phenotypic reversal by Hh inhibitors, Tg(Ptf1a-Gal4/UAS:GFP-UAS:Ihha) and control embryos were treated with the maximal tolerable dose (MTD) of either cyclopamine (15uM, Smo inhibitor) or HPI-4 [32] (5uM, ciliogenesis inhibitor working at downstream of Smo). Hh expression during embryonic periods induced pancreatic morphologic changes. Instead of a well-formed posterior pancreas in control, the Hh-secreting pancreas revealed a relatively prominent head with a short, slender, and tortuous posteriorly-growing pancreas. Whereas the length ratio of the posterior pancreas and head was between 1.5 and 2.0 in control at 5 dpf, it was roughly 1.0 in the Hh-expressing pancreas, which was used as criterion for reversibility. The pancreatic phenotypes were effectively reversed by either HPI-4 or cyclopamine treatment when evaluated by fluorescence imaging (Fig. 9A, B).

Next, groups of 12-day old Tg(Ptf1a-Gal4/UAS:GFP-UAS:Ihha) larvae were treated with Hh inhibitors for an extended period of up to 6 weeks. On histologic observation, the maximal tolerable dose (5uM) of HPI-4effectively prevented pancreatic fibrosis but induced prominent fatty infiltration of the pancreas (Fig.9C), which might need further investigation to have a further understanding of the underlying mechanism. However, contrary to HPI-4, cyclopamine failed to inhibit pancreatic fibrosis. This failure was possibly resulted from a low dose, due to dose-

limiting toxicity (MTD: 500nm in juvenile fish) or from a different mechanism itself as the HPI-4 directly disturbs ciliogenesis leading to the disruption of Gli1/Gli2 activity.

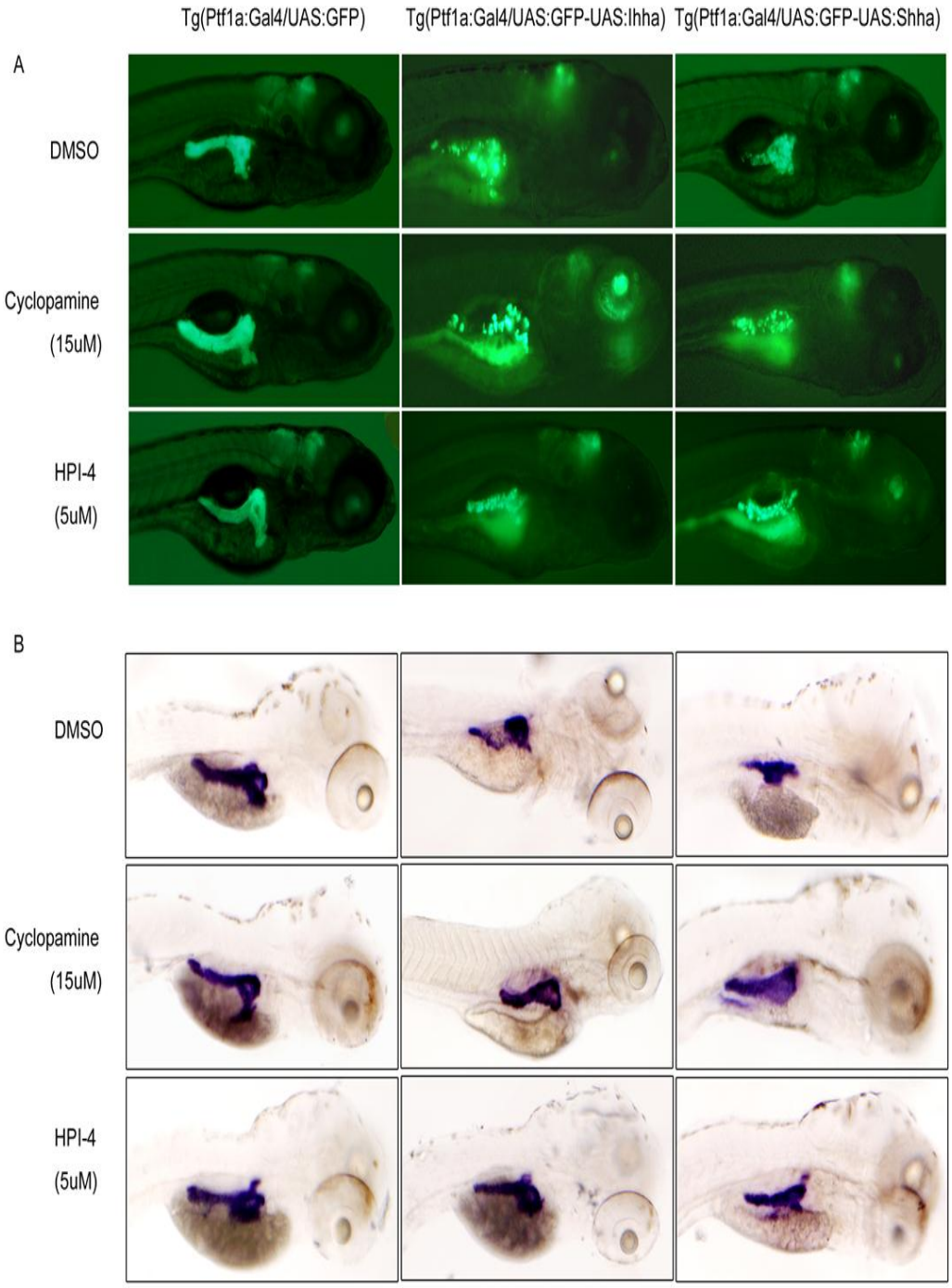
Tg(Ptf1a:Gal4/UAS:GFP)
Tg(Ptf1a:Gal4/UAS:GFP-UAS:Ihha)
Tg(Ptf1a:Gal4/UAS:GFP-UAS:Shha)
A
DMSO
Cyclopamine
(15uM)
HPI-4
(5uM)
B
DMSO
Cyclopamine
(15uM)
HPI-4
(5uM)

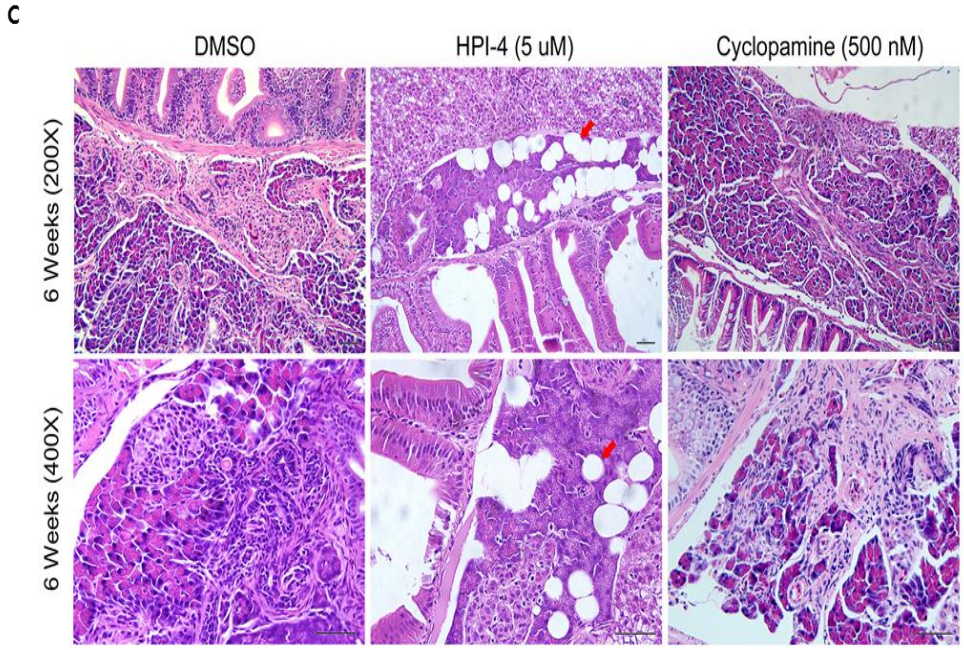

Figure 9. Phenotypic reversal by Hh inhibitors. (A) Reversal of pancreatic phenotypes in embryos. Embryos were treated with either HPI-4 or cyclopamine from 32 hpf until 5 dpf. Neither HPI-4 nor cyclopamine at the indicated concentrations impairs pancreatic development in controls. A well-formed pancreas in control produces a 1.5 to 2.0 times longer posterior pancreas compared to the head. Hh-expression induces a short and slender posterior pancreas showing the ratio between the body and head by approximately 1.0. By the criterion for reversal of the 1.5 times or longer posterior pancreas, the Hh-induced pancreatic phenotypes are effectively reversed by either HPI-4 or cyclopamine treatment. (B) Whole mount ISH for ptf1a 32and 5dpf.(C) Prevention of pancreatic fibrosis by a long-term treatment with Hh inhibitors. 12 day-old Ihha-expressing larvae were treated with Hh inhibitors for up to 6 weeks. In the HPI-4 treated group (12 out of 16 survived), there is no evidence of pancreatic fibrosis but a somewhat prominent fatty infiltration (red arrows). Contrary to HPI-4, cyclopamine failed to inhibit pancreatic fibrosis in the surviving 11 zebrafish out of 14. Bars, 50 μm.

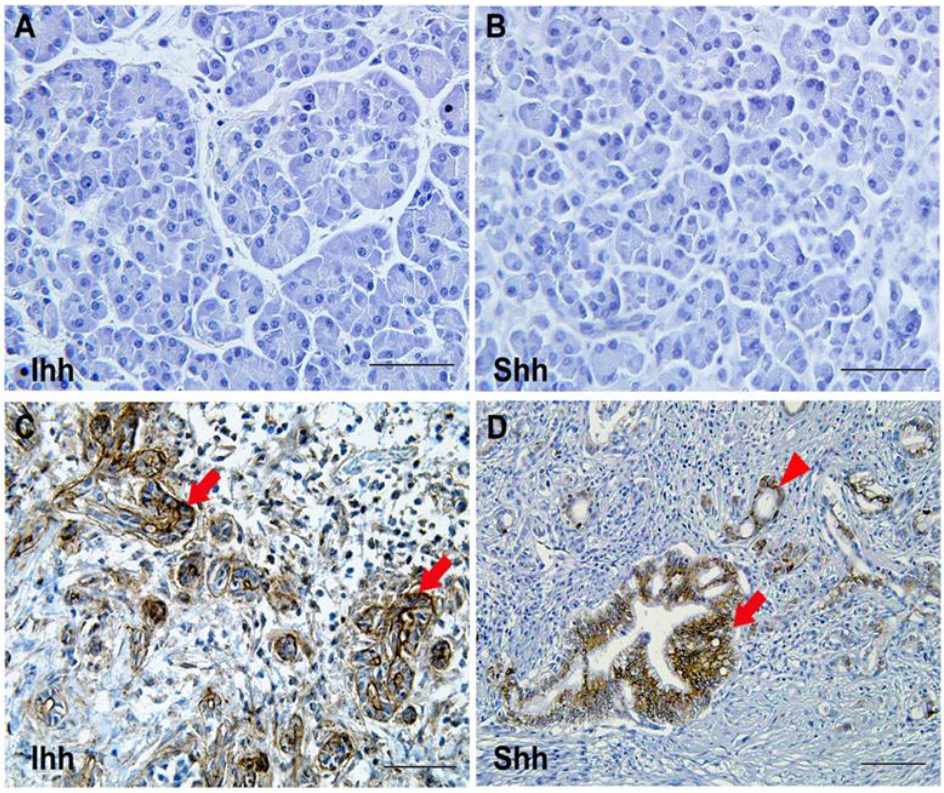

Figure 10. IHC for hedgehog ligands in human pancreas. (A, B) Immunostaining for Ihh and Shh in normal pancreas showing nil expression. (C) IHC for Ihh in chronic pancreatitis. Metaplastic ducts are strong positive for Ihh expression (arrows). (D) IHC for Shh in pancreatic cancer. Ductal cancer cells (arrow) and neighboring metaplastic ducts (arrowhead) are positive for Shh expression. Microscopic images are 400X. Bars, 50 μm.

5. Discussion

For the first time, current study presents a zebrafish model to study pancreatic fibrosis in which molecular events relevant to Hh-induced fibrosis can be explored. Zebrafish have recently been seen to simulate human disease in both molecular and histopathologic levels [18, 33]. In order to investigate the effect of Hh signaling in the pancreas, an experiment in which zebrafish orthologs of Hh ligands are over-expressed in the Ptf1a domain have been conducted. Along with a recent series of studies [10,15, 20,34], the result provides strong *in vivo* evidence that Hh signaling operates in a paracrine mode in the pancreas.

Among the three members of Hh ligands, Ihh and Shh expression is broader and strictly controlled in various organs, including the gastrointestinal system [5, 6, 35] Dhh expression is largely restricted to the gonads during the development [3, 36]. Thus subtypes of Ihh and Shh that are duplicated in zebrafish were chosen. Despite more prominent fibrosis by Shh expression, virtually identical phenotypes support functional redundancy between Ihh and Shh.

The canonical Hh pathway involves ligands, receptors, intracellular mediators, and transcription factors. In the present study, aberrant expression of Ihha and Shha molecules in the exocrine pancreas caused progressive fibrosis by paracrine action. This leads to the destruction of acinar structures which mimics desmoplasia occurring in human chronic pancreatitis and pancreatic cancer. Although the paracrine action of Hh signaling during embryonic development has been well-documented [14, 37], there

have been debates on whether it works through a cell autonomous or non-autonomous mechanism, or both in pathologic conditions. *In vitro* studies have provided evidence of the autocrine activation of Hh signaling in keratinocytes, medulloblastoma, and renal cell carcinoma cells [17, 38, 39]. This is, however, not the case in the gastrointestinal tract and the pancreas, where Hh seems to work in an exclusively paracrine manner. Moreover, a similar mode of action has been demonstrated in fibrosis of the lungs and liver [11, 13,40]. Other studies have also demonstrated that Hh molecules directly enhanced migration and proliferation of fibroblasts in those organs [10, 41]. The study provides *in vivo* evidence that secreted Hh ligands cause pancreatic fibrosis by paracrine activation of responsive cells. The embryonic phenotypes in current models are not dramatic, they simply show morphologic changes of the exocrine pancreas. The development of the endocrine pancreas as well as other endodermal organs including the liver and the intestine were not affected by Hh over-expression. The exocrine markers such as trypsin, elastase, and CPA are properly and timely expressed in acinar cells. These findings strongly support the fact that Hh-expressing acinar cells are not influenced by this signaling but undergo proper differentiation. Although it is not clear whether the mode of action is dependent on cell type, the result suggests that a paracrine mechanism is highly involved in the pancreas.

Chronic pancreatitis and pancreatic cancer represent human diseases that are accompanied by progressive pancreatic fibrosis. In both conditions, Hh ligands are considerably over-expressed in metaplastic ductal and cancer cells and play central roles in (Fig. 10) [7, 8, 19]. Pancreatic stellate cells residing in the vicinity of the acini

are the main source of proliferating fibroblasts in human disease. In the current models, the majority of the proliferating myofibroblasts in the pancreas seem to originate from the muscle layer of the bowel in the vicinity of the pancreas. Muscle layers of the large pancreatic ductal wall are a second source of proliferating myofibroblasts, as evidenced by thickened muscle layers which are immuno-reactive to α-SMA and Smo. The putative pancreatic stellate cells identified in the control pancreas by immuno-staining can be the third source of Hh-responsive cells. Therefore, it seems that Hh ligands indiscriminately recruit and activate myofibroblasts within the vicinity of Hh-secreting acinar cells. The pro-migratory effects of Hh signaling in multiple cell types have been well-documented, including neuronal and vascular endothelial cells as well as myofibroblasts [42-45]. The activation of Hh signaling is concentration dependent, and secreted ligands are effective up to 300um, which is the maximal distance they can reach by an unclear mechanism of molecular movement [46]. The close proximity between the pancreas and bowel in zebrafish allows secreted Hh molecules to reach and attract myofibroblasts from the gut wall. It is not clear if this phenomenon also occurs in the human pancreas, in which the distance between the pancreas and gut is much longer. It was also demonstrated that Hh-responsive myofibroblasts and ductular cells invariably express downstream components of Hh signaling. However, none of the acinar cells expressed these genes at either the mRNA or protein level. It is unclear as to how the Hh signaling exerts paracrine action in the pancreas, so it is crucial to determine responsiveness to secreted Hh molecules. In the current study, Hh-responsive myofibroblasts invariable expressed Ptc1 and Smo even in control,

suggesting that expression of Ptc1 or Smo, or both determines Hh-responsiveness. Considering that Hh signaling is initiated by ligand-binding to the Ptc receptor, expression of the Ptc gene is mandatory for the initiation of Hh signaling. A recent observation has implicated that over-expression of Smo in pancreatic cancer-associated fibroblasts is a potential determinant for Hh-responsiveness [20]. It would be interesting to see whether forced co-expression of either Ptc1 or Smo, along with Hh ligands, might induce Hh responsiveness in acinar cells.

This study suggests that the aberrant expression of Hh molecules does not induce tumors. The study have followed the transgenic zebrafish for more than one year without observing any evidence of tumor foci or PanIn-like lesions; as opposite to Pdx1-Shh mice that developed metaplastic duct and PanIn-like lesions with over-expressed Ptc1 and Smo [19]. The discrepancy may be attributed to the difference in the regulatory element driving Hh expression or to the biologic difference between teleosts and mammals. Otherwise, the metaplastic duct and PanIn-like lesions in Pdx1-Shh mice may actually be the counterparts of proliferating ductular structures found in our models.

TGFß1 and MMPs as important mediators of Hh signaling have been identified. Recent observations have demonstrated that Hh signaling accelerates pancreatic tumorigenesis through tumor-stromal interaction by providing favorable conditions for tumor cells [21, 34]. The induction of TGFß1and MMPs expression in ductular cells gives an important hint as to how Hh signaling provides a favorable environment for tumor-stromal interaction during pancreatic tumorigenesis. Also, it provides theoretical

background evidence that inhibition of Hh signaling is beneficial for the treatment of pancreatic cancer. In fact, recent observation has suggested that inhibition of Hh signaling can provide additional benefits to anti-tumor effects of conventional chemotherapy [47, 48]. A cross-sectional study has strictly demonstrated co-expression of TGFß1 and Hh molecules in epithelial compartments [13], and crosstalk between Shh and TGFß pathway has also been documented *in vivo* during embryonic development [49]. *In vitro* studies have shown that TGFß cooperates with canonical Hh signaling to activate Gli proteins and Hh target gene expression [50, 51], and exogenous Shh induces TGFß secretion in gastric cancer cells [52]. Therefore, the emergence of TGFß1-expressing ductular cells in current models harbors important implications. Though requisites for Hh-responsiveness need to be investigated, epithelial cells are indeed capable of responding to Hh ligands. Moreover, TGFß1 may be one of the targets that are induced by Gli-mediated transcriptional regulation, which may aggravate pre-existing conditions such as chronic pancreatitis and pancreatic cancer. The TGFß1 expression, however, is not primarily responsible for pancreatic fibrosis because fibrotic change was evident even at the first month when TGFß1-secreting ductular proliferation was not observed.

Similarly, MMPs play roles by remodeling the extracellular environment, which is an important step in the progression of fibrosis as well as tumorigenesis. In this study, Hh-responsive cells demonstrated the striking up-regulation of MMP9 with modest elevation of MMP2 and MT1-MMPs.This factor is consistent with *in vitro* observations that have demonstrated either exogenous Hh molecules or ectopic

expression of Gli1 or Hh molecules induced MT1-MMP and MMP9 in cultured cells [53, 54]. MMPs induced by Hh signaling remodel the extracellular matrix and promote migration of activated Hh-responsive cells, which accelerates the fibrotic process. The *in vivo* environment enables exploration of epiphenomena manifested by the complex interaction of different types of cells. Thus, reflection of what really happens in the context of the physiologic and pathologic conditions is more than an *in vitro* study can provide.

While chronic pancreatitis accompanies the infiltration of inflammatory cells, the pancreatic pathology in these Hh-expressing zebrafish lacks an inflammatory reaction. Considering that the eventual pancreatic dysfunction in human chronic pancreatitis results from long-standing fibrotic change, acinar destruction and prevention of fibrosis is one of the main therapeutic targets. As a model, the zebrafish uniquely allows *in vivo* screening for small molecules, in which the effect of given drugs as well as toxicity can be simultaneously monitored under physiologic conditions. A visible short-term phenotype can facilitate high-throughput screening of candidate drugs. Although this model could not thoroughly explain how the morphologies of a developing pancreas were changed by Hh expression, the study could observe phenotypic reversal by treatment with Hh inhibitors. The study also demonstrated that pancreatic fibrosis and destruction were effectively prevented by the treatment of HPI-4, a ciliogenesis inhibitor, but not with cyclopamine. Although failure by cyclopamine may be attributed to the dose limitation such as the high toxicity in the larval stage, this finding implies that targeting downstream of Smo may be beneficial for obtaining a therapeutic effect.

Though the mechanism for differential sensitivity between embryos and larvae was unclear at the time, the acquisition of a toxicity profile in a physiologic context is an additional benefit of using the zebrafish as a model for drug screening. This study provides *in vivo* evidence that inhibition of Hh signaling is a viable option for the prevention of pancreatic fibrosis which has a detrimental effect on chronic pancreatitis and pancreatic cancer.

In conclusion, aberrant expression of either Ihha or Shha causes progressive pancreatic fibrosis through paracrine activation of Hh-responsive cells. This study identified TGFß and MMPs as important genes induced by Hh signaling in responsive cells. These transgenic models will be a valuable platform in exploring the mechanism of fibrogenic pancreatic diseases caused by Hh signaling activation.

6. References-

1. Berman DM, Karhadkar SS, Maitra A (2003) Widespread requirement for hedgehog ligand stimulation in growth of digestive tract tumours. Nature 425:846-851.
2. Hooper JE, Scott MP (2005) Communicating with hedgehogs. Nature Rev Mol Cell Biol 6:306-317.
3. Bitgood MJ, Shen L, McMahon AP (2005) Sertoli cell signaling by Desert hedgehog regulates the male germline. Curr Biol 6:298–304.
4. Wijgerde M, Ooms M, Hoogerbrugge JW, Grootegoed JA (2005) Hedgehog signaling in mouse ovary: Indian hedgehog and desert hedgehog from granulosa cells induce target gene expression in developing theca cells. Endocrinology 146:3558–3566.
5. Madison BB, Braunstein K, Kuizon E, Portman K, Qiao XT, et al (2005) Epithelial hedgehog signals pattern the intestinal crypt-villus axis. Development 132:279–289.
6. Brink GR (2007) Hedgehog signaling in development and homeostasis of the gastrointestinal tract. Physiol Rev 87:1343–1375.
7. Kayed H, Kleeff J, KelegS,Büchler MW, FriessH (2003) Distribution of Indian hedgehog and its receptors patched and smoothened in human chronic pancreatitis. J Endocrinol 178:467–478.
8. Kayed H, Kleeff J, Keleg S, Guo J, Ketterer K, et al (2004) Indian hedgehog signaling pathway: Expression and regulation in pancreatic cancer. Int J Cancer 110:668–676.
9. Prasad NB, Biankin AV, Fukushima N, Maitra A, Dhara S, et al (2005) Gene expression profiles in pancreatic intraepithelial neoplasia reflect the effects of hedgehog signaling on pancreatic ductal epithelial cells. Cancer Res 65:1619-1626.
10. Shinozaki S, Ohnishi H, Hama K, Kita H, Yamamoto H, et al (2008) Indian

hedgehog promotes the migration of rat activated pancreatic stellate cells by increasing membrane type-1 matrix metalloproteinase on the plasma membrane. J Cell Physiol 216:38-46.

11. Lin N, Tang Z, Deng M, Zhong Y, Lin J, et al (2008) Hedgehog-mediated paracrine interaction between hepatic stellate cells and marrow-derived mesenchymal stem cells. Biochem Biophy Res Comm 372:260-265.
12. Omenetti A, Porrello A, Jung Y, Yang L, Popov Y, et al (2008) Hedgehog signaling regulates epithelial-mesenchymal transition during biliary fibrosis in rodents and humans. J Clin Invest 118:3331–3342.
13. Stewart GA, Hoyne GF, Ahmad SA, Jarman E, Wallace WAH, et al (2003) Expression of the developmental Sonic hedgehog (Shh) signaling pathway is up-regulated in chronic lung fibrosis and the Shh receptor patched 1 is present in circulating T lymphocytes. J Pathol 199:488-495.
14. Kolterud Å, Grosse AS, Zacharias WJ, Walton KD, Kretovich KE, et al (2009) Paracrine hedgehog signaling in stomach and intestine: New roles for hedgehog in gastrointestinal patterning. Gastroenterology 137:618-628.
15. Bailey JM, Swanson BJ, Hamada T, Eggers JP, Singh PK, et al (2008) Sonic hedgehog promotes desmoplasia in pancreatic cancer. Clin Cancer Res 14:5995-6004.
16. Wicking C, Smyth I, Bale A (1999) The hedgehog signaling pathway in tumorigenesis and development. Oncogene 18:7844-7851.
17. Berman DM, Karhadkar SS, Hallahan AR, Prichard JI, Eberhart CG, et al (2002) Medulloblastoma growth inhibition by hedgehog pathway blockade. Science 297:1559–1561.
18. Park SW, Davison JM, Rhee J, Hruban RH, Maitra A, et al (2008) Oncogenic Kras induces progenitor cell expansion and malignant transformation in zebrafish exocrine pancreas. Gastroenterology 124:2080-2090.
19. Thayer SP, de Magliano MP, Heiser PW, Nielsen CM, Roberts DJ, et al (2003) Hedgehog is an early and late mediator of pancreatic cancer tumorigenesis. Nature 425:851-856.

20. Walter K, Omura N, Hong SM, Griffith M, Vincent A, et al (2010) Overexpression of smoothened activates the sonic hedgehog signaling pathway in pancreatic cancer-associated fibroblasts. Clin Cancer Res 16:1781-1789.
21. Yauch RL, Gould SE, Scales SJ, Tang T, Tian H, et al (2008) A paracrine requirement for hedgehog signaling in cancer. Nature 455:406–410.
22. Hao LT, Burghes AHM, Beattie CE. (2011) Generation and Characterization of a genetic zebrafish model of SMA carrying the human SMN2 gene. Mol Neurodegener 6:24.
23. Davison J, Park SW, Rhee JM, Leach SD (2008) Characterization of Kras-Mediated Pancreatic Tumorigenesis in Zebrafish. Methods Enzymol 438:391-417.
24. Pisharath H, Parsons MJ (2009) Nitroreductase-mediated cell ablation in transgenic zebrafish embryos. Methods Mol Biol 546:133-143.
25. Ober EA, Field HA, Stainier DYR (2003) From endoderm formation to liver and pancreas development in zebrafish. Mech Dev 120:5–18.
26. Cheng PY, Lin CC, Wu CS, Lu YF, Lin CY, Chung CC, et al (2008) Zebrafish*cdx1b* regulates expression of downstream factors of Nodal signaling during early endoderm formation. Development 135:941-952.
27. Jiang J, Hui CC (2008) Hedgehog signaling in development and cancer. Develop Cell 15:801-812.
28. Nolan-Stevaux O, Lau J, Truitt ML, Chu GC, Hebrok M, et al (2009) Gli1 is regulated through Smoothened-independent mechanisms in neoplastic pancreatic ducts and mediated PDAC cell survival and transformation. Genes & Dev 23: 24-36.
29. Du SJ, Dienhart M (2000) Gli2 mediation of hedgehog signals in slow muscle induction in zebrafish. Differentiation 67:84-91.
30. Lipinski RJ, Gipp JJ, Zhang J, Doles JD, Bushman W (2006) Unique and complimentary activities of the Gli transcription factors in Hedgehog signaling. Exp Cell Res 312:1925-1938.

31. Mimeault M, Batra SK (2010)Frequent Deregulations in the Hedgehog Signaling Network and Cross-Talks with the Epidermal Growth Factor Receptor Pathway Involved in Cancer Progression and Targeted Therapies. Pharmacol Rev 62:497-524.
32. Hyman JM, Firestone AJ, Heine VM, Zhao Y, Ocasio CA, et al (2009) Small-molecule inhibitors reveal multiple strategies for hedgehog pathway blockade. Proc Natl Acad Sci USA 106:14132-14137.
33. Haramis APG, Hurlstone A, van der Velden Y, Begthel H, van den Born M, et al (2006) Adenomatous polyposis coli-deficient zebrafish are susceptible to digestive tract neoplasia. Embo Rep7:444-449.
34. Tian H, Callahan CA, DuPree KJ, Darbonne WC, Ahn CP, et al (2009) Hedgehog signaling is restricted to the stromal compartment during pancreatic carcinogenesis. Proc Natl Acad Sci USA 106:4254-4259.
35. Dyer MA, Farrington SM, Mohn D, Munday JR, Baron MH, et al (2001) Indian hedgehog activates hematopoiesis and vasculogenesis and can respecify prospective neuroectodermal cell fate in the mouse embryo. Development 128:1717–1730.
36. Yao HH, Whoriskey W, Capel B (2002) Desert Hedgehog/Patched 1 signaling specifies fetal Leydig cell fate in testis organogenesis. Genes & Dev16:1433–1440.
37. Ingham PW, McMahon AP (2001) Hedgehog signaling in animal development: paradigms and principles. Genes & Dev15:3059-3087.
38. Bigelow RLH, Jen EY, Delehedde M, Chari NS, McDonnell TJ (2005) Sonic hedgehog induces epidermal growth factor dependent matrix infiltration in HaCaT Keratinocytes. J Invest Dermatol 124:457-465.
39. Dormoy V, Danilin S, Lindner V, Thomas L, Rothhut S, et al (2009) The sonic hedgehog signaling pathway is reactivated in human renal cell carcinoma and plays orchestral role in tumor growth. Mol Cancer 8:123-138.
40. Sicklick JK, Li YX, Choi SS, Qi Y, Chen W, et al (2005) Role for hedgehog signaling in hepatic stellate cell activation and viability. Lab Invest 85:1368-

1380.

41. Yang L, Wang Y, Mao H, Fleig S, Omenetti A, et al (2008) Sonic hedgehog is an autocrine viability factor for myofibroblastic hepatic stellate cells. J Hepatol 48:98-106.
42. Deshpande G, Swanhart L, Chiang P, Schedl P (2001) Hedgehog signaling in germ cell migration. Cell 106:759-769.
43. Gering M, Patient R (2005) Hedgehog signaling is required for adult blood stem cell formation in zebrafish embryos. Dev Cell 8:389-400.
44. Kolpak A, Zhang J, Bao ZZ (2005) Sonic hedgehog has a dual effect on the growth of retinal ganglion axons depending on its concentration. J Neurosci 25:3432-3441.
45. Asai J, Takenaka H, Kusano KF, Masaaki I, Luedemann C, et al (2006) Topical sonic hedgehog gene therapy accelerates wound healing in diabetes by enhancing endothelial progenitor cell-mediated microvascular remodeling. Circulation 113:2413–2424.
46. Zhu AJ, Scott MP (2004) Incredible journey: How do development signals travel through tissue? Genes & Dev 18:2985-2997.
47. Mueller MT, Hermann PC, Witthauer J, Rubio-Viqueira B, Leicht SF, et al (2009) Combined targeted treatment to eliminate tumorigenic cancer stem cells in human pancreatic cancer. Gastroenterology 139:1102-1113.
48. Oliver KP, Jacobetz MA, Davidson CJ, Gopinathan A, Mclntyre D, et al (2009). Inhibition of Hedgehog signaling enhances delivery of chemotherapy in a mouse model of pancreatic cancer. Science 324:1457-1461.
49. Li M, Li C, Liu Y, Hu L, Borok Z, et al (2008) Mesodermal deletion of transforming growth factor ß- receptor II disrupts lung epithelial morphogenesis. J Biol Chem 283:36257-36264.
50. Karhadkar SS, Bova GS, Abdallah N, Dhara S, Gardner D, et al (2004) Hedgehog signaling in prostate regeneration, neoplasia and metastasis. Nature 431:707-12.
51. Dennler S, Andre´ J, Alexaki I, Li A, Magnaldo T, et al (2007)Induction of

sonic hedgehog mediators by transforming growth factor-beta: Smad3-dependent activation of Gli2 and Gli1 expression *in vitro* and *in vivo*. Cancer Res 67:6981–6986.

52. Yoo YA, Kang MY, Kim JS, Oh SC, et al (2008)Sonic hedgehog signaling promotes motility and invasiveness of gastric cancer cells through TGFß-mediated activation of the ALK-Smad3 pathway. Carcinogenesis 29:480-490.
53. Nagai S, Nakamura M, Yanai K, Wada J, Akiyoshi T, et al (2008) Gli1 contributes to the invasiveness of pancreatic cancer through matrix metalloproteinase-9 activation. Cancer Sci 99:1377-1384.
54. Liao X, Siu MK, Au CW, Wong ES, Chan HY, et al (2009)Aberrant activation of hedgehog signaling pathway in ovarian cancers: effect on prognosis, cell invasion and differentiation. Carcinogenesis 30:131-140.

Liver - specific expression using LFABP regulatory element

Chapter 2

Interleukin-6 mediated chronic inflammation induces hepatocellular carcinoma in transgenic zebrafish

1. Abstract

Chronic inflammation is an important process leading to carcinogenesis. Therefore targeting and controlling inflammation can be a promising cancer therapy. Inflammation is often caused by a variety of inflammatory cytokines. Interleukin-6 (IL-6), a pleiotrophic cytokine, is not only involved in the regulation of regenerative process, but also in immune and inflammatory responses in various carcinogenesis including liver cancer. Yet, the nature of its involvement in tumorigenesis is still unclear. Although animal models have been widely used to elucidate the nature of IL-6's involvement in hepatic tumorigenesis, to date, no animal model revealing direct consequence of the inflammatory IL-6 expression and hepatic tumorigenesis have been suggested. In this study, an *in vivo* hepatic tumorigenesis model using transgenic zebrafish was generated to demonstrate IL-6 driven tumorigenesis. Transgene expression under the regulation of LFABP promoter driving hIL6 gene was found starting from embryonic day 4 and persisted until adulthood. Interestingly, the aberrant hIL6 gene expression, specifically expressed in the zebrafish liver, caused a chronic inflammation accompanying infiltration of inflammatory cells of myeloid and B cell lineage. The inflammation induced cell damage and compensatory proliferation. This eventually resulted in the generation of precancerous dysplastic lesions including clear cell foci, large cell changes, and eosinophilic and also basophilic bodies. Hepatocellular carcinoma developed in a subset of the transgenics was finally observed.

Molecular analyses revealed up-regulation of majority of the components involved in the IL-6 driven pathway during inflammatory process as evidenced by quantitative RT-PCR and Western blot, supporting that the aberrant high level of IL-6 production in the liver causes hepatic tumorigenesis. Among the downstream pathway from IL-6, while PI3K/Akt pathway activation was confined to inflammatory cells, activation of Jak/Stat3 pathway was noted in inflammed hepatocytes as well as in cells at dysplatic foci, suggesting Jak/Stat3 pathway played dominant role in the hepatic tumorigenesis. *Conclusion:* As far as we know, the current transgenic zebrafish most closely mimic hepatic carcinogenesis in human induced by chronic B or C viral infection at both cellular and molecular level. We provide a straightforward evidence of relationship between chronic inflammation and tumorigenesis, and reinforces the pivotal role of IL-6 in inflammation-associated hepatocellular carcinoma.

Key words: Transgenic zebrafish, Interleukin-6, Inflammation, Dysplastic foci, Hepatocellular carcinoma

2. Introduction

The liver is the largest internal organ and plays a major role in systemic metabolism in human. The organ must not only be able to produce biochemicals necessary for digestions, it must also be able to protect against damage by ingested agents, drugs. Hepatic immune system functions to identify, detoxify, and neutralize pathogens and failure of this immune system can cause chronic inflammation which leads to hepatic carcinogenesis. It is well known that the immune-mediated liver

damage is played by apoptotic death pathway, whereas acute liver damage caused from a variety of drugs and poisons is occurred by oxidative damage of the hepatic cells.[1-2]

IL-6 is a highly versatile cytokine which was originally characterized as a regulator that stimulates the final maturation of B cell. [17] This cytokine is also known to promote hepatic survival by stimulating liver regeneration. [3-5] IL-6 is closely related to NF-κB which increases the IL-6 secretion following hepatectomy. Upon binding of the IL-6 to its receptor, Janus Kinase (JAK) is activated and in turn the kinase activates the MAPK and STAT3 pathways, blocking and reducing apoptotic cascade and oxidative injury, respectively. [6, 7, 13] This results in promoting hepatic regeneration by a rapid transition from quiescence into cell cycle of hepatocytes. Thus, IL-6 plays a crucial role in regulating the regeneration of hepatocytes after hepatectomy, functioning as a critical proregenerative factor and acute-phase inducer in the liver injury.

In contrast, however, growing evidences indicating that IL-6 levels are elevated in various cancer tumorigeneses associated with chronic inflammation have been reported in different cancer types. Inappropriately high level of IL-6 production has been detected in breast cancer mammospheres.[8] A non-small-cell lung adenocarcinoma has also provided additional evidence for the involvement of IL-6 in tumorigenesis.[9] These reports raise the question that elevating the cytokine level is implicated in tumorigenesis. In fact, a previous study showed that high IL-6 level rather inhibit liver regeneration by increasing expression of p21, the cyclin dependent kinase inhibitor

(CDKI), after hepatectomy in mice.[14] Taken together with the reports showing IL-6 as a proregenerative factor of hepatocytes, IL-6 contains both pro- and anti-mitogenic actions, suggesting that its signaling process might be regulated by a negative feedback loop. STAT3 is a transcription factor involved in inflammation and tumorigenesis. In response to IL-6, the transcription factor is translocated to nucleus and turns on strong negative feedback loops involving suppressor of cytokine signaling 3 (SOCS3), the major negative regulator of IL-6 dependent signaling.[24] This event that leads to STAT3 regulation in human HCC is not fully understood.

In the past decade, zebrafish has been used as an experimental model for human diseases, including human liver cancer.[10-12] It has been demonstrated that the zebrafish and human tumor have molecular and cellular conservation at various levels, indicating the potential of zebrafish for modeling human cancer. [15-16] In the present study, a novel transgenic zebrafish line was generated and validated to demonstrate a clear *in vivo* evidence that the hepatic expression of IL-6 induces chronic inflammation leading to hepatic tumorigenesis.

3. Materials and Methods

1. Transgene constructs and transgenesis.

All constructs used in our study were sequenced and verified using the appropriate primers listed in Table 1. For transgenesis, LFABP-Gal4 and UAS-hIL6 fish were

established and crossed for targeted expression of transgene in the liver by a binary expression system (Fig. 1A).[28-29] Using polymerase with a proofreading function (Invitrogen, Grand Island, NY), 2.8kb upstream of LFABP gene was PCR-amplified as referenced by a previous report.[19] The PCR product was then cloned into ApaI/NcoI site of pUAS-GFP-Kras-pA construct, replacing the pUAS region to give a construct of pLFABP-GFP-Kras-pA. Gal4VP16 sequence was also PCR-amplified by using F-Gal4-NcoI/R-Gal4-ClaI primer and inserted into NcoI/ClaI sites of pLFABP-GFP-Kras-pA to generate pLFABP-Gal4VP16-pA. Human interleukin-6 cDNA was purchased from Open Biosystems (Huntsville, AL). This cDNA was then cloned into mluI/nheI sites of the pUAS-GFPpA-Kras to give pUAS-IL6pA-Kras. To facilitate identification of transgenics, Cmcl2-GFP (for Cardiac expression of GFP) was PCR-amplified and cloned into the pUAS-IL6pA-Kras which gives the final construct, pUAS-hIL6-pA-Cmcl2-GFP-pA. pUAS-RFP was prepared by placing RFP sequence under the pUAS promoter.

Each injection mixture was prepared by reconstituting Tol2-transposase mRNA (20 ng/ul) and transgene construct (20 ng/ul) in Danieu's buffer mixed with 0.03% phenol red. UAS-RFP embryos at single-cell stage were transferred to a molded agarose dish and 4 pL of the injection mixture of pLFABP-Gal4VP16-pA was introduced by yolk injection using a MMPI-2 microinjector. F0 founder embryos showing RFP expression in the liver were selected under a fluorescence microscope (Olympus, Japan). The embryos were raised and bred to give a birth to F1 Tg (LFABP-Gal4) zebrafish. Injection mixture of pUAS-hIL6-pA-Cmcl2-GFP-pA was introduced into AB (wild

type) embryos and cardiac GFP was utilized as a biomarker for gene transmission. By crossing Tg (LFABP-Gal4 / UAS-RFP) and Tg (UAS-hIL6-CG), transgenic zebrafish expressing hIL6 in the liver was established. All transgenes were transmitted in normal Mendelian ratio.

2. Animal stocks and embryo care.

All zebrafish were raised in a standardized aquaria system (Genomic-Design Co., Daejeon, Korea) according to standard protocols at 28°C on a 14- to 10-hour light and dark cycle. Embryos to be processed for whole mount analyses were placed in an E3 media with 0.003% phenylthiourea at 24 hpf to inhibit pigmentation. This experiment strictly followed the Guidelines for the Welfare and Use of Animals in Cancer Research.

3. Histology, immunohistochemistry staining (IHC).

Histologic evaluation was performed using 4-μm sections of 4% paraformaldehyde-fixed, paraffin-embedded tissues. Hematoxylin and eosin (H&E) staining was performed according to standard protocols. [21] Gene expression analyses were carried out either by IHC if an antibody cross-reactive to zebrafish was available, or by ISH as previously described. [15, 21] The sections were deparaffinized and rehydrated, and were then subjected to antigen retrieval performed according to several recommended methods. The endogenous peroxidase activity was blocked using 0.3% hydrogen

peroxide. Primary antibodies were rabbit anti-IL6 (1:200), rabbit anti-Caspase 3 (1:100), mouse anti-proliferating cell nuclear antigen (PCNA) (1:2000), rabbit anti-JAK1 (1:200), from Abcam (Cambridge, MA), mouse anti-phospho-PI3K (1:100), goat anti-AFP (1:200), from Santa cruz Biotechnology, Inc. (Santa Cruz, CA), rabbit anti-phospho-Tuberin/TSC2 (1:200), rabbit anti-phospho-mTOR (1:200), rabbit anti-phospho-4EBP1 (1:200), rabbit anti-phospho-RS6K(1:200), rabbit anti-Stat3 (1:200), and rabbit anti-phospho-Stat3 (1:200), from Cell Signaling (Danvers, MA). The primary antibodies were applied and incubated for overnight at 4 °C. After washing, the HRP-conjugated secondary antibody was applied, and samples were further incubated for 60 min at room temperature. Finally, the sections were colored using REAL EnVision Detection System, Peroxidase/DAB+, Rabbit/Mouse Kit (DAKO**,** Hamburg, Germany). For observation, slides were counterstained with hematoxylin and mounted with Histomount (Zymed, San Francisco, CA).

4. In situ hybridization (ISH).

To generate a riboprobe for hIL6, cDNA was amplified by PCR (hIL-6 sense: 5'-ATAACGCGTACCATGAACTCCTTCTCCACAAGC-3', antisense; 5'-ATAGCTAGCCTACATTTGCCGAAGAGCCC-3 ') then cloned into pCRII vector (Invitrogen, Carlsbad, CA), a TA cloning vector. Plasmids were linearized and antisense riboprobe was generated by in vitro transcription using digoxigenin labelling mixture (Roche Diagnostics GmbH, Mannheim, Germany). Control sense probes were run in parallel for all experiments. Experiments were performed using either whole

embryos or 4um section slides. Specimens were fixed in 4% paraformaldehyde (PFA) on rotate for overnight at 4 °C, dehydrated in a graded methanol series and stored in 100% MeOH. Samples were reconstituted in PBS with 0.1% Tween20 (PBST) and treated with 5mg/ml Proteinase K for 20 min 20 min at room temperature. Rehydrated samples were prehybridized with 50% formamide, 5X SSC, 50ug/mL heparin, 9.2 mM citric acid, 0.1% Tween-20, and 500ug/mL Torula yeast RNA (Sigma, St. Louis, MO) for 3 h at 65℃ followed by overnight hybridization with DIG-labeled RNA. Post-hybridization washes were done at 68 °C at least 4 hours as follows 2 washes in 2×SSC 0.1% Tween-20 for 10 minutes, one wash in 2×SSC 0.1% Tween-20 for 10 minutes followed by two washes in 0.2×SSC 0.1% Tween-20 for 30 minutes. All washing solutions were pre-warmed to 65℃. Subsequently, specimens were rinsed twice with PBST. Tissue was incubated in Anti-DIG alkaline phosphatase antibody (Roche) in blocking overnight at 4 °C. Tissue was washed in PBST After extensive washing, samples are visualized by incubating with NBT/BCIP AP substrate solution (Roche Diagnostics GmbH) in 0.1 M Tris–HCl, pH 9.5, 0.1 M NaCl, 50 mM MgCl2, 0.1% Tween 20. Whole mount embryos were immersed in glycerol for better visualization. The sections were counterstained with neutral red and mounted with Histomount.

5. Imaging

An Olympus MVX10 was used for whole mount embryo imaging. Photographs from slide sections or live embryos were obtained using an Olympus BX51 or a confocal microscopy (Carl Zeiss 700, Germany).

6. RT-PCR

Real-time PCR was performed by using dissected liver tissue from **3**-month-old zebrafish. The co-expressed GFP enabled precise dissection of the tissue. For each group, samples were collected from 3-4 zebrafish and using TRIzol reagent® (Invitrogen, Carlsbad, CA). cDNA was synthesized using a Maxima First Strand cDNA Synthesis Kit for RT-qPCR (Thermo Scientific Fermentas, K1641, Glen Burnie, MD, USA). Quantitative real-time PCR was performed using Maxima SYBR Green/ROX qPCR Master Mix (Thermo Scientific Fermentas, K0222, Glen Burnie, MD, USA) and the 7300 Real Time PCR System (Applied Biosystems, Foster city, CA). Samples were triplicated and all experiments were repeated three times using individually prepared samples. Primer sequences for RT-RCR are shown in Table 2.

7. Western blotting

Whole cell extracts were prepared from liver of zebrafish as described previously [28] A 20 mg sample of whole cell extract was separated on an 10% SDS–polyacrylamide gel and transferred to PVDF (Polyvinylidene fluoride) membrane (Amersham, GE Health, Sweden) using semidry transfer (GenScript NJ, USA). Filters were stained for 10 minutes with Ponceau S, blocked for 1 h in 5% nonfat dry milk in phosphate-buffered saline (PBS) with 0.1% Tween 20, incubated over night at 4℃ with a primary antibody in blocking buffer, washed 4 times with PBST, and incubated for 1h with horseradish peroxidase-conjugated secondary antibody. Labeled proteins were detected by ECL reagents and Hyperfilm ECL (Amersham Biosciences).

8. Treatment with IL6 pathway inhibitors

To counteract active Il6 signaling in live zebrafish, BKM 120 (PI3K inhibitor sc-364437; Santa Cruz Biotechnology, Santa Cruz, CA). AZD 1480(JAK1 inhibitor sc-364735; Santa Cruz Biotechnology, Santa Cruz, CA) and Cucurbitacin I (Stat3 inhibitor sc-203010; Santa Cruz Biotechnology, Santa Cruz, CA)were used to block downstream signaling. To determine treatment doses, 8-weeks old embryos were treated with a serial escalation of each inhibitor for 7days. Of the Maximal tolerable doses (MTDs) that caused fatality no more than 25% were selected; which were 1uM, 10nM, and 10nM for BKM120 **(**BKM120 is a potent and cell permeable inhibitor of the PI 3-kinase family. Specifically inhibits p110α, p110β, p110γ and p110δ with IC_{50} of 52 nM, 166 nM, 262 nM and 116 nM, respectively) , AZD1480(AZD1480 is a novel ATP-competitive inhibitor of JAK1 (IC_{50} = 1.3 nM) and JAK2 (IC_{50} = 0.26 nM)), and Cucurbitacin I(HL-60: IC_{50} = 0.1 nM (human); U-937: IC_{50} = 0.3 nM (human); HT-1080: IC_{50} = 0.47 nM (human); HT-29: IC_{50} = 190 nM (human); Integrin αL: IC_{50} = 950 nM (human)) respectively. First, groups (20 per group) of 6–weeks old LFABP-Gal4/UAS-hIL6 juvenile fish were separately treated with the each inhibitor in 1L-water tanks up to 8 weeks then processed for histology.

9. Statistical analyses

Statistical analyses were performed using SPSS ver. 11 software. $P < 0.05$ was considered to be a statistically significant difference. All tests were performed with SPSS 10.1 software (SPSS Inc., Chicago, IL, USA).

4. Results

1. Sustained expression of hIL6 induces chronic inflammation in the liver.

Different transgenic zebrafish lines to demonstrate hIL6 driven tumorigenesis have been generated. In order to do this, independent transgenic lines of Tg (UAS-hIL6-CG) were established and crossed with Tg (LFABP-Gal4 / UAS-RFP). Binary expression by a Gal4-UAS system has allowed a faithful expression of the hIL6 gene in the zebrafish liver (Fig. 1A). RFP expression and ISH experiment confirmed that the transgene expression was apparently detected from 4 days post-fertilization (dpf) and persisted until adulthood, suggesting that the stable Tg lines, LFABP-Gal4 / UAS-RFP / UAS-hIL6-CG and LFABP-Gal4/UAS-RFP for experimental and control lines, respectively, were established (Fig. 1B). By selecting the transgenic lines under a fluorescence microscope, the heterozygote zebrafish were then maintained and used for all experiments. The result showed that a sustained expression of hIL6 specifically in the hepatocytes induced chronic inflammatory change of the liver (Fig. 2). Massive infiltration of inflammatory cells was noted at 1 month of age in hepatic sinusoids and intrahepatic vessels, which was ruthlessly appeared in all transgenic zebrafish expressing hIL6 gene in hepatocytes. The infiltrated inflammatory cells then caused destruction of normal hepatic architecture (Fig. 2).

Inflammatory changes of the liver induced cell damage and compensatory proliferation of hepatocytes, which resulted in increased reactivity to active caspase 3, PCNA immunostaining, and cyclinD (Fig. 3). Infiltrated inflammatory cells were identified by ISH for myeloid and B cell lineage. While control liver was scanty of

inflammatory cells, IL6 expression markedly increased myeloid and B cells in the liver (Fig3).

2. Hepatocellular tumorigenesis caused by hIL6 expression.

Dysplastic foci began to appear at 2 months of age. Various precancerous lesions were noted in the liver of hIL6-expressing transgenic zebrafish, including clear cell bodies, eosinophilic and also basophilic cell bodies (Fig. 4). A typical cytology of hepatocellular carcinoma such as eosinophilic granular cytoplasm, rounded nuclei and prominent nucleoli was often detected from the observation. Large cell changes and hyaline bodies which are also the characteristics of tumorigenesis were shown in the transgenic zebrafish liver. Furthermore, individual liver of the transgenic zebrafish frequently harbors multiple foci of dysplasia of different types, indicating that carcinogenic process was polygonally occurred from multiple areas. Further investigation of the transgenic zebrafish observed that dysplastic foci were occurred in all transgenic zebrafish at 3 months of age, revealing 100% penetrance. Among the dysplastic foci, clear cell bodies were the most common phenotype. Overt hepatocellular carcinoma began to appear at 6 months of age. Taken together, our histological observation revealed that the hIL6-expressing transgenic zebrafish has developed a hepatocellualr carcinoma. Immunohistochemical staining revealed markedly increased reactivity to PCNA in dysplatic area (Fig. 4k). Overt HCC cells were positive to αFP (Fig. 4l).

3. Up-regulation of inflammatory and carcinogenic pathway by the

chronic expression of hIL6.

Upon binding of IL6 to its receptor, pleiotropic effects are transduced through different intracellular signalings, which includes PI3K-Akt pathway, Jak/Stat3 pathway, and Ras-Raf-Mapk pathway. PI3K-Akt pathway is an intracellular signaling pathway important for carcinogenesis, contributing to cellular proliferation and survival.[29] Jak/Stat3 pathway is also known for tumor cell survival through the up-regulation of anti-apoptotic genes and function of Ras-Raf-Mapk pathway is to transduce signals for cell growth, division and differentiation.[30, 31] Thus, a list of genes that might be modulated by the aberrant expression of hIL6 in these pathways was selected and summarized into three categories, inflammation, survival, and proliferation for quantitative real-time PCR (qRT-PCR) (Primers are listed in Table 2). For this qRT-PCR experiment, whole livers collected from four zebrafishes of each group were used. The result indicated that chronic expression of hIL6 induced up-regulation of various components of the pathways (Fig. 5). The genes involved in inflammatory process such as c-Myc, Pim1, Socs1a, Socs2, Socs4, and Tgfb1a were especially noted to be increased by many folds. Among these, interestingly, c-Myc known as a regulator of cell growth showed over 20 fold increasing of its expression. The most prominent expression change was observed from Surv2, a member of Survivin family containing anti-apoptotic activity. Other genes involved in PI3K-Akt and Jak/Stat3 pathways were also up-regulated, suggesting that sustained expression of hIL6 has induced activation of inflammatory and carcinogenic pathway.

To further determine whether the molecular up-regulation is actually caused by the

chronic expression of hIL6, western blot analyses were done (Fig. 5C). The experiment was done using pooled samples of dissected livers from 3-month old transgenic zebrafish. As shown in the fugure 3C, the transgenic zebrafish contained high level of hIL6 expression while non-transgenic zebrafish did not show the protein expression. This is consistent with the RT-PCR result (Fig. 5). Antibody against pMAPK1, pPI3K, and pSTAT3 clearly detected the proteins that show up-regulation in the transgenic zebrafish. The result showed a consistency with the gene expression analyses, suggesting that hIL6 expression has actually activated all downstream signaling pathways in the zebrafish liver.

4. Histologic analyses by IHC and ISH revealed predominant activation of Jak/Stat3 pathway in the hepatocellular tumorigenesis.

Our molecular analysis revealed that IL6 action in conducting tumorigenesis involves up-regulation of downstream genes in inflammatory pathway. The inflammation associated tumorigenesis of the transgenic zebrafish liver might be resulted from Jak/Stat3 signaling. To find out this, immunohistochemical analysis and ISH were done (Fig. 6,7). In fact, antibody against caspase 3 showed a clear positive visualization in abundant hepatocytes of the transgenic zebrafish liver, suggesting that induced cell death occurs, whereas control did not show any positive sign (Fig. 3c and d). Strong reactivity of hepatocytes in dysplatic foci to PCNA suggested that the dysplastic foci were true neoplastic lesions. To delineate PI3K/Akt pathway,

immunostaining was performed for pPI3K, pAkt, pTuberin, and pRS6k. Among the dysplastic foci, only hepatocytes showing large cell change were reactive to pTuberin, pRS6k, and pAkt, while immunostaining against pPI3K in hepatocytes of the dysplastic foci were not reactive (Fig6). Interstingly immunoreactivity to pPI3K was noted in infiltrated inflammatory cells. These finding suggested that activation of PI3K/Akt signaling is not a crucial finding in IL6-induced hepatic carcinogenesis. On the contrary, immunoreactivity to pStat3 was robust in non-neoplastic inflamed hepatocytes, hepatocytes in dysplastic foci, and in hepatocellular carcinoma, suggesting activation of Jak/Stat3 pathway played an important role in IL6-induced carcinogenesis (Fig 7). Downstream genes induced by active Jak/Stat3 pathway were evaluated by ISH. As expected hepatocytes in inflammation and dysplactic foci revealed robust expression of those genes, suggesting actual activation of Jak/Stat3 pathway in IL6-expressing hepatocytes. Above findings suggest Jak/Stat3 is a crucial pathway leading to carcinogenesis in the current IL6-induced HCC model.

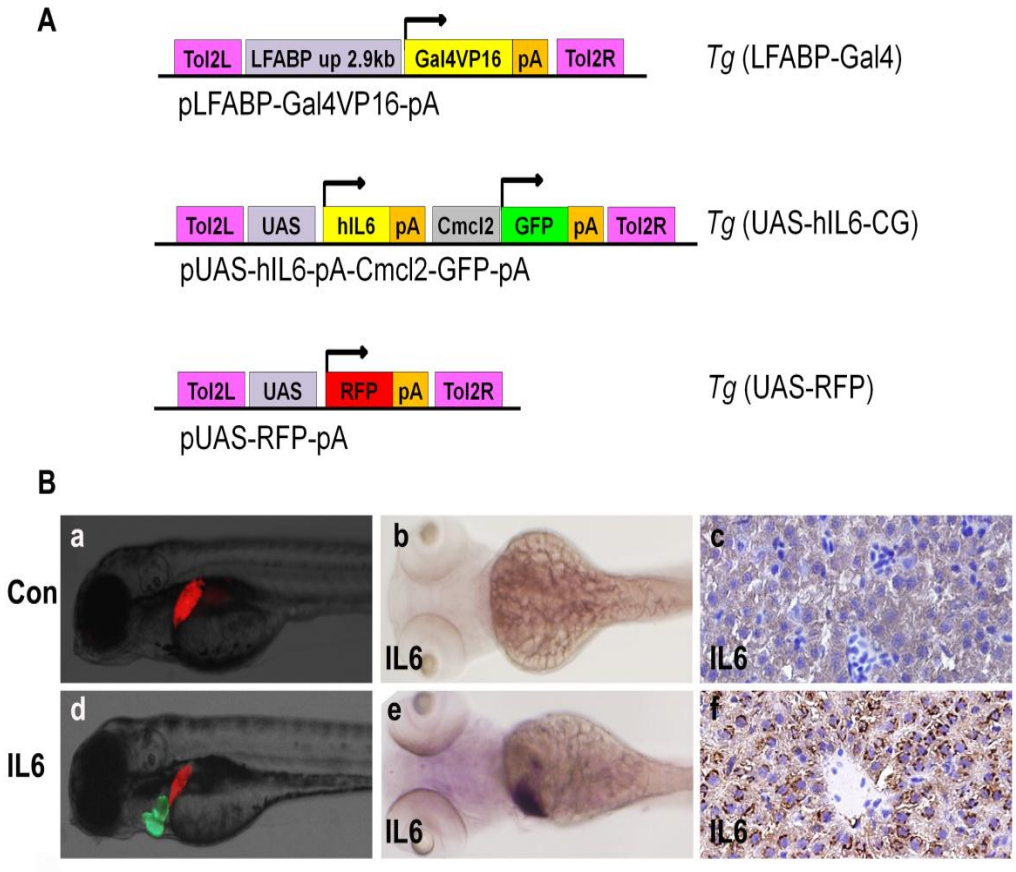

Fig 1. Transgenesis. A. Strategy of transgenesis. Transgenic constructs allowing Tol2-mediated transgenesis. Experimental line was maintained as Tg (LFABP-Gal4) / (UAS-RFP) / (UAS-hIL6) and control line as Tg (LFABP-Gal4) / (UAS-RFP). **B.** Transgene expression. a-c Tg(LFABP-Gal4/UAS-RFP) zebrafish. d-f. Tg(LFABP-Gal4) / (UAS-RFP) / (UAS-IL6-CG). Transgene expression is noted as red fluorescence in the liver and as green fluorescence in the heart. Cardiac GFP are to facilitate selection of transgenic embryos. b,e. ISH for IL6 in 4 dpf transgenic embryos showing strict RNA expression in the liver. c,f. IHC for IL6 in liver section from 2 month old zebrafish showing expression in hepatocytes. Microscopic images are 400X. Bars, 50 μm.

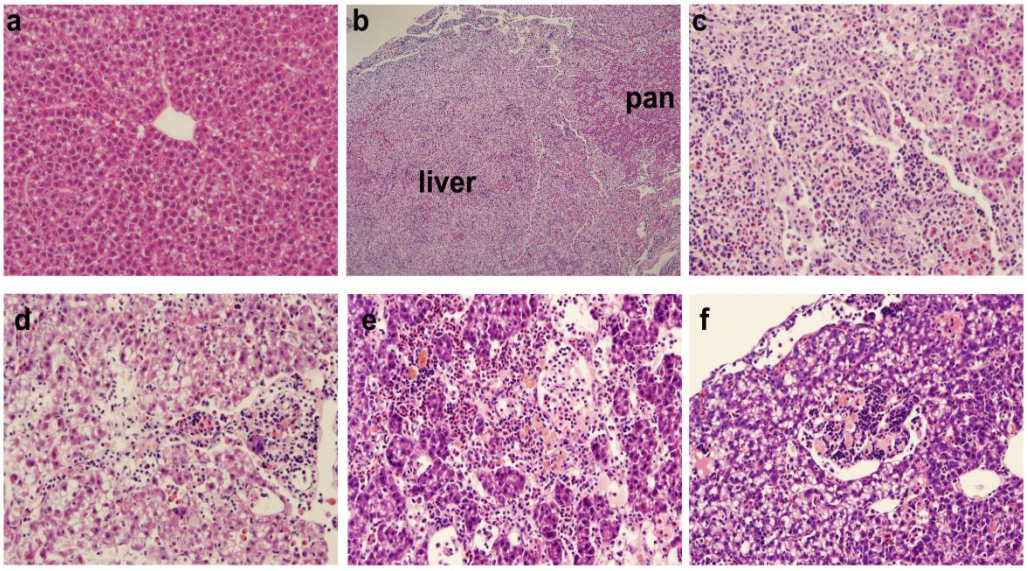

Fig 2. Liver inflammation by IL6 expression. a. Control. b-f. Tg(LFABP-Gal4/UAS-IL6) zebrafish. Variable degree of chronic inflammation of the liver is frankly evident at 1 month of age. b. Massive infiltration of inflammatory cells destructs liver architecture. e. Inflammatory cells in hepatic sinusoids. f. Inflammatory cells in the hepatic vasculature.

Table 1. Primers used for the generation of transgene contructs.

Primers	Sequence
F-LFABP-Apa1	5’-ACTAGGGCCCTCGATCTGCTGCAGTTCGAA-3’
R-LFABP-Nco1	5’-ATACCATGGGCTTTCTGGAGAAGCTCAAC-3’
F-Gal4VP16-Nco1	5’-ATACCATGGAGATGAAGCTACTGTCTTCTATCG-3’
R-Gal4VP16-Cla1	5’-ACTAATCGATCTACATATCCAGAGCGCCG-3’
F-hIL6-Mlu1	5’-ATAACGCGTACCATGAACTCCTTCTCCACAAGC-3’
R-hIL6-Nhe1	5’-ATAGCTAGCCTACATTTGCCGAAGAGCCC-3’
F-Cmcl2-Nde1	5’-GAATTCCATATGAAAGCTTAAATCAGTTGTGT -3’
F-EGFP-Xho1	5’-ATACTCGAGCTCAAGCTTATGGTGAGCAAGGGCGAGGAG-3’
R-EGFP- Cla1	5’-ACTAATCGATTTACTTGTACAGCTCGTCCAT-3’
F-RFP -Nco1	5’-ACTACCATGGCCTCTTTGCTGAAGAAGA -3’
R-RFP- Cla1	5’-CCATCGATTCAGTTGTGGCCCAGCTTGG-3’
F-UAS-Xho1	5’-ATACTCGAGCTCTGCTAACCATGTTCATG-3’
F-UAS-Seq	5’-TCAGCCTCACTTTGAGCTCC-3’

F-UAS-Seq was used for sequence verification of constructs. Underlined GCCACC sequence was inserted for Underlines, restriction enzyme sequences

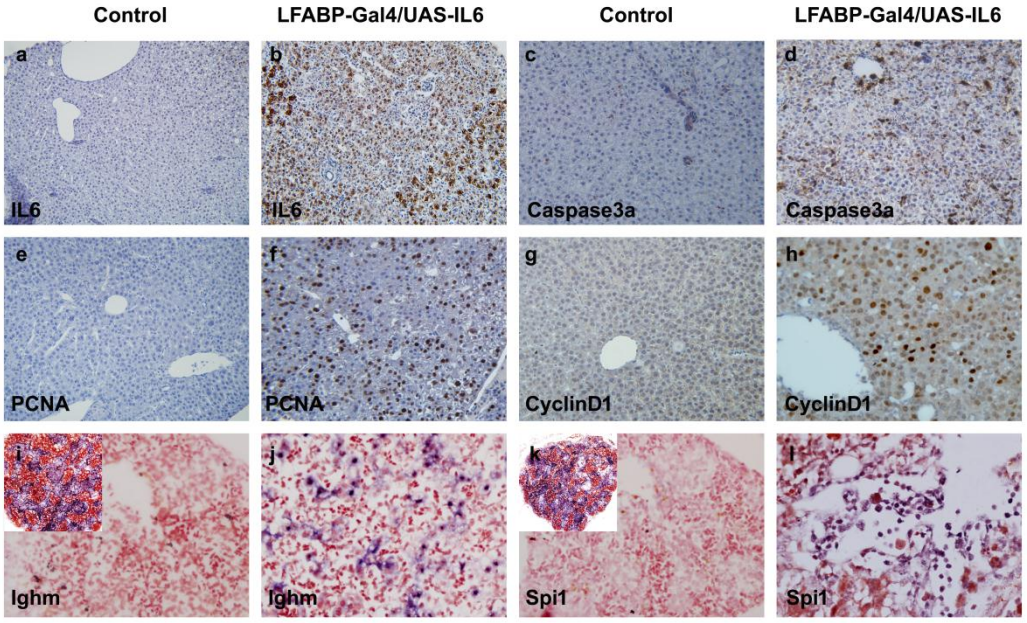

Fig 3. Chronic inflammation induced cell damage and proliferation. a,b. IHC for IL6. Inflammed hepatocytes are positive for IL6. c,d. IHC for caspase3a showing increased cells with positivity e,f. IHC for PCNA showing markedly increased positivity in IL6-expressing liver. g,h. Immunoreactivity to cyclinD1 was also markedly increased. i,j. ISH for Ighm, a B-cell marker, showing some infiltrated inflammatory cells positive for Ighm. k,l. ISH for Spi1, a myeloid marker, showing reactive cells. i,k. Inlet image is spleen as positive internal control. Microscopic images are 400X. Bars, 50 μm.

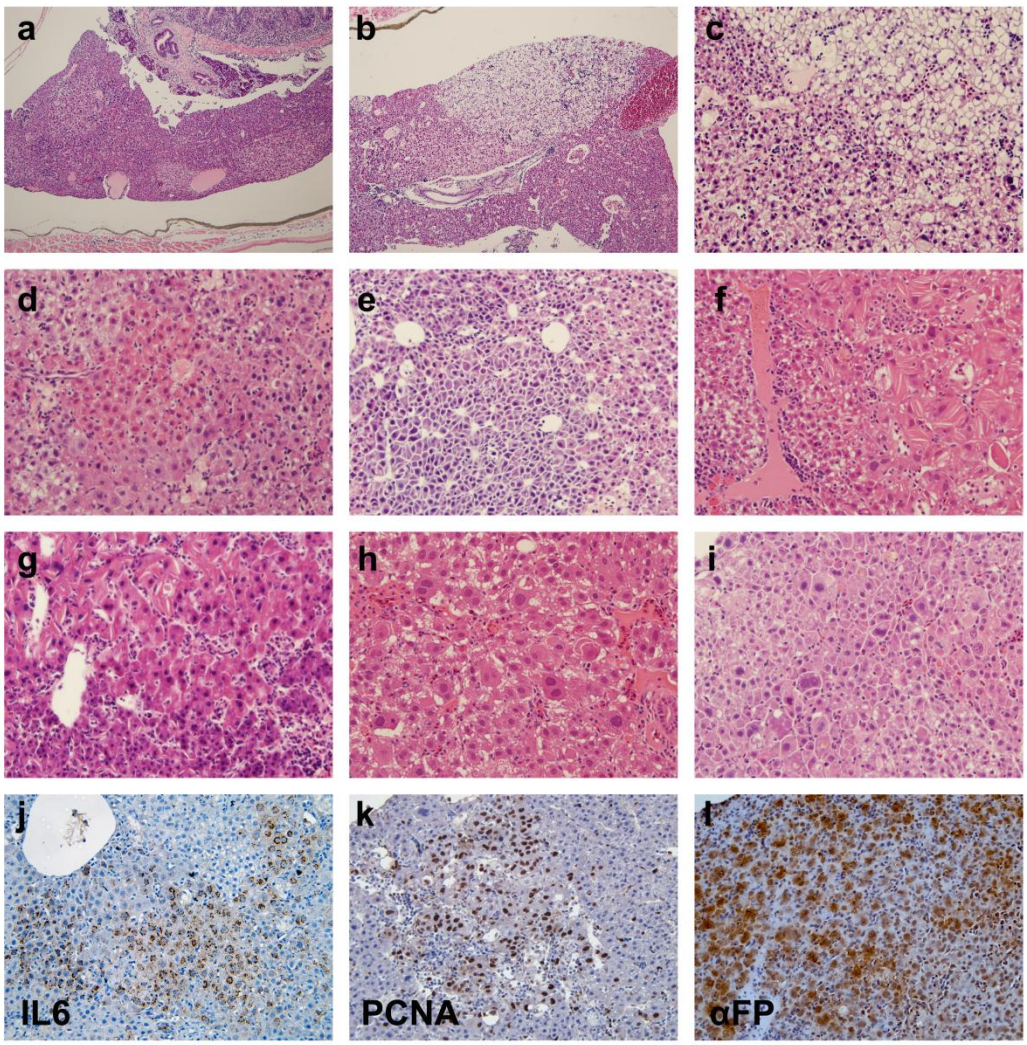

Fig 4. Histologic changes of the liver by interleukin 6 expression. a-i. H&E stain. a,b. Low power (100X) views showing multiple foci of dysplasia. c. High power (400X) view of a clear cell body. Hepatocytes adjacent to the clear cell body also show anaplasia. d. An eosinophilic cell body. e. A basophilic cell body. f. Hyaline-like body changes of hepatocytes suggesting altered cytoskeleton. g,h. Large cell changes of hepatocytes. i. Overt hepatocellular carcinoma showing severe cellular anaplasia and occasional mitosis. j. IHC for IL6. Dysplatic hepatocytes are positive for IL6. k. IHC for PCNA showing markedly increased positive cell at a dysplatic focus. l. Immunostaing for αFP in an area of HCC showing frequent positive cells. Microscopic images are 400X. Bars, 50 μm.

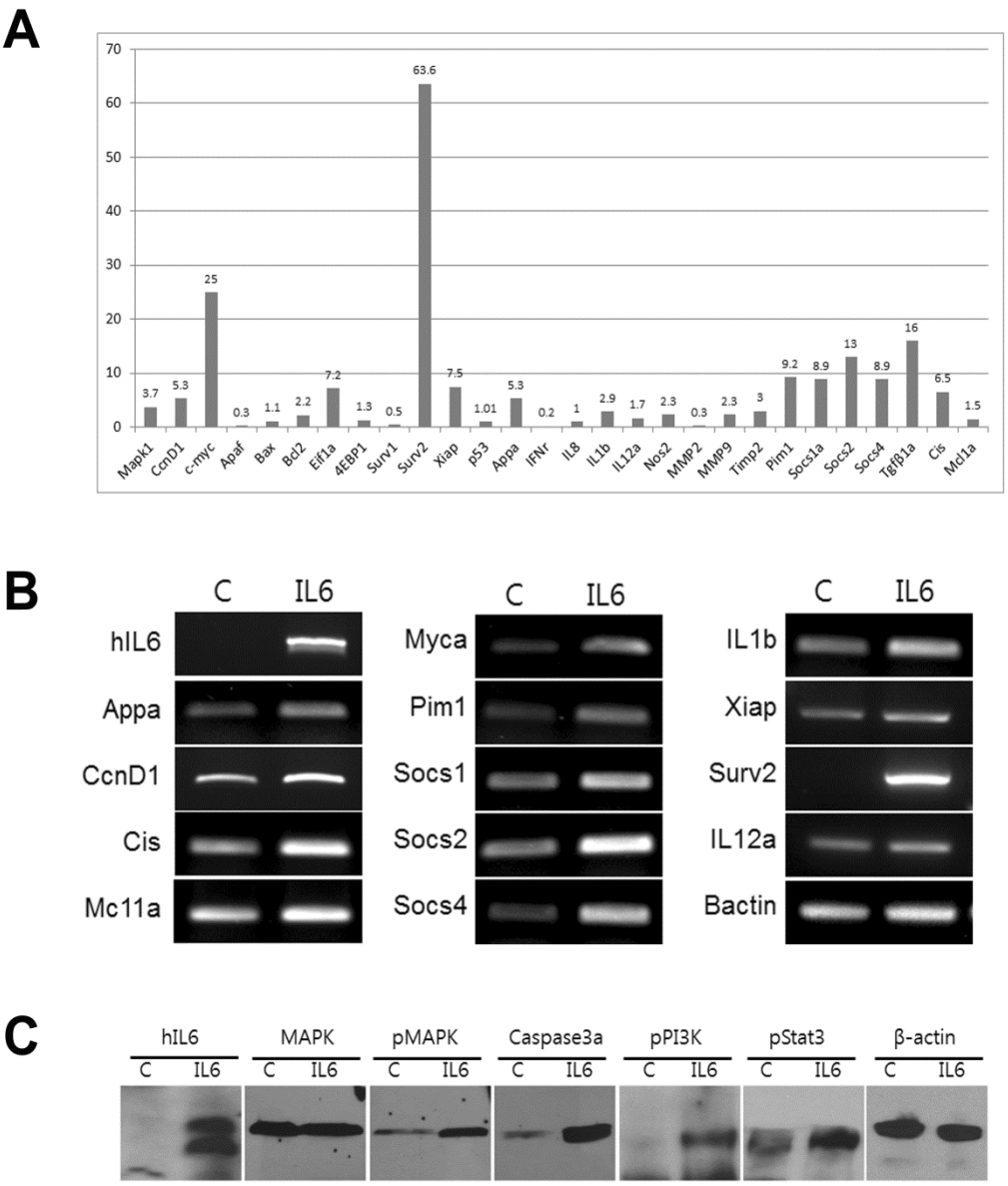

Fig 5. RT-PCR and Western blot. Samples were prepared from whole livers dissected under a fluorescence microscopy from 3-month old zebrafish. (A) Real-time RT-PCR showing differential expression of the components of the PI3K-Akt, Jak/Stat3 pathway, and Ras-Raf-Mapk pathway. Most genes induced by Jak/Stat3 pathway including Appa, c-Myc, Socs1a, Socs2, Socs2, Cis, Pim1 are up-regulated. Note the

prominent up-regulation of Myca and surv2. (B) Electrophoretic images of RT-PCR products recapitulate real-time PCR findings. (C) A western blot hybridization showing up-regulation of active phosphorylated downstream compoments. hIL6, 26 kD; MAPK1, 52 kD; p-MAPK1, 52 kD; p- PI3K, 85 kD; p-STAT3, 86 kD; Caspase3-A, 35 kD; ß-actin, 45 kD. C, Tg(LFABP-Gal4/UAS:RFP); IL6, Tg(LFABP-Gal4/UAS:Hil6-CG/UAS-RFP). (* $P<0.05$ versus control.

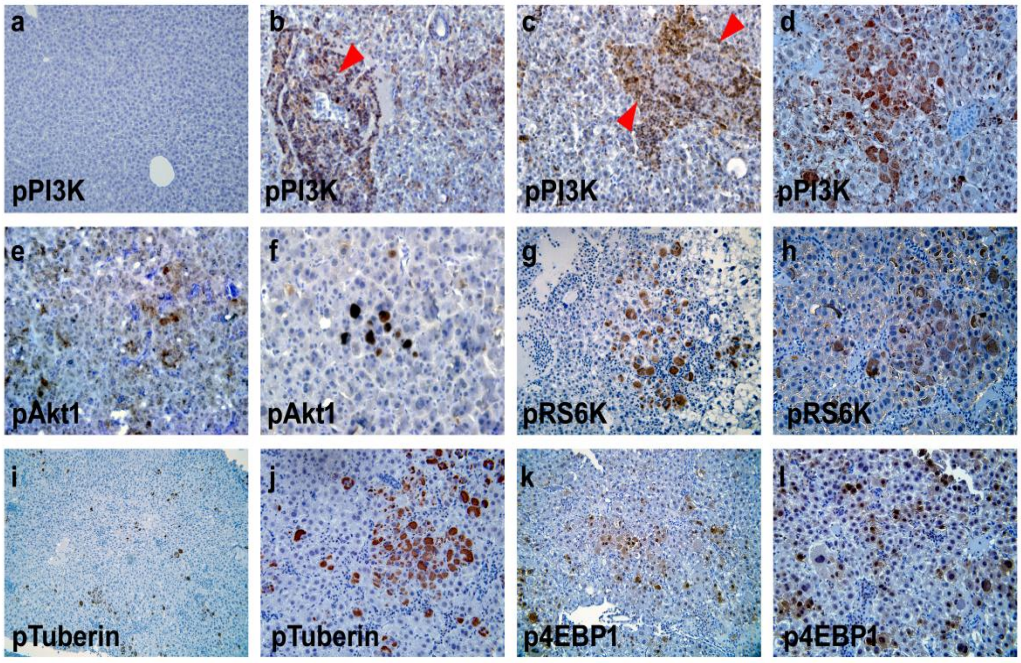

Fig 6. IHC for components of PI3K pathway. As downstream components IHC was done for active forms of PI3K, Akt, 70S6K, tuberin, and 4EBP1. a. Control. b-i. Tg(LFABP-Gal4/UAS-IL6). a-d. IHC for phophorylated form of PI3K showing positive staining only in infiltrated inflammatory cells. However, dysplatic hepatocytes with large cell chages are positive for pPI3K. e,f. IHC for pAkt with HCC at 9 monhts reveals small subset of tumor cells positive. g,h. IHC for pRS6K showing positive reaction only in hepatocytes with large cell changes. i,j. pTuberin staining is also positive in large cells. k,l. IHC for p4EBP1 showing positive saining in hepatocytes with large cell changes. Bars, 50 μm.

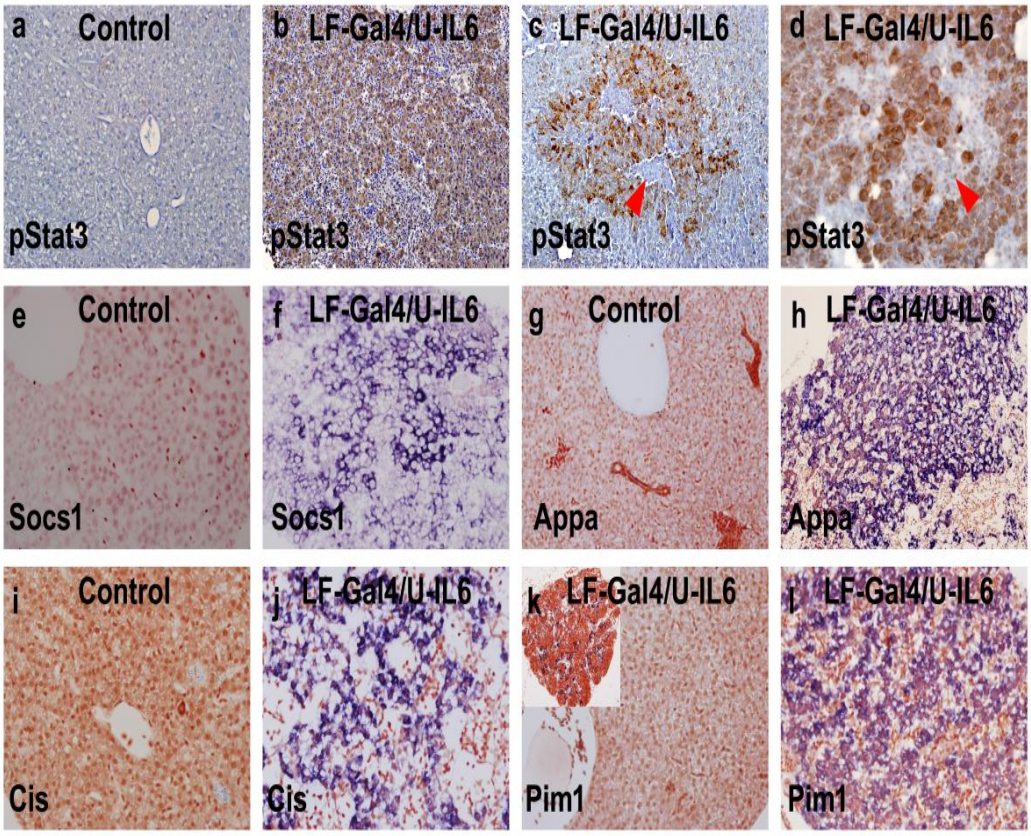

Fig 7. IHC for Jak/Stat3 components. a-d. IHC for pStat3. Virtually all hepatocytes are positive for pStat3 in Tg(LFABP-Gal4/UAS-IL6). c. Note that hepatocytes in dysplastic focus are strongly reactive pStat3. c,d. While hepatocytes are postive for pStat3, infiltrating inflammatory cells are not (red arrowhead). e-i. ISH for genes induced by Jak/Stat3 pathway. Inflammed and dysplastic hepatocytes express Socs1, Appa, Cis, and Pim1. k. Inlet image is spleen as positive internal control. Bars, 50 μm.

Table 2. Primers used for RT-PCR.

.Genes	Sense (5'-3')	Antisense (5'-3')	Product length (bp)
zAppa	TTATTCCCGATGCAGCTCTT	ATGGGTATAGACCGCACGGT	151
zApaf	ATGGAGGAACGTGCCCGCA	GGCCTTGCTGAGCACTTTTG	141
zBax	ATACGGGCAGTGGCAATGAC	GTTTATGGCTGGGGTCACAC	153
zBcl2	GGACTGATGGGGCTGAAGAG	CCTCCTTCACTGCGTCTAGA	171
zβ-Actin	ATGGATGAGGAAATCGCTGC	CTTTCTGTCCCATGCCAACC	151
zCcnD1	GCACCAGTTGTTTTGCTGCG	GACCTCGAGCATCCACGTCG	196
zCis	TGCCTTTCTCTTCACCGAGA	AACAGAGTGGGCCTCACTGG	152
zMc11a	AGTTTGGATTTTAGGCGAAC	AACAAATCGACCGTCCAGCT	183
z4EBP1	ATGTCCATGGGCAGTCAGAAG	GCAGGAACTTTCGGTCATAG	169
zEif1a	GACTGCTGAACCGGAAACTT	CCTCCACGGTGTCAAACTTT	200

zErk1	CTGGAGTCGGTGAAGGGACA	GCTGGCAGTAGGTCTGGTGT	169
zIL1b	CATGCGGGCAATATGAAGTC	CATTTTGTGCTGCGAAGTCC	170
zIL12a	ATGAAGATCTGTATTGTGATTAGCA	AAAACCAGCAAACAAGTCCT	177
zMCl1a	AGTTTGGATTTTAGGCGAAC	AACAAATCGACCGTCCAGCT	183
zMCl1b	ATGTTCGCTGGAAGAAACAA	ATAATCTCCCGCGTGTCCAT	197
zMyca	GAACGGCATTCGTTAAACACAA	TGGGCAGCAGTTCGAATTT	202
zPim1	AATTCAACACATTTGCTCACATT	TTTTGCAACATGCTTGATGG	191
zSocs1a	ATGGTGGCGCACAGTTCAGT	TGCATAGTTGAACGGCTTGA	153
zSocs2	ATGACCTGTCACTCATCCGAC	GGCTTCATTGGCTGTCAGGC	162
zSocs4	ATGTCTGAGAGGAAGACCAAAAACT	AGATCGAGCAGTCTGTTCGT	168
zSocs9	CCACTGCCTCGTTCCTGATT	CGAGAACAGGTAATCCTCCT	151
zSurv1	TGGATCTTGCAAGTGATGATCA	TTCCCATCCTTCCAGCTCTT	200

zSurv2	AAGACTTCAGACTTTTTCCGAG	GTGAAGAAAGGCACAGTTGG	214
zTimp2	ATGAAGAGCGTCAGGAGCTGTA	GCTTGATCGGGTTCCCATAA	199
zTgfb1a	GTTGGTTTGCTTGGTGCTGA	ATCTTCTGTCCGTCGTCGTC	186
zXiap	ATGGCACACTCAACTCATAATGG	GGCACTGCAGCTGAAACATT	192
zIFNg	ATGGATTCCTGCCTCAAAATG	TCCAACCCAATCCTTTGCAA	171
zNOS2	ATGGGAAGACAAGCACAAACCA	GCCGCTTTGTGATGAAGTGA	158
zIL8	ATGACCAGCAAAATCATTTCAGTGTG	AAATCTTTACAGTGTGGGCTTG	188
zP53	TAT TCA GCC CCC AGG TGG TG	GGA TAG TCG CTT GTC TCC GG	162

5. Discussion

In the present study, hIL6 gene was introduced into zebrafish and investigated that aberrant expression of the hIL6 has caused hepatocellular carcinogenesis. Although zebrafish has been used as an animal model system in the study of various human diseases, none of study expressing a human gene in the system to show its direct function has been reported. IL6 is a well known cytokine playing a crucial role in liver regeneration and also hepatic tumorigenesis depending on its expression condition.[3-5, 9] This pleiotrophic cytokine acts through signal transduction pathways.[6-8] Among the pathways, STAT3 plays very important roles in inflammation and tumorigenesis of liver. STAT3 which belongs to the STAT protein family consisting of seven member is especially known to be a key element in tumor initiation and progression.[25-26] Normal activation of STAT3 by phosphorylation in response to IL6 leads to turn on transcription of many downstream genes involved in development, while abnormal persistent activation of the element contributes to tumorigenesis and chronic inflammation, suggesting that STAT3 has dual role. Thus, our study focuses on inflammatory response and tumorigenesis by IL6/STAT3 signal using zebrafish model.

To do this, different transgenic zebrafish lines containing sustained expression of hIL6 gene which targets specifically to liver were generated (Fig. 1). Binary expression system using Gal4-UAS has provided a stable expression of the gene in all transgenic zebrafish and immunohistochemical experiments have well confirmed induction of chronic inflammatory change of the liver (Fig. 2,3). To determine the developmental progression of inflammation, the phenotype at different developmental stages of the

transgenic zebrafish was characterized. In our observation, massive infiltration of inflammatory cells was noted at 1 month of age in hepatic sinusoids and intrahepatic vessels in all transgenic zebrafishes expressing hIL6 gene (Fig. 2). At 2 months old of the hIL6-expressing transgenic zebrafish, dysplastic foci with various precancerous lesions began to appear in the liver (Fig. 4). The lesions included an appearance of clear cell bodies, eosinophilic and also basophilic cell bodies (Fig. 4). The results suggest that the persistent expression of hIL6 causes inflammation and tumorigenesis in zebrafish liver.

Further investigation of the tumorigenesis was done by molecular and immunochemical analyses (Fig. 5-7). Since IL6 plays roles in liver regeneration and tumorigenesis by regulating intracellular signal transduction, an advantage of determining differential expression of the downstream genes involved in the signal transduction pathways was taken to show that the hepatocellular tumorigenesis is caused by the action of the chronic expression of hIL6 in the transgenic zebrafish. The RT-PCR experiment with hIL6 primer clearly showed the over-expression of hIL6 gene in the transgenic zebrafish while the gene was not detected in non-transgenic zebrafish (Fig. 5b) and a consistency of this result was confirmed by a western blot analysis (Fig. 5c). The result suggests that a stable sustained expression of the hIL6 transgene was successfully achieved in the zebrafish model system. Since the cytokine IL6 has a role in enhancing cellular proliferation and hindering apoptosis by downregulating different pathways during inflammation and tumorigenesis, qRT-PCR experiment against few selected genes that might be involved in the pathways of PI3K-

Akt, Jak/Stat3, and Ras-Raf-Mapk was done. These three pathways are known to be activated upon response to IL6 binding to its membrane receptor, gp130, and control an array of dwonstream molecules involved in cell survival and proliferation.[13] From the qRT-PCR result, their differential expression pattern into three categories, inflammation, survival, and proliferation was summarized (Fig. 5a). The results revealed that many of the genes are up-regulated. Among these, up-regulation of c-myc and Survivin genes are prominently noted. These two genes are known to play important roles in various carcinogenesis. The c-myc is known as a critical regulator of cell growth and upon stimulation of the IL6 receptor, the gene expression is rapidly induced by increasing STAT3.[33] Furthermore, a very recent report has revealed that c-myc expression is dependent on IL6 stimulation to up-regulate rRNA transcription and the enhanced rRNA transcription stimulates MDM2-mediated proteasomal degradation of p53.[36] This result suggests that IL6 also downregulates p53 expression leading to chronic inflammation and tumorigenesis. Survivin is a member of the inhibitors of apoptosis protein family that directly inhibits caspase-3 and caspase-7 activity and its over-expression has been reported in various cancer.[34-35] Pim1, a serine-threonine kinase, is also known to suppress apoptosis and promote cell cycle progression.[32] Taken together, our qRT-PCR results suggested that the intracellular signaling activated by hIL6 enhances cell proliferation and reducing apoptosis inducing the liver inflammation and tumorigenesis in the zebrafish.

This is the first study reporting persistent expression of human IL6 in the liver induces chronic inflammation, dysplasia, and overt hepatocellular carcinoma in

transgenic zebrafish. Under normal circumstance, inflammation-associated expression of IL6 might have protective role of preventing hepatocyte death. Inappropriate or uncontrolled expression, however, can be detrimental to the liver causing accentuation of inflammatory process, cell damage and death, and eventually generation of dysplastic foci and hepatocellular carcinoma. Although the immunohistochemical analysis suggested that activation of Jak/Stat3 pathway played an important role in IL6-induced carcinogenesis in the zebrafish liver (Fig. 7), further investigation is necessary to demonstate its mechanism. For this reason, currently, inhibition analysis of the IL6 pathway responsible for the hepatocellular carcinogenesis (i.e., Jak/Stat3 pathway) is undergoing. The analysis will take us further insight into revealing the mechanism of chronic inflammation caused by IL6.

6. References

1. Kaplowitz NK, DeLeve LD. Druginduced liver disease. Marcel Dekker Inc. New York, New York, USA. 2003; 773 pp
2. Kanzler S, Galle PR. Apoptosis and the liver. Semin Cancer Biol 2000**;**10:173–184.
3. Taub R, Greenbaum LE, Peng Y. 1999. Transcriptional regulatory signals define cytokine dependent and independent pathways in liver regeneration. Semin Liver Dis 1999;19:117–127.
4. Kovalovich K. Interleukin-6 protects against Fas-mediated death by establishing a critical level of anti-apoptotic hepatic proteins FLIP, Bcl-2, and Bcl-xL. J Biol Chem 2001; 276:26605–26613.
5. Galun E, Zeira E, Pappo O, Peters M, Rose-John S. Liver regeneration induced by a designer human IL-6/sIL-6R fusion protein reverses severe hepatocellular injury. FASEB J 2000;14:1979–1987.
6. Taub R. Hepatoprotection via the IL-6/Stat3 pathway. J Clin Invest 2003;112:978-980.
7. Kuma S, Inaba M, Ogata H, Inaba K, Okumura T. Effect of human recombinant interleukin-6 on the proliferation of mouse hepatocytes in the primary culture. Immunobiology 1990;180: 235–242.
8. Sansone P. IL-6 triggers malignant features in mammospheres from human ductal breast carcinoma and normal mammary gland. J Clin Invest 2007;117:3988–4002.
9. Gao SP, Mark KG, Leslie K, Pao W, Motoi N, Gerald WL, Travis WD, Bornmann W, Veach D, Clarkson B, Bromberg JF. Mutations in the EGFR kinase domain mediate STAT3 activation via IL-6 production in human lung adenocarcinomas. J Clin Invest 2007;117:3846-3856
10. Lieschke GJ, Currie PD. Animal models of human disease: zebrafish swim into view. Nat Rev Genet 2007;8:353-367.

11. Liu S, Leach SD. Zebrafish models for cancer. Annu Rev Pathol 2011;6:71-93.
12. Lam SH, Wu YL, Vega VB, Miller LD, Spitsbergen J, Tong Y, Zhan H, Govindarajan KR, Lee S, Mathavan S. Conservation of gene expression signatures between zebrafish and human liver tumors and tumor progression. Nat. Biotechnol 2006;24:73-75.
13. Cressman DE, Diamond RH, Taub R. Rapid activation of the Stat3 transcription complex in liver regeneration. HEPATOLOGY 1995;21:1443-1449.
14. Wustefeld T, Rakemann T, Kubicka S, Manns MP, Trautwein C. Hyperstimulation with interleukin 6 inhibits cell cycle progression after hepatectomy in mice. HEPATOLOGY 2000;32:514-522.
15. Jung IH, Jung DE, Park YN, Song SY, Park SW. Aberrant Hedgehog ligand induce progressive pancreatic fibrosis by paracrine activation of myofibrolasts and ductular cells in transgenic zebrafish. PLoS ONE 2011;6:1-15
16. Jung IH, Leem GL, Jung DE, Park SW. Glioma is formed by active Akt1 alone and promoted by active Rac1 in transgenic zebrafish. Neuro-Oncology 2013;
17. Hirano T, Yasukawa K, Harada H, Taga T, Watanabe Y, Matsuda T, Kashiwamura S, Nakajima K, Koyama K, Iwamatsu A. Complementary DNA for a novel human interleukin (BSF-2) that induces B lymphocytes to produce immunoglobulin. Nature 1986;324:73–76.
18. Pisharath H, Parsons MJ. Nitroreductase-mediated cell ablation in transgenic zebrafish embryos. Methods Mol Biol 2009;546:133-143.
19. Her GM, Cheng CH, Hong JR, Sundaram GS, Wu JL. Imbalance in liver homeostasis leading to hyperplasia by overexpressing either one of the Bcl-2- related genes, zfBLP1 and zfMcl-1a. Dev Dyn 2006;235:515–523.
20. Workman P, Aboagye EO, Balkwill F. Guidelines for the welfare and use of animals in cancer research. Br J Cancer 2010;102:1555-1577.

21. Park SW, Davison JM, Rhee J, Hruban RH, Maitra A, Leach SD. Oncogenic KRAS induces progenitor cell expansion and malignant transformation in zebrafish exocrine pancreas. Gastroenterology 2008;134:2080-2090.
22. Janezic G, Widni EE, Haxhija EQ, Stradner M, Frohlich E, Weinberg AM. Proliferation analysis of the growth plate after diaphyseal midshaft fracture by 5'-bromo-2'-deoxy-uridine. Virchows Arch 2010;457:77-85.
23. Davison JM, Woo Park S, Rhee JM, Leach SD. Characterization of Kras-mediated pancreatic tumorigenesis in zebrafish. Methods Enzymol 2008;438:391-417.
24. Kubo M, Hanada T, Yoshimura A. Suppressors of cytokine signaling and immunity. Nat Immunol 2003;4:1169-1176.
25. Buettner R, Mora LB, Jove R. Activated STAT signaling in human tumors provides novel molecular targets for therapeutic intervention. Clin Cancer Res 2002;8(4):945-954.
26. Yu H, Pardoll D Jove R. STATs in cancer inflammation and immunity: A leading role for STAT3. Nat Rev Cancer 2009;9(11):798-809.
27. Mantovani A, Allavena P, Sica A, Balkwill F. Cancer-related inflammation. Nature 2008;454:436–444.
28. Airaksinen S, Rabergh CMI, Sistonen L, Nikinmaa M. Effects of heat shock and hypoxia on protein synthesis in rainbow trout (*Oncorhynchus mykiss*) cells. J Exp Biol 1998;201:2543–2551.
29. Morgensztern D, McLeod HL. PI3K/Akt/mTOR pathway as a target for cancer therapy. Anti-cancer Drugs16 (8): 797–803.
30. Yu H, Pardoll D, Jove R. STATs in cancer inflammation and immunity: a leading role for STAT3. Nat Rev Cancer 2009;9:798-809.
31. Molina JR, Adjei AA. The Ras/Raf/MAPK Pathway. J Thorac Oncol 2006;1: 7–9.
32. Bachmann M, Moroy T. The serine/threonine kinase Pim-1. Int J Biochem Cell Biol 2005;37: 726–730.

33. Kiuchi N, Nakajima K, Ichiba M, Fukada T, Narimatsu M, Mizuno K et al. STAT3 is required for the gp130-mediated full activation of the c-myc gene. J Exp Med 1999; 189: 63–73.
34. Mita AC, Mita MM, Nawrocki ST, Giles FJ (2008) Survivin: key regulator of mitosis and apoptosis and novel target for cancer therapeutics. Clin Cancer Res 14:5000-5005. 10.1158/1078-0432.CCR-08- 0746PubMed: 18698017.
35. Waligórska-Stachura J, Jankowska A, Waśko R, et al. Survivin – prognostic tumor biomarker in human neoplasms – review. Ginekol Pol. 2012;83(7):537–540.
36. Brighenti E, Calabrese C, Liguori G, Giannone FA, Trerè D, Montanaro L, Derenzini M. Interleukin 6 downregulates p53 expression and activity by stimulating ribosome biogenesis: a new pathway connecting inflammation to cancer. Oncogene. 2014;1-11

Intestine - specific expression

Chapter 3. Platform for intestine - specific expression of transgenes.

1. Abstract

In an effort to completion of zebrafish model platform of gastrointestinal expression, transgenic zebrafish has been established by using Cre-Loxp system (Tg(IFABP-CreERT2pA-Cmcl2-mcherry)). In this system, tamoxifen-dependent transcription factor CreERT2 was expressed under the control of the regulatory element of zebrafish intestinal fatty acid binding protein (IFABP) gene. Transgene CreERT2 expression was confirmed by ISH for Cre in 4 dpf embryos.

This platform line will be crossed with transgenic zebrafish in which transgene is expressed by recombinational excision of Loxp-stop-Loxp sequence by CreERT2 such as (Tg(UBB-Loxp-mCherry-Loxp-GFPKras^{G12D}). This strategy is used to induce expression of the transgene spcifically to intestinal organ and the established platform will be a valuable model for the study of human intestinal diseases.

Key words: Transgenic zebrafish, IFABP, DCLK1a, Cre-loxp-Cre system.

2. Introduction

Zebrafish (*Danio rerio*) has been used as an animal model system for developmental biology since 1980 and the system is now used to define the mechanism of tumorigenesis in recent years.[1,2] Zebrafish is about 3-4cm long when the fish is fully grown up at 10 weeks of generation cycle and contains 25 chromosomes. The fish interestingly conserves most of the genes found in human despite its diversity occurred 3 billion years ago.

Study in developmental biology, genetics, and tumorigenesis with zebrafish model system has different advantages; cost effectiveness, genomic similarity to human, huge production of progeny, and a short period of reproduction with 48 hours.[3,4] Also, the embryo can be easily detected under a fluorescence microscope when appropriate fluorescence biomarkers are used, allowing organ dependent expression of transgenes. [5] Since zebrafish undergoes with in vitro fertilization, researcher can easily manipulate transgenes for gain-of-function and knock-out purposes. For these, the animal system has been applied to investigate molecular and cellular mechanism of tumorigenesis since 2000.[6-11]

Using BAC or plasmid transgene constructs, F0 founder fishes can be cultivated and reproduced for F1 progeny containing the transgene expression. In our organ specific expression study of the genes involved in intestinal tumorigenesis, ptf1a and elastase2 is used for pancreas expression and the same as true for LFABP (Liver fatty acid binding protein) and IFABP (intestinal fatty acid binding protein) [12-14] for liver and intestine, respectively. DCLK1a gene can also be used to drive transgene expression in

the progenitor compartment of intestine.[15-20] For transgene expression analysis, Gal4-UAS system and/or LoxP-CreERT system are effectively used. In the system, Gal4 or CreERT contributes to organ specific expression from the transgene constructs under UAS or Loxp-stop-Loxp. Cre LoxP system allows temporal and spatial expression of the transgenes at desired developmental stages of the zebrafish. This strategy can be achieved by treating Tamoxifen which binds to Cre Recombinase (CreERT2), cutting Loxp-stop-Loxp sequence and inducing recombination of the transgenes. Cre/loxP system overcomes this problem because the system can control the expression of particular genes in specific tissues and stages during development. To make this system working, targeted gene under a tissue-specific and stage-specific promoter has flanked by loxP sites. The loxP sites are then recognized by Tamoxifen-dependent Cre recombinase, excising the gene at specific stages during development. Another strategy can be done to facilitate transgenic efficiency by using Tol2 which is recognized by T3 transposase. Introducing transgene constructs with transposase mRNA into fertilized eggs of zebrafish causes transpostion of the gene into zebrafish chromosome. [21-23]

Gastrointestinal tract is an important system in which food is digested from esophagus to intestine for nutritional absorption and storage. Different cancers, however, occurred in the gastrointestinal tracts such as esophagus cancer, stomach cancer, colorectal cancer, liver cancer, pancreas cancer, and biliary tract cancer take 42% of total cancers occurred in Korea. Therefore, purpose of the present study is to develop zebrafish model system which demonstrates human cancer disease [24,25]

3. Materials and Methods

1. Transgene constructs and transgenesis.

This present experiment involves Loxp-Cre system for induced expression of transgene. To do this, first, CreERT2 gene was PCR-amplified and cloned into Mlu1/Nhe1 site of pUAS-GFPpA-Cmcl2-mCherry to generate pUAS-CreERT2pA-Cmcl2-mCherry. Then, for intestine specific expression of transgene, upstream 3.0kb regulatory sequence of zIFABP (IFABP2) gene was PCR amplified from BAC DNA (CH73-34B5) and inserted into Apa1/Mlu1 site to generate the final transgene construct, pIFABP-CreERT2pA-Cmcl2-mcherry (table 1). All constructs used in this study were sequenced and verified using the appropriate primers listed in Table 1. Each injection mixture was prepared by reconstituting Tol2-transposase mRNA (20 ng/ul) and transgene construct (20 ng/ul) in Danieu's buffer mixed with 0.03% phenol red. AB embryos at single-cell stage were transferred to a molded agarose dish and 4 pL of the injection mixture of pIFABP-CreERT2pA-Cmcl2-mcherry was introduced by yolk injection using a MMPI-2 microinjector. F0 founder embryos showing robust cardiac mCherry expression were selected under a fluorescence microscope (Olympus, Japan). The embryos were then raised and bred to give a birth to F1 embryos showing non-mosaic mCherry expression in the heart. Intestinal expression of CreERT2 was confirmed by ISH for Cre using 4 dpf-old transgenic embryos. Transgenic embryos, Tg(UBB-Loxp-mCherry-Loxp-GFPKrasG12D) were kind gift from Park of Johns Hopkins Medical Institution. By crossing Tg(IFABP-CreERT2pA-

Cmcl2-mcherry) and Tg (UBB-Loxp-mCherry-Loxp-GFPKrasG12D), transgenic zebrafish in which dominant-active Kras gene is expressed by tamoxifen induction was established. All transgenes were transmitted in normal Mendelian ratio.

2. Animal stocks and embryo care.

All zebrafish were raised in a standardized aquaria system (Genomic-Design Co., Daejeon, Korea) according to standard protocols at 28°C on a 14- to 10-hour light and dark cycle. Embryos to be processed for whole mount analyses were placed in an E3 media with 0.003% phenylthiourea at 24 hpf to inhibit pigmentation. This experiment strictly followed the Guidelines for the Welfare and Use of Animals in Cancer Research.

3. In situ hybridization (ISH).

PCR amplification was done by using One-Step RT-PCR kit (Invitrogen) and amplified particial conding sequence was purified by gel extraction kit (Qiagen) and used for probe synthesis. (CreER sense: 5'-ATAACGCGTACCATGTCCAATTTACTGACCGTA-3', antisense; 5'-CTAATACGACTCACTATAGGGATTGCCCCTGTTTCACTATC'). The amplified sequence was inserted into PCRII vector. Then, PCRII plasmid with coding sequence was linearized and antisense riboprobe was generated by in vitro transcription using digoxigenin labelling mixture (Roche Diagnostics GmbH, Mannheim, Germany). Control sense probes were run in parallel for all experiments. Experiments were performed using either whole embryos or 4um

section slides. Specimens were fixed in 4% paraformaldehyde (PFA) on rotate for overnight at 4 ℃, dehydrated in a graded methanol series and stored in 100% MeOH. Samples were reconstituted in PBS with 0.1% Tween20 (PBST) and treated with 5mg/ml Proteinase K for 20 min 20 min at room temperature. Rehydrated samples were prehybridized with 50% formamide, 5X SSC, 50ug/mL heparin, 9.2 mM citric acid, 0.1% Tween-20, and 500ug/mL Torula yeast RNA (Sigma, St. Louis, MO) for 3 h at 65℃ followed by overnight hybridization with DIG-labeled RNA. Post-hybridization washes were done at 68 ℃ at least 4 hours as follows 2 washes in 2×SSC 0.1% Tween-20 for 10 minutes, one wash in 2×SSC 0.1% Tween-20 for 10 minutes followed by two washes in 0.2×SSC 0.1% Tween-20 for 30 minutes. All washing solutions were pre-warmed to 65℃. Subsequently, specimens were rinsed twice with PBST. Tissue was incubated in Anti-DIG alkaline phosphatase antibody (Roche) in blocking overnight at 4 ℃. Tissue was washed in PBST After extensive washing, samples are visualized by incubating with NBT/BCIP AP substrate solution (Roche Diagnostics GmbH) in 0.1 M Tris–HCl, pH 9.5, 0.1 M NaCl, 50 mM MgCl2, 0.1% Tween 20. Whole mount embryos were immersed in glycerol for better visualization. The sections were counterstained with neutral red and mounted with Histomount.

5. Imaging

Olympus MVX10 was used for whole mount embryo imaging.

4. Results

1. Strategy of intestine-specific expression platform

To achieve intestinal specific gene expression, CreERT2 gene has been put under IFABP promoter which is specifically expressed in intestine, establishing a Cre-lox-Cre system of the IFABP-CreERT2 (GI tract) transgenic lines of zebrafish (Fig. 1). CMV-loxp-stop-loxp-K-RAS (G12V) construct has also been used and the oncogene, K-RAS, has been induced for selective expression (Fig.2A). Tamoxifen treatment was done at 1 month after birth of zebrafish.

2. Expression analysis of intestine-specific transgene

For intestinal expression analysis, CreERT and molecular biomarker genes were used appropriately to tract their transgenic expressions in intestinal organs of zebrafish. The results revealed intestinal specific expression of CreERT in IFABP-CreERT transgenic lines. (Fig. 2) This established platform will be a useful experimental model system in demonstrating human gastrointestinal diseases.

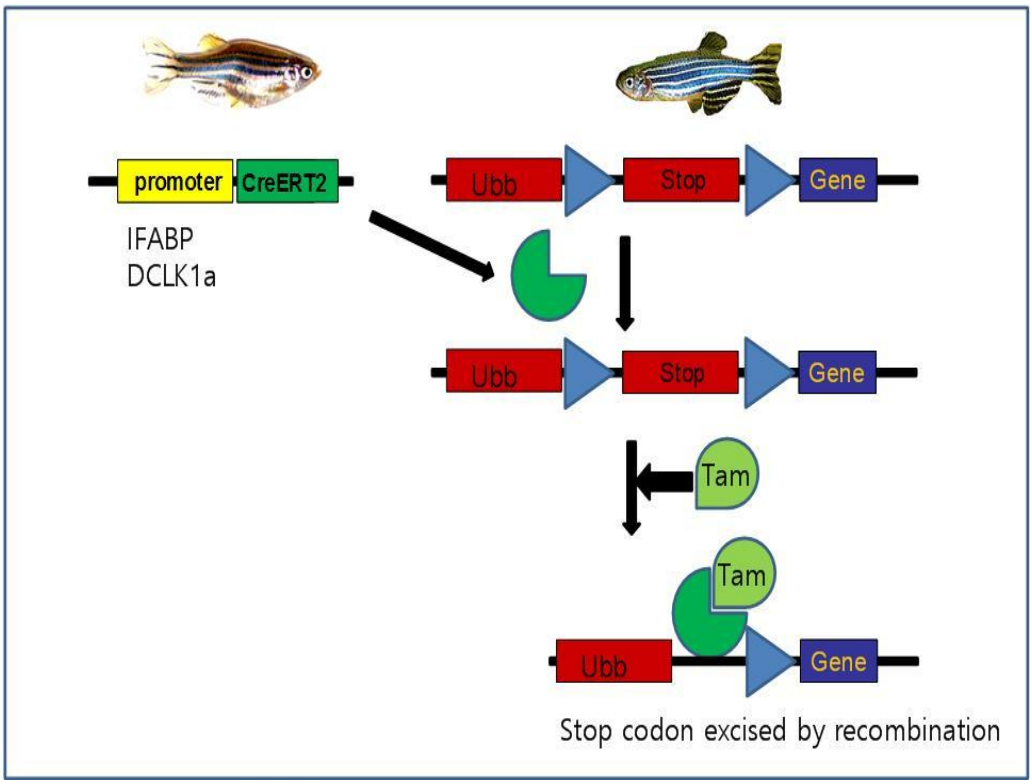

Fig 1. Schematic illustration of Cre-loxp-Cre system. CreERT2 recombinase expressed under the control of IFABP or DCLK1a regulatory element excises Loxp-stop-Loxp sequence under the presence of tamoxifen, which induces downstream gene in intestine-speficic manner.

Table 1. Primers used for the generation of transgene contructs.

F-UAS-Seq was used for sequence verification of constructs. Underlined GCCACC sequence was inserted for

Primers	Sequence
F1-CreER-Mlu1	5'-ATAACGCGTACCATGTCCAATTTACTGACCGTA-3'
R1-CreER-Nhe1	5'-ATAGCTAGCTCAAGCTGTGGCAGGGAAAC-3'
F0-EGFP-Mlu1	5'- ATAACGCGTATGGTGAGCAAGGGCGAGGAG-3'
R6-EGFP-Cla	5'-ACTAATCGATTTACTTGTACAGCTCGTCCAT-3'
F1-zFABP2-u3k-Apa1	5'- ACTAGGGCCCACCTCCGTCTTGTGGTACAA-3'
R2-zFABP2-Mlu1	5'- ATAACGCGTCCCGTTGAAGGTCATGATGA-3'
F1-zDCLK1a-Apa	5'- ACTAGGGCCCATTGAGACATGCCCCTGTCT -3'
R1-zDCLK1a-Mlu	5'- ATAACGCGTTTCGTATTGCAGCATGTTGA-3'

Underlines, restriction enzyme sequences

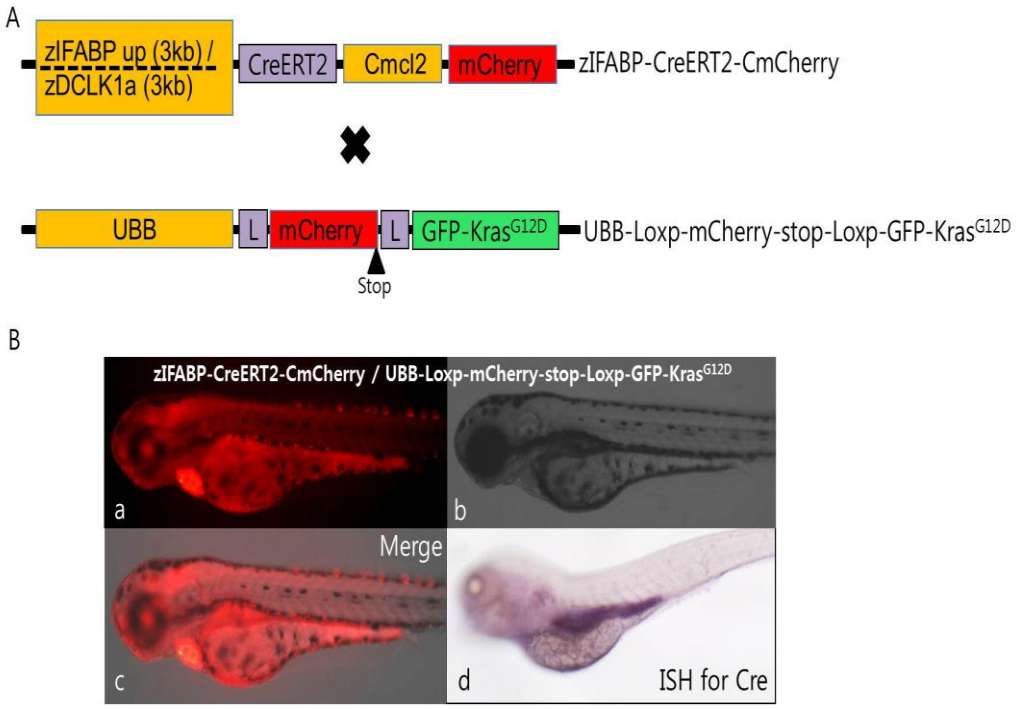

Fig 2. Targeted expression of transgenes in embryos. (A) Transgene construct for Cre-Loxp system. Spatio-temporally restricted expression of Gene, L: Loxp, IFABP: intestinal fatty acid binding protein, UBB: Ubiquitin B, DCLK1a: doublecortin-like kinase 1a, GFP-KrasG12D: dominant-active Kras as fusion gene (B) Transgenic embryos at 96 hpf. a. Inverted fluorescence image. b. Bright field image. c. Merged image. Red flurescence of moderate intensity at whole body and strong red at heart confirm the presence of both treansgenic construct. d. ISH for Cre showing robust expression at intestine.

5. Discussion

Gene expression analysis during embryonic development of animal model system requires specialized techniques especially when the transgene expression is toxic to the embryo because the embryo dies before development into aldut stage. For this reason, selecting an expression startegy of the transgene at particular developmenatal stage is very important. Gal4-UAS system and/or LoxP-CreERT system can be an effective choice for this type of expression analysis. In the system, Gal4 or CreERT contributes to organ specific expression from the transgene constructs under UAS or Loxp-stop-Loxp. Cre LoxP system allows temporal and spatial expression of the transgenes at desired developmental stages of the zebrafish becuase the transgene expression can be controlled by treating Tamoxifen which binds to Cre Recombinase (CreERT2), cutting Loxp-stop-Loxp sequence and inducing recombination of the transgenes.

Purpose of this study is to establish an expression platform that can be identified specifically in intestine. IFABP or DCLK1a is a useful regulatory element to make a transgene expression in intestinal organs. Thus, IFABP has been chosen to drive CreERT in differentiated intestinal cells. In this preliminary study, CreERT2 expression was detected by ISH in zebrafish intestine, suggesting that the transgene is expressed at desired developmental stages.

Establishing an intestine specific expression platform is important for human gastrointestinal cancer study. Althogh the present study is preliminary and requires further confirmation, the study suggests that zebrafish is a very useful model system for the study of human cancer disease.

6. References

1. Delvecchio C, Tiefenbach J, Krause HM (2011) The zebrafish: a powerful platform for in vivo, HTS drug discovery. Assay Drug Dev Technol 9: 354-361.
2. Lewis KE, Eisen JS (2003) From cells to circuits: development of the zebrafish spinal cord. Progress in Neurobiology 69: 419-449.
3. Chen JW, Galloway JL (2014) The development of zebrafish tendon and ligament progenitors. Development 141: 2035-2045.
4. Miyares RL, de Rezende VB, Farber SA (2014) Zebrafish yolk lipid processing: a tractable tool for the study of vertebrate lipid transport and metabolism. Dis Model Mech.
5. Jung IH, Jung DE, Park YN, Song SY, Park SW (2011) Aberrant Hedgehog ligands induce progressive pancreatic fibrosis by paracrine activation of myofibroblasts and ductular cells in transgenic zebrafish. PLoS One 6: e27941.
6. Jung IH, Leem GL, Jung DE, Kim MH, Kim EY, et al. (2013) Glioma is formed by active Akt1 alone and promoted by active Rac1 in transgenic zebrafish. Neuro Oncol 15: 290-304.
7. Lang V, Pallara C, Zabala A, Lobato-Gil S, Lopitz-Otsoa F, et al. (2014) Tetramerization-defects of p53 result in aberrant ubiquitylation and transcriptional activity. Mol Oncol.
8. Witjes JA, Gomella LG, Stenzl A, Chang SS, Zaak D, et al. (2014) Safety of Hexaminolevulinate for Blue Light Cystoscopy in Bladder Cancer. A Combined Analysis of the Trials Used for Registration and Postmarketing Data. Urology.
9. Castinetti F, Qi XP, Walz MK, Maia AL, Sanso G, et al. (2014) Outcomes of adrenal-sparing surgery or total adrenalectomy in phaeochromocytoma associated with multiple endocrine neoplasia type 2: an international retrospective population-based study. Lancet Oncol 15: 648-655.

10. Sloothaak DA, Grewal S, Doornewaard H, van Duijvendijk P, Tanis PJ, et al. (2014) Lymph node size as a predictor of lymphatic staging in colonic cancer. Br J Surg 101: 701-706.
11. Haidle AM, Zabierek AA, Childers KK, Rosenstein C, Mathur A, et al. (2014) Thiophene carboxamide inhibitors of JAK2 as potential treatments for myleoproliferative neoplasms. Bioorg Med Chem Lett 24: 1968-1973.
12. Schurink M, Scholten IG, Kooi EM, Hulzebos CV, Kox RG, et al. (2014) Intestinal Fatty Acid-Binding Protein in Neonates with Imminent Necrotizing Enterocolitis. Neonatology 106: 49-54.
13. de Geronimo E, Rodriguez Sawicki L, Bottasso Arias N, Franchini GR, Zamarreno F, et al. (2014) IFABP portal region insertion during membrane interaction depends on phospholipid composition. Biochim Biophys Acta 1841: 141-150.
14. Lagakos WS, Guan X, Ho SY, Sawicki LR, Corsico B, et al. (2013) Liver fatty acid-binding protein binds monoacylglycerol in vitro and in mouse liver cytosol. J Biol Chem 288: 19805-19815.
15. Kantara C, O'Connell M, Sarkar S, Moya S, Ullrich R, et al. (2014) Curcumin Promotes Autophagic Survival of a Subset of Colon Cancer Stem Cells, Which Are Ablated by DCLK1-siRNA. Cancer Res 74: 2487-2498.
16. 16. Ong BA, Vega KJ, Houchen CW (2014) Intestinal stem cells and the colorectal cancer microenvironment. World J Gastroenterol 20: 1898-1909.
17. Vedeld HM, Skotheim RI, Lothe RA, Lind GE (2014) The recently suggested intestinal cancer stem cell marker DCLK1 is an epigenetic biomarker for colorectal cancer. Epigenetics 9: 346-350.
18. May R, Qu D, Weygant N, Chandrakesan P, Ali N, et al. (2014) Brief report: Dclk1 deletion in tuft cells results in impaired epithelial repair after radiation injury. Stem Cells 32: 822-827.
19. Bailey JM, Alsina J, Rasheed ZA, McAllister FM, Fu YY, et al. (2014) DCLK1 marks a morphologically distinct subpopulation of cells with stem cell properties in preinvasive pancreatic cancer. Gastroenterology 146: 245-

256.

20. Nakanishi Y, Seno H, Fukuoka A, Ueo T, Yamaga Y, et al. (2013) Dclk1 distinguishes between tumor and normal stem cells in the intestine. Nat Genet 45: 98-103.
21. Pan X, Wan H, Chia W, Tong Y, Gong Z (2005) Demonstration of site-directed recombination in transgenic zebrafish using the Cre/loxP system. Transgenic Research 14: 217-223.
22. Reinert RB, Kantz J, Misfeldt AA, Poffenberger G, Gannon M, et al. (2012) Tamoxifen-Induced Cre-loxP Recombination Is Prolonged in Pancreatic Islets of Adult Mice. PLoS One 7: e33529.
23. Yoshikawa S, Kawakami K, Zhao XC (2008) G2R Cre reporter transgenic zebrafish. Dev Dyn 237: 2460-2465.
24. Park SW, Davison JM, Rhee J, Hruban RH, Maitra A, et al. (2008) Oncogenic KRAS induces progenitor cell expansion and malignant transformation in zebrafish exocrine pancreas. Gastroenterology 134: 2080-2090.
25. Davison JM, Woo Park S, Rhee JM, Leach SD (2008) Characterization of Kras-mediated pancreatic tumorigenesis in zebrafish. Methods Enzymol 438: 391-417.
26. Abe G, Suster ML, Kawakami K (2011) Tol2-mediated transgenesis, gene trapping, enhancer trapping, and the Gal4-UAS system. Methods Cell Biol 104: 23-49.
27. Hoegler KJ, Distel M, Koster RW, Horne JH (2011) Targeting olfactory bulb neurons using combined in vivo electroporation and Gal4-based enhancer trap zebrafish lines. J Vis Exp.
28. Gray C, Loynes CA, Whyte MK, Crossman DC, Renshaw SA, et al. (2011) Simultaneous intravital imaging of macrophage and neutrophil behaviour during inflammation using a novel transgenic zebrafish. Thromb Haemost 105: 811-819.
29. Asakawa K, Kawakami K (2009) The Tol2-mediated Gal4-UAS method for

gene and enhancer trapping in zebrafish. Methods 49: 275-281.

30. Scott EK (2009) The Gal4/UAS toolbox in zebrafish: new approaches for defining behavioral circuits. J Neurochem 110: 441-456.

31. Scheer N, Campos-Ortega JA (1999) Use of the Gal4-UAS technique for targeted gene expression in the zebrafish. Mech Dev 80: 153-158.

국 문 요 약

형질 전환 기법을 활용한 제브라피쉬 소화기질환 모델의 개발과 응용

연세대학교 대학원
나노메디컬협동과정
정인혜

제브라피쉬(Danio rerio)는 1980년대 발생생물학 모델로 이용되기 시작하였고, 2000년대부터 종양생물학 모델로 가치가 부각되었다. 3년생 열대담수어인 제브라피쉬는 성어의 크기가 3-4cm이고 세대기간 10주이며 25쌍의 염색체를 지니며, 진화상으로 3억년 전에 인류의 공통 조상에서 분리가 되었음에도 유전자가 보존되어 있어 인간이 가지는 거의 모든 유전자를 보유하고 있다. 이 외에도 제브라피쉬는 발생학, 유전학, 종양생물학 연구에 있어서 몇 가지 장점을 지닌다. 첫째, 초기비용과 유지비용이 낮아 비용효과적이다. 둘째, 백서에는 미치지 못하지만 초파리나 선형동물에 비하여 유전적으로 인간과 매우 유사하다. 셋째, 다수의 수정란을 생산하기 때문에 저비용 고효율 연구가 가능하다. 넷째, 배아가 투명하고 48시간의 짧은 발생기간을 가지기 때문에 실시간 관찰이 가능하다. 기관 특이적으로 형광단백과 같은 생물표지자를 발현시키면 생체에서 실시간으로 특정기관의 관찰이 가능하고 배아단계에서는 세포 수준의 추적이 가능해서 발생생물학 연구에 매우 유용하다. 다섯째, 체외수정을 하기 때문에 수정란의 난황으로 손쉽게 유전물질을 주입하여 유전자조작(gain-of-function, knock-out)이 용이하다. 이러한 장점에 기인하여 1981년에 모델로 수립된 이후 급속한 발전과 전파를 거쳐 발생생물학과 유전학 연구의 핵심적인 모델의 하나로 정립되었다.

2000년 이후 형질전환 제브라피쉬 혈액암 모델을 시작으로 다양한 제브라피쉬 형질전환 암모델이 수립되기 시작하였으며 매년 수립되는 모델의 수가 증가하고 있는 추세이다. 손쉽게 벤치 사이드에서 형질전환을 할 수 있다는 장점은 유전자의 기관특이적 발현을 통한 종양유전자의 연구가 진행된 계기가 되었다. 질병모델의 수립은 기관특이적 전환유전자의 발현을 이용하는 형질전환 기법이 흔히 이용되고 있다. 형질전환은 원래의 세포에는 없는 DNA를 외부에서 투여하여 세포의 유전 형질을 변환시키는 분자생물학적 기법을 말한다. 형질전환에는 다양한 기법과 전략이 개발되어 있으나, 흔히 실험실에서 형질전환을 위한 BAC 또는 plasmid를 조작하여 전환유전자 콘스트럭트를 제작한 다음 수정란으로 미세주입하여 염색체로 삽입시키는 방법이 이용된다. 특정 기관의 질병모델 개발을 위해서는 기관특이적인 유전자 발현을 유도하는 전략을 이용한다. 소화기계는 식도, 위, 장 등 음식물의 이동 및 흡수 경로가 되는 위장관, 음식물의 소화를 유발하는 소화액을 분비하는 췌장, 담도 및 각종 단백을 생산하고 영양분을 저장하는 간을 포함하는 시스템이다. 소화기계에는 식도암, 위암, 대장 직장암, 간암, 췌장암, 담도암 등 다양한 암종이 발생하고 있고 국내에서 전체 암의 42%를 차지하고 있어 국가보건의 주요 이슈이기도 하다. 소화기계 질병모델의 체계적인 구축을 위해서는 이들 장기에 기관특이적으로 질병 관련 유전자를 발현할 수 있는 플랫포옴의 개발이 필요하다. 연구자는 소화기계 기관별 특이적인 전환유전자를 발현할 수 있는 모델 플랫포옴을 구축하고 형질전환주를 수립하여 구축된 모델이 실제 인간의 질병을 모방할 수 있는지 규명하고자 본 연구를 진행하였다.

소화기계의 기관특이적 유전자 발현을 위하여 췌장은 ptf1a, 간은 Liver fatty acid binding protein (LFABP), 위장관은 intestinal fatty acid binding protein (IFABP) 조절인자를 이용하였다. 전환유전자의 발현은 Gal4-UAS 시스템 또는 LoxP-CreERT 시스템을 이용하였다. 이는 전환유전자의 이소성 발현을 최소화하기 위한 전략으로 Gal4 또는 CreERT가 고도로 기관특이적인

발현을 보이도록 구축한 형질전환주를 기반으로 하여, UAS 하방 또는 Loxp-stop-Loxp 하방에 유전자를 클로닝하여 별개의 형질전환주를 수립한 뒤 교배를 통하여 원하는 기관에 전환유전자가 발현되도록 하였다. Cre LoxP 시스템은 시공간적 발현조절이 가능하여 목표 장기에서 발현되는 Cre Recombinase(CreERT2)와 원하는 시기에 외부에서 투여하는 Tamoxifen과 결합한 뒤 loxP-stop-loxP 서열을 절단, 재조합하면 전환유전자가 발현되도록 하였다. 또한 연구자는 형질전환의 효율을 높이기 위하여 삽입하고자 하는 DNA 서열의 5’ 및 3’에 T3 transposase가 인식하는 Tol2 서열을 넣었다. 형질전환을 위한 수정란내 미세주입시 transposase mRNA와 형질전환 콘스트럭트 플라스미드를 함께 주입하면 transposase에 의하여 Tol2 서열 사이의 DNA가 염색체로 강제 치환되기 때문에 형질전환의 효율을 극대화 할 수 있다. 상기 시스템을 활용하여 연구자는 소화기관 선택적으로 종양유전자를 발현하는 형질전환 제브라피쉬 모델 플랫포옴을 구축하고 유전자 발현에 의한 표현형을 분자/세포 생물학 수준에 검증함으로써 제브라피쉬 모델 시스템의 유용성을 확립하고자 하였다. ptf1a 유전자는 인간과 백서에서 망막, 소뇌, 췌장의 발생에 핵심적인 기능을 하는 전사인자이다. 제브라피쉬에서도 마찬가지로 발생시 망막, 후뇌, 외분비췌장에 발현된다. 차이점으로 인간과 백서에서는 내, 외분비췌장 모두의 발생에 필수적이지만 제브라피쉬에서는 외분비췌장의 발생에만 관여하기 때문에 외분비췌장 특이적인 유전자발현을 유도하는데 적합한 유전자이다. 분화전 전구세포에서 발현되는 ptf1a 유전자를 포함하는 BAC DNA를 재조합방식으로 조작하여 ptf1a-Gal4 형질전환주를 구축하였고, UAS-Shh 및 UAS-Ihh 형질전환주를 구축하여 고배함으로써 ptf1a 영역에 hedgehog 리간드가 발현되는 이중 형질전환주를 구축하였다.

형질전환주의 표현형을 분석하여 hedgehog 신호의 활성화는 paracrine 기전을 통하여 췌장의 섬유화가 유발됨을 제브라피쉬 형질전환주를 통하여 in vivo에서 규명하였다. Hedgehog 경로의 활성화에 의해 췌장 섬유화가 발생함을

보여주며 이는 인간의 만성췌장염 및 췌장암에서 나타나는 췌장 섬유화와 조직학적 및 분자생물학적으로 매우 유사함을 확인하였다.

본 연구자는 제브라피쉬에서 발생 단계부터 간특이적으로 유전자가 발현되는 형질전환 플랫포옴을 구축하기 위하여 liver fatty acid binding protein (LFABP)를 선택하여 5‘ upstream 2.9kb (조절서열)를 클로닝하였다. LFABP 조절서열의 특이성을 분석하기 위하여 LFABP-GFP 콘스트럭트를 제작하여 형질전환 제브라피쉬를 수립하여 확인하였다. 간의 만성염증을 촉진시켜 간암 발생에 중요한 역할을 하는 IL-6 유전자를 선정하였고, UAS-hIL6-CG 형질전환주를 별도로 수립하여 LFABP-Gal4 / UAS-RFP 전환주와 교배함으로써 간 특이적으로 hIL6를 발현하는 triple 형질전환주를(LFABP-Gal4 / UAS-RFP / UAS-hIL6-CG) 수립하였다. hIL6 발현은 간에 만성적인 염증세포의 침윤과 이에 따른 간세포의 손상과 재생을 유발하였고, 생후 3개월부터 다양한 이형성을 유발하였다. 6개월에는 만성염증성 변화와 아울러 AFP 양성인 간세포암이 발생하였다.

분자수준에서의 분석상 hIL6의 발현은 PI3K/Akt, Jak/Stat3, Raf/MAPK 신호경로를 활성화 시킴이 확인되었다. 면역염색상 대부분의 간세포와, 이형성세포, 간암세포에 활성화된 pStat3가 강양성을 보여 만성염증에 따른 간암 발생과정에서 Jak/Stat3 신호경로가 주요한 역할을 함을 시사하였다. 반면에 pPI3K는 간세포보다는 주로 침윤된 염증세포에서 발현을 보였다. 이상의 결과는 강력한 염증유발 유전자인 hIL6의 간특이적 발현에 의하여 발생하는 간세포암화 과정에서 Jak/Stat3가 주도적인 역할을 하고 있음을 의미한다.

위장관 발현주는 Gal4자체의 독성으로 인하여 생존이 불가하여 IFABP - CreERT 형질전환주 수립을 통하여 시공간적 발현 조절이 가능한 형질 전환 전략으로 전환하였다. Cre-lox-Cre 시스템은 recombination을 통하여 유전자 재조합을 유발하면 지속적으로 유전자발현이 유도된다. 제브라피쉬 IFABP 유

전자의 5' 조절서열 3kb를 성공적으로 클로닝하였고, 위장관 특이적 Cre-lox-Cre 시스템을 구축하기 위하여 IFABP-CreERT2-CmC 형질전환주를 수립하였으며, CreERT2의 위장관 특이적 발현을 ISH을 통하여 확인하였다. 플랫포옴이 되는 IFABP-CreERT2주는 CMV-loxp-stop-loxp-transgene 주와 교배하여 Cre-LoxP 시스템에 의하여 발현이 유도되는 위장관모델주를 수립하는데 이용할 예정이다.

이상의 결과로 연구자는 제브라피쉬 소화관 발현 모델 플랫포옴을 성공적으로 구축하였다. 췌장특이적 발현은 Ptf1a, 간특이적 발현은 LFABP, 장관특이적 발현은 IFABP 유전자의 조절염기서열에 의해 각각 유도되는 시스템이며, Gal4-UAS 또는 Cre-LoxP 시스템에 의해 발현이 조절된다. 수립된 플랫포옴주를 바탕으로 별도로 수립하는 UAS-유전자, 또는 LSL-유전자 형질전환주와 교배함으로써 binary expression 시스템을 손쉽게 완성할 수 있다. 다양한 종양 발생관련 유전자를 이용하여 단기간 내에 원하는 장기에 유전자를 발현하는 형질전환주를 수립할 수 있으며 이러한 시스템은 향후 제브라피쉬가 종양생물학 연구를 위한 모델로서의 가치가 확장되는데 일조할 것으로 판단한다.

핵심이 되는 말: 형질전환, 제브라피쉬, 췌장, 간, 장관, Ptf1a, LFABP, IFABP, Hedgehog, Interleukin-6, 섬유화, 간세포암.